NUREG/CR–4599
BMI–2173
Vol. 3, No. 2

Short Cracks in Piping and Piping Welds

Semiannual Report
October 1992 – March 1993

Prepared by
G. M. Wilkowski, F. Brust, R. Francini,
N. Ghadiali, T. Kilinski, P. Krishnaswamy, R. Mohan,
C. W. Marschall, S. Rahman, A. Rosenfield, and P. Scott

Battelle

Prepared for
U.S. Nuclear Regulatory Commission

AVAILABILITY NOTICE

Availability of Reference Materials Cited in NRC Publications

Most documents cited in NRC publications will be available from one of the following sources:

1. The NRC Public Document Room, 2120 L Street, NW., Lower Level, Washington, DC 20555-0001

2. The Superintendent of Documents, U.S. Government Printing Office, Mail Stop SSOP, Washington, DC 20402-9328

3. The National Technical Information Service, Springfield, VA 22161

Although the listing that follows represents the majority of documents cited in NRC publications, it is not intended to be exhaustive.

Referenced documents available for inspection and copying for a fee from the NRC Public Document Room include NRC correspondence and internal NRC memoranda; NRC bulletins, circulars, information notices, inspection and investigation notices; licensee event reports; vendor reports and correspondence; Commission papers; and applicant and licensee documents and correspondence.

The following documents in the NUREG series are available for purchase from the GPO Sales Program: formal NRC staff and contractor reports, NRC-sponsored conference proceedings, international agreement reports, grant publications, and NRC booklets and brochures. Also available are regulatory guides, NRC regulations in the *Code of Federal Regulations*, and *Nuclear Regulatory Commission Issuances*.

Documents available from the National Technical Information Service include NUREG-series reports and technical reports prepared by other Federal agencies and reports prepared by the Atomic Energy Commission, forerunner agency to the Nuclear Regulatory Commission.

Documents available from public and special technical libraries include all open literature items, such as books, journal articles, and transactions. *Federal Register* notices, Federal and State legislation, and congressional reports can usually be obtained from these libraries.

Documents such as theses, dissertations, foreign reports and translations, and non-NRC conference proceedings are available for purchase from the organization sponsoring the publication cited.

Single copies of NRC draft reports are available free, to the extent of supply, upon written request to the Office of Administration, Distribution and Mail Services Section, U.S. Nuclear Regulatory Commission, Washington, DC 20555-0001.

Copies of industry codes and standards used in a substantive manner in the NRC regulatory process are maintained at the NRC Library, 7920 Norfolk Avenue, Bethesda, Maryland, for use by the public. Codes and standards are usually copyrighted and may be purchased from the originating organization or, if they are American National Standards, from the American National Standards Institute, 1430 Broadway, New York, NY 10018.

DISCLAIMER NOTICE

This report was prepared as an account of work sponsored by an agency of the United States Government. Neither the United States Government nor any agency thereof, or any of their employees, makes any warranty, expressed or implied, or assumes any legal liability of responsibility for any third party's use, or the results of such use, of any information, apparatus, product or process disclosed in this report, or represents that its use by such third party would not infringe privately owned rights.

NUREG/CR–4599
BMI–2173
Vol. 3, No. 2

Short Cracks in Piping and Piping Welds

Semiannual Report
October 1992 – March 1993

Manuscript Completed: February 1994
Date Published: March 1994

Prepared by
G. M. Wilkowski, F. Brust, R. Francini,
N. Ghadiali, T. Kilinski, P. Krishnaswamy, R. Mohan,
C. W. Marschall, S. Rahman, A. Rosenfield, and P. Scott

Battelle
505 King Avenue
Columbus, OH 43201

Prepared for
Division of Engineering
Office of Nuclear Regulatory Research
U.S. Nuclear Regulatory Commission
Washington, DC 20555
NRC FIN B5702

ABSTRACT

This is the sixth semiannual report of the U.S. Nuclear Regulatory Commission's research program entitled "Short Cracks in Piping and Piping Welds." This 4-year program began in March 1990. The program objective is to verify and improve fracture analyses for circumferentially cracked large-diameter nuclear piping with crack sizes typically used in leak-before-break analyses, in-service flaw evaluations, or other related piping structural integrity concerns.

In the through-wall-cracked pipe evaluations, three analytical efforts were undertaken: (1) verification of J-deformation plasticity under nonproportional loading, (2) use of past stainless as-welded and solution-annealed identically flawed pipe experiments to examine the effect of weld metal strength on various J-estimation schemes, and (3) development of new F, V, and h functions for the GE/EPRI method involving short circumferential through-wall cracks in pipes under tension loading.

In the surface-cracked pipe evaluations, work was completed on: (1) material characterization efforts on a Babcock & Wilcox carbon-manganese-molybdenum submerged arc weld metal, and (2) a 3D finite-element mesh refinement study.

Efforts were initiated in the fracture of bimetallic weld fusion line toughness evaluations. The initial studies showed a soft region in the ferritic steel about 1 to 2 mm from the fusion line, and unusual fracture behavior was found to occur in the fusion-line Charpy tests.

The dynamic strain aging experimental efforts were completed with J-R curve tests that confirmed the screening criterion for a material that behaved quite differently than the ferritic base metals examined to date.

A new version of NRCPIPE, Version 1.4g, has been released with updated manuals.

Numerous other efforts were also undertaken, as follows: (1) an analytical effort on validation of J_M and J_D fracture parameters, (2) an assessment of the toughness of stainless steel SAW fusion lines, (3) updating the PIFRAC data base, (4) converting past Degraded Piping Program pipe fracture experimental data files from HP to IBM format, (5) expanding the data base of circumferentially cracked-pipe experiments, and (6) a new effort to assess the changes of critical flaw sizes if ASME Section III changes the elastic stress limits from $3S_m$ to $7S_m$.

Part of the program also involves cooperating with the ASME Section XI Pipe Flaw Evaluation Working Group. A Charpy energy based EPFM flaw evaluation procedure for axial cracks, presented in the last semiannual report, was further developed for circumferential cracks during this reporting period. We also showed that the α-modified GE/EPRI method gives non-unique solutions with the same input data, and hence should not be used.

CONTENTS

CONTENTS

CONTENTS

CONTENTS

LIST OF FIGURES

LIST OF FIGURES

LIST OF FIGURES

LIST OF TABLES

PREVIOUS REPORTS IN SERIES

Previous Reports from this Program

"Short Cracks in Piping and Piping Welds," First Semiannual Report, NUREG/CR-4599, Vol. 1, No. 1, March 1991.

"Short Cracks in Piping and Piping Welds," Second Semiannual Report, NUREG/CR-4599, Vol. 1, No. 2, April 1992.

"Short Cracks in Piping and Piping Welds," Third Semiannual Report, NUREG/CR-4599, Vol. 2, No. 1, September 1992.

"Short Cracks in Piping and Piping Welds," Fourth Semiannual Report, NUREG/CR-4599, Vol. 2, No. 2, February 1993.

"Short Cracks in Piping and Piping Welds," Fifth Semiannual Report, NUREG/CR-4599, Vol. 3, No. 1, October, 1993.

Previous Related Documents from NRC's Degraded Piping Program

"Degraded Piping Program - Phase II," Semiannual Report, NUREG/CR-4082, Vol. 1, October 1984.

"Degraded Piping Program - Phase II," Semiannual Report, NUREG/CR-4082, Vol. 2, June 1985.

"Degraded Piping Program - Phase II," Semiannual Report, NUREG/CR-4082, Vol. 3, March 1986.

"Degraded Piping Program - Phase II," Semiannual Report, NUREG/CR-4082, Vol. 4, July 1986.

"Degraded Piping Program - Phase II," Semiannual Report, NUREG/CR-4082, Vol. 5, December 1986.

"Degraded Piping Program - Phase II," Semiannual Report, NUREG/CR-4082, Vol. 6, April 1988.

"Degraded Piping Program - Phase II," Semiannual Report, NUREG/CR-4082, Vol. 7, March 1989.

"Degraded Piping Program - Phase II," Semiannual Report, NUREG/CR-4082, Vol. 8, March 1989.

"NRC Leak-Before-Break (LBB.NRC) Analysis Method for Circumferentially Through-Wall Cracked Pipes Under Axial Plus Bending Loads," Topical Report, NUREG/CR-4572, March 1986.

"Elastic-Plastic Finite Element Analysis of Crack Growth in Large Compact Tension and Circumferentially Through-Wall-Cracked Pipe Specimen--Results of the First Battelle/NRC Analysis Round Robin," Topical Report, NUREG/CR-4573 September 1986.

"An Experimental and Analytical Assessment of Circumferential Through-Wall Cracked Pipes Under Pure Bending," Topical Report, NUREG/CR-4574, June 1986.

"Predictions of J-R Curves With Large Crack Growth From Small Specimen Data," Topical Report, NUREG/CR-4575, August 1986.

"An Assessment of Circumferentially Complex-Cracked Pipe Subjected to Bending," Topical Report, NUREG/CR-4687, September 1986.

"Analysis of Cracks in Stainless Steel TIG Welds," Topical Report, NUREG/CR4806, November 1986.

"Approximate Methods for Fracture Analyses of Through-Wall Cracked Pipes," Topical Report, NUREG/CR-4853, January 1987.

"Assessment of Design Basis for Load-Carrying Capacity of Weld-Overlay Repair," Topical Report, NUREG/CR-4877, February 1987.

"Analysis of Experiments on Stainless Steel Flux Welds," Topical Report, NUREG/CR-4878, February 1987.

"Experimental and Analytical Assessment of Circumferentially Surface-Cracked Pipes Under Bending," Topical Report, NUREG/CR-4872, April 1987.

Previous Related Documents from NRC's International Piping Integrity Research Group (IPIRG) Program

"Evaluation and Refinement of Leak-Rate Estimation Models," NUREG/CR-5128, April 1991.

"Loading Rate Effects on Strength and Fracture Toughness of Pipe Steels Used in Task 1 of the IPIRG Program," Topical Report, NUREG/CR-6098, October 1993.

EXECUTIVE SUMMARY

The U.S. Nuclear Regulatory Commission's (NRC) program "Short Cracks in Piping and Piping Welds Research" began in March of 1990 and will extend for four years. The program objective is to verify and improve fracture analyses for circumferentially cracked large-diameter nuclear piping using integrated results from analytical, material characterization, and full-scale pipe fracture efforts. Only quasi-static loading rates are evaluated, since the NRC's International Piping Integrity Research Group (IPIRG) Program is evaluating the effects of seismic loading rates on cracked piping systems.

The term "short cracks" encompasses crack sizes typically considered in leak-before-break (LBB) or pragmatic in-service flaw evaluations. The size of a typical leak-before-break (LBB) crack for a large diameter pipe is 6 percent of the circumference, which is much less than the 20 to 40 percent ratios investigated in many past pipe fracture programs.

During this period, one new subtask was added to the program. This was Subtask 8.6, "Evaluation of ASME Section III Allowable Stress Limits". This was a relatively simple analysis to assess the change in the flaw sizes that result if the elastic stress limits are increased from $3S_m$ to $7S_m$.

Some key results in the various tasks during this reporting period are given below.

Short Through-Wall Cracked Pipe

The full-scale pipe fracture efforts and material characterization efforts associated with this task are completed. There were three analysis activities during this reporting period. The first examined the differences in J values using deformation versus incremental plasticity in finite element analyses for cases of loading at constant internal pressure and increasing bending moment, i.e., examining the effect of nonproportional loading. The error in the deformation plasticity analysis was less than 1 percent. This is good news for several reasons. Deformation plasticity analyses are much more cost effective and are the basis of many of the existing J-estimation schemes; also, the degree of nonproportional loading of practical concern was found to have insignificant effect on J.

The second analysis activity was an evaluation of stainless steel SAW as-welded versus solution-annealed "identical" through-wall-cracked pipe experiments from the Degraded Piping Program - Phase II. The solution annealing increased the C(T) specimen weld-metal J-R curve, but lowered the weld metal stress-strain curve. Since typical pipe fracture analyses use the base metal stress-strain curve and the weld J-R curve, these were good experiments to use to evaluate the weld metal modified J-estimation scheme (LBB.ENG3) developed earlier in this program. The analyses showed very slight improvement when using the LBB.ENG3 analyses compared with existing analyses and, more importantly that the J-R curve from the thicker (25.4 mm) C(T) specimens was more conservative than the J-R curve from the thinner (14 mm) thick pipe experiments.

The last effort undertaken was the development of F, V, and h functions for the GE/EPRI J-estimation method for tension loading of short circumferential through-wall cracks, i.e., θ/π = 1/16 and 1/8.

Short Surface-Cracked Pipe

The material properties characterizations for a Babcock and Wilcox (B&W) carbon-manganese-molybdenum weld (DP2-F49W) were completed. This weld procedure was used in most B&W carbon steel piping, and there were no prior J-R curve data on this weld procedure. This weld procedure is to be used in the last remaining pipe experiment in this task.

Finite element analyses were completed to examine the mesh refinement requirements for a circumferentially surface-cracked pipe. There was insufficient refinement with five elements in the ligament, even with an increase in the number of iterations. Meshes with seven or more elements showed convergence and gave adequate results.

Bimetallic Welds

This task was initiated during this reporting period. Material characterization efforts are well under way, and one large pipe test will be conducted with a crack located close to the fusion line of a bimetallic weld in a cold-leg pipe from a cancelled Combustion Engineering plant that is a nominal 36-inch diameter schedule 160 pipe.

The material characterization efforts showed a softer region in the ferritic steel about 1 to 2 mm from the bimetallic weld fusion line. Also, the Charpy data on the fusion line of the ferritic steel to the stainless steel weld remain quite puzzling. The specimens were oriented as if the cracks are growing as a circumferential through-wall crack in the pipe fusion line. Interestingly, the cracks split and turned 90 degrees as if they would suddenly become axial through-wall cracks in the ferritic base metal. A metallurgical evaluation gave no obvious reason for this splitting. The results of the splitting was that the cracks in the Charpy test were arrested and the specimens were not broken, resulting in very high impact energies.

Dynamic Strain Aging

J-R curve tests were completed to confirm if a particular carbon steel SAW was susceptible to dynamic crack jumps at higher temperatures as indicated by the high temperature hardness dynamic strain aging screening criterion. The results confirmed the dynamic strain aging screening criterion. This completes all the experimental work. Analysis of the toughness during a dynamic strain aging induced crack jump are under way. This analysis effort will be the final technical activity in this task. A topical report will then be written on all these results.

Crack Opening Area Evaluations

A statistical analysis was conducted on the J-R curve toughness of stainless steel base metals based on the probabilistic work conducted earlier. The results showed a higher scatter than anticipated, which was due to the presence of an inclusion that existed in the ligament of the specimen. The work also showed that additional care had to be taken in the methods used to extrapolate the J-R curves, which may affect the results of the past probabilistic work.

NRCPIPE Improvements

Version 1.4g of the NRCPIPE code was completed and released with a new user's manual. The changes were mainly to improve the user-friendly aspects of the program.

Additional Efforts

This task includes several unrelated technical activities that have started since the beginning of the program. These include: (1) a validation of J_M relative to J_D, (2) an assessment of the toughness of stainless steel SAW fusion line toughness, (3) updating the PIFRAC data base, (4) converting Degraded Piping Program - Phase II pipe experiment data files from HP to IBM format, (5) compiling a data base of circumferential cracked pipe experiments, and (6) a new effort to assess the changes of the flaw sizes if ASME Section III changes the elastic stress limits from $3S_m$ to $7S_m$. The progress of these efforts and their status are summarized in this report.

Interprogram Cooperation and Program Management

As part of the interprogram cooperative efforts, working with the ASME Section XI Pipe Flaw Evaluation Task Group is a key aspect of the technology transfer of results of this program to practical application. During this time period, three technical activities were conducted: (1) a comparison of the Charpy energy based elastic-plastic fracture mechanics axial surface crack analysis with the current ASME ferritic pipe axial crack EPFM tables for a material with J_{Ic} of kJ/m^2 (600 $in\text{-}lb/in^2$), (2) the development of a circumferential surface-cracked pipe Charpy energy based EPFM analysis, and (3) an evaluation of the Zahoor α-modified GE/EPRI analysis.

The comparison of the ASME axial crack EPFM table values with experimental data and the Charpy energy based EPFM criterion, presented in the last semiannual report, showed that the ASME tables were very conservative and that Charpy energy EPFM criterion and the experimental data showed that all the conditions in the tables were actually limit-load failures.

A Charpy-energy-based EPFM criterion was developed as a possible replacement for the current Z factors. This criterion eliminated many of the problems in using the current Z-factor approach. For instance, a Z factor can be calculated for any material using its Charpy energy rather than limiting the Z factor to two material categories, hence there is a smooth transition from EPFM to limit load.

The final effort examined the moment and crack-opening displacement predictions for the α-modification to the GE/EPRI method. This work showed that the α-modified method does not provide a unique numerical solution and hence should not be used.

Major Conclusions

Major conclusions to date are:

- Short circumferential through-wall flaws fail closer to limit-load (net-section-collapse) predictions than the longer flaws tested in past programs.

The significance of this to LBB analyses is that typically the circumferential flaw lengths in large diameter pipe (28 inches or larger) are quite short, approximately 6 percent of the circumference. This short length means that: (1) the failure loads are not as sensitive to toughness variations, and (2) when using a criterion such as the ASME Z-factor approach, which is based on long circumferential flaws, there is an extra degree of conservatism. However, for small diameter pipe (i.e., 4 to 6 inches), the LBB through-wall-crack size may be up to 30 percent of the circumference. Hence these pipes would be more sensitive to toughness variations, and the ASME Section XI Z-factor based criterion would be more appropriate. It is possible to develop engineering corrections to the Z-factor approach that would account for crack length, as well as diameter, to have a more consistent fracture analysis for LBB of any size pipe.

- From the surface-cracked pipe results, it was found that the effect of R/t ratio on the Net-Section-Collapse analysis predicted loads were consistent for large crack (d/t = .66 and θ/π = 0.5) experiments from the Degraded Piping Program and short cracked (d/t = .50 and θ/π = 0.25) pipe experiments from this program. The trend is that as R/t increases, the failure load decreases relative to the Net-Section-Collapse predicted failure load.

- A dynamic strain aging screening criterion using high temperature hardness testing was developed and verified. This criterion could be used non-destructively in situ or for specifying new piping steels. The occurrence of dynamic crack jumps induced by dynamic strain aging has been found to be very probabilistic in nature and has been experienced more frequently in pipe tests than in laboratory tests, i.e., C(T) specimens.

ACKNOWLEDGMENTS

This work is supported by the U.S. Nuclear Regulatory Commission through the Materials Engineering Branch of the Office of Nuclear Regulatory Research under Contract No. NRC-04-90-069. Mr. A. Hiser is the NRC program manager.

We would also like to thank others at Battelle who have helped in these efforts. Technicians who have contributed to the initial efforts are: Mr. R. Gertler, Mr. P. Held, Mr. P. Mincer, Mr. D. Rider, Mr. J. Ryan, Mr. D. Shoemaker, and Mr. J. Woods. We thank Mrs. V. Kreachbaum for typing this report, Dr. A. Hopper and Mr. M. Steve for editorial review comments, and Mr. D. Hayes for drafting assistance.

NOMENCLATURE

1. SYMBOLS

a	Half the crack length
c	Half the mean circumferential crack length
C_1	Remaining ligament of surface crack
C′	Coefficient used to fit J-resistance curve
C	Empirical constant used in DPZP analysis
CVP	Charpy upper-shelf energy
d	Flaw depth
D	Nominal outside pipe diameter
D_m	Mean pipe diameter
E	Young's modulus
F	Function relating elastic stress intensity factor to stress in GE/EPRI estimation scheme
F′	Constant used in original Ramberg-Osgood equation
f_{int}	Initial porosity of the material
h_1,h_2,h_3,h_4	Functions tabulated in GE/EPRI method
J_2	Second invariant of the stress tensor in plastic flow theory
J	J-integral fracture parameter
J_D	Deformation J
J_D-R	Deformation J-Resistance curve
J_i	J-integral at crack initiation but not necessarily a valid J_{Ic} by ASTM E813-81
J_{Ic}	J at crack initiation under Mode I loading
J_M	Modified value of J integral

J_P	Plastic component of J-integral
J-R, J_R	J-integral resistance (curve)
K_I	Mode I stress intensity factor
m	Exponent used to fit J-resistance curve
M	Moment
n	Ramberg-Osgood strain-hardening exponent
n_1	x_1 component of outward normal to Γ
p	Pressure
P	Tension load due to internal pressure
P_e	Thermal expansion stress
P_o	Failure load
r	A normalizing constant
R_i	Inside radius
R_m	Mean pipe radius
s	Standard deviation
S_m	ASME design stress
S_u	ASME ultimate stress
S_y	ASME yield strength
t	Thickness of pipe wall
T	Temperature
T	Second-order term in the asymptotic expansion of the elastic crack-tip stress field
V_1, V_2, V_3	Displacement functions in GE/EPRI analysis
Z	A stress multiplier in the ASME IWB-3640 and -3650 analyses

Y	Vector
α	Ramberg-Osgood parameter
β	Fully plastic neutral axis angle
Δa	Increment of crack growth
δ_p	Plastic component of displacement
ϵ	Strain
ϵ_o	Reference strain, σ_o/E
η	Geometric factor used in J-integral analysis
θ	Half-crack angle
μ	Statistical mean
σ	Stress
σ_f	Flow stress
σ_{nsc}	Net-strain-collapse analysis predicted failure stress
σ_u	Ultimate stress
σ_y	Yield stress

2. ACRONYMS AND INITIALISMS

ABACRACK	Computer code to generate finite element meshes for surface cracks
ABAQUS	Finite element computer code
AEC	Atomic Energy Commission (U.S.)
AGA	American Gas Association
ASME	American Society of Mechanical Engineers
ASTM	American Society for Testing and Materials
BMI	Battelle Memorial Institute

BMFT	Bundesministerimm für Forschung und Technologie (Germany)
B&W	Babcock and Wilcox
BWR	Boiling Water Reactor
CC	Complex crack
CEGB	Central Electricity Generating Board (U.K.)
CIRCUMCK.WK1	Lotus® database of circumferentially cracked pipe fracture experiments
CISE	Centro Informazioni Studi Esperienze (Italy)
CS	Carbon steel
CTOA	Crack-tip-opening angle
C(T)	Compact (tension) specimen
CVP	Charpy V-notch upper-shelf energy
DEGB	Double-ended guillotine break
DOS	Disk Operating System
DP^3II	Degraded Piping Program - Phase II
DPZP	Dimensionless Plastic-Zone-Parameter
DSA	Dynamic strain aging
DTRC	David Taylor Research Center (U.S.)
EDF	Electricite de France
ENEA	Comitato Nazionale per L'Energia Nucleare e delle Energie Alternative (Italy)
EPFM	Elastic-plastic fracture mechanics
EPRI	Electric Power Research Institute (U.S.)
FE	Finite element
FEM	Finite element method

GEAP	General Electric Atomic Power (Report)
HP	Hewlett Packard (computer)
IBM	International Business Machine (computer)
IPIRG	International Piping Integrity Research Group
JAERI	Japanese Atomic Energy Research Institute
KWU	Kraftwerk Union Aktiengesellschaft (Germany)
LBB	Leak-before-break
LBB.ENG2	Circumferential TWC analysis method developed at Battelle
LBB.ENG3	Modified LBB.ENG2 method for cracks in welds
LBB.NRC	TWC analysis method developed at NRC-NRR
L-C	Longitudinal-circumferential orientation (direction of through-wall crack growth around pipe circumference)
L-R	Longitudinal-radial orientation (direction of circumferential surface crack growth)
LWR	Light Water Reactor
MITI	Ministry of International Trade and Industry (Japan)
MPA	Staatliche Materialprüfungsanstalt (University of Stuttgart, Germany)
NED	Nuclear Engineering and Design (Journal)
NRC	Nuclear Regulatory Commission (U.S.)
NRCDP	National Research Center for Disaster Prevention (Japan)
NRC-NRR	Nuclear Regulatory Commission - Office of Nuclear Reactor Regulation
NRC-RES	Nuclear Regulatory Commission - Office of Nuclear Regulatory Research
NRCPIPE	PC computer program for circumferential TWC analyses
NRCPIPES	PC computer program for circumferential SC analyses
NUREG/CR	Nuclear Regulatory Commission Contractor Report

NUPEC	Nuclear Power Engineering Test Center (Japan)
P&B	Pressure and bend
PC	Personal computer
PIFRAC	Piping fracture database
PWR	Pressurized water reactor
ROFIT	Computer code to calculate Ramberg-Osgood parameters
SAM	Seismic anchor motion
SAW	Submerged-arc weld
SC	Surface crack
SC.TKP	Surface crack analysis using thick pipe approximations
SC.TNP	Surface crack analysis using thin pipe approximations
SEM	Scanning electron microscope
SMAW	Shielded metal arc weld
SQUIRT	Seepage Quantification of Upsets in Reactor Tubes, a leak-rate computer program
S.R.P	Standard Review Plan
STA	Science and Technology Agency (Japan)
TIG	Tungsten inert gas (weld)
TWC	Through-wall crack, through-wall-cracked
USNRC	United States Nuclear Regulatory Commission
VAX	Mainframe computer
WRC	Welding Research Council (U.S.)

1. INTRODUCTION

The "Short Cracks in Piping and Piping Welds" program was initiated to address Nuclear Regulatory Commission (NRC) licensing needs and to resolve some critical findings from the NRC's Degraded Piping Program. The term "short cracks" refers to the type of cracks assessed in leak-before-break (LBB) or pragmatic in-service flaw evaluations. A typical LBB-size crack for a large-diameter pipe is 6 percent of the circumference, which is much less than the circumferential lengths of 20 to 40 percent investigated in other pipe fracture programs conducted in the past. Hence, the term "short cracks" in this project does not refer to microscopic cracks that are of interest to the aerospace industry.

The 4-year program started on March 23, 1990. This sixth semiannual report describes progress in all the tasks during the period April through September 1992, and provides information on plans for the next 12 months.

The nine tasks addressed in this program are:

(1) Short through-wall-cracked (TWC) pipe evaluations
(2) Short surface-cracked (SC) pipe evaluations
(3) Bimetallic weld crack evaluations
(4) Dynamic strain aging and crack instabilities evaluations
(5) Fracture evaluations of anisotropic pipe
(6) Crack-opening-area evaluations
(7) NRCPIPE Code improvements
(8) Additional efforts
(9) Interprogram cooperation and program management.

Of these, work was conducted in all but Task 5 (Fracture Evaluations of Pipe Anisotropy) during this period. The Task 3 efforts on fracture of bimetallic welds were initiated during this time period. In addition, several subtasks were initiated in Task 8.

Table 1.1 gives an updated summary of the pipe experiments conducted in this program. Most of the tasks involve integrated analytical, material characterization, and full-scale pipe fracture experimental efforts. This program addresses only circumferential cracks in straight pipe under quasi-static loading rates. Seismic loading rate behavior of cracked pipe is being investigated in the NRC's Second International Piping Integrity Research Program (IPIRG-2).

Table 1.1 Current matrix of pipe experiments

Expt. No.	Diameter, in.	Schedule	Material	Temperature	Test Date
Unpressurized through-wall-cracked pipe experiments					
1.1.1.21	28	60	A515 Gr60	288C (550F)	10/25/90
1.1.1.23	28	80	TP316L SAW	288C (550F)	5/23/91
1.1.1.24	24	80	A333 Gr6 SAW	288C (550F)	3/13/92
1.1.1.26	4	80	TP316LN	22C (72F)	2/27/91
Unpressurized uncracked pipe experiment					
1.1.1.25	28	60	A515 Gr60	288C (550F)	2/07/92
Bimetallic weld fusion line experiments - TWC					
1.1.1.27	36	160	A516/SS-SAW	288C (550F)	(10/93)*
Unpressurized surface-cracked pipe experiments					
1.2.1.20	16	30	TP316	99C (210F)	1/15/92
1.2.1.21	6	XXS	TP304	288C (550F)	4/16/91
1.2.1.22	6	40	TP304	288C (550F)	3/15/91
Pressurized surface-cracked pipe experiments					
1.2.3.15	28	60	A515 Gr60	288C (550F)	11/08/91
1.2.3.16	28	80	TP316L SAW	288C (550F)	9/05/91
1.2.3.17	24	100	A106B SAW	288C (550F)	(1/94)*

* Planned test date.

2. TASK 1 SHORT TWC PIPE EVALUATIONS

2.1 Task Objective

The objective of this task is to modify and verify analyses for short through-wall-cracked (TWC) pipe using existing and new data on large-diameter pipe.

2.2 Task Rationale

The results of this task will help to refine the fracture analyses in leak-before-break (LBB) procedures used to evaluate through-wall cracks in large-diameter pipes.

2.3 Task Approach

The five subtasks in this task are:

Subtask 1.1	Material characterization for short TWC pipe experiments
Subtask 1.2	Upgrading of the large-pipe testing system
Subtask 1.3	Large-diameter pipe fracture experiments
Subtask 1.4	Analysis for short through-wall cracks in pipes
Subtask 1.5	Topical report.

Subtask 1.1 has been completed and discussed in previous semiannual reports. As stated in the previous semiannual report, Subtask 1.2 was eliminated. The data record book for Experiment 1.1.1.24 in Subtask 1.3 was submitted to the NRC, thus completing this subtask. Progress in Subtask 1.4 is described below.

2.3.1 Subtask 1.4 Analyses for Short Through-Wall Cracks in Pipes

2.3.1.1 Objective

The objective of this subtask is to develop, improve, and verify the engineering analyses for short circumferential through-wall-cracked pipe.

2.3.1.2 Rationale

The short through-wall-cracked pipe analysis improvements are aimed at LBB fracture evaluations for larger-diameter pipe.

2.3.1.3 Approach

The four activities in this subtask are:

Activity 1.4.1	Improve short through-wall-cracked pipe analysis and compare predictions with existing data
Activity 1.4.2	Analyze large-diameter pipe TWC test results
Activity 1.4.3	Analyze through-wall cracks in welds.
Activity 1.4.4	Develop new GE/EPRI functions.

During this reporting period, Activities 1.4.1, 1.4.3, and 1.4.4 were active. Progress in these activities is reported here.

2.3.1.4 Progress

Activity 1.4.1 Improve Short Through-Wall-Cracked Pipe Analysis and Compare Predictions with Existing Data

The four separate efforts in this activity are:

(a) Numerically assess the effect of plastic ovalization on the validity of J
(b) Determine pipe ovalization effects on limit-load analysis
(c) Improve F, V, and h functions
(d) Compare predictions from improved analyses with existing data.

Only Activity 1.4.1(c) was active and the progress is described below.

The effort in this activity involves computation of F, V, and h functions for circumferentially cracked pipes under combined bending and tension. The calculation of these functions using 3-D analysis of short TWC pipes under pure bending has shown that the GE/EPRI functions (Ref. 2.1) are in error as they were developed using shell elements that are generally stiffer than 3-D brick elements. In this activity, these functions will be re-computed using ABAQUS (Ref. 2.2) using 20-noded 3-D brick elements for several sets of values of crack length (θ/π), mean-radius-to-thickness ratio (R_m/t), and hardening parameter (n).

Deformation and Flow Theories - In developing constitutive equations for work-hardening materials, two basic approaches can be used to calculate the above influence functions. The first formulation uses deformation theory in the form of a total stress-strain relation. This theory assumes that the state of stress determines the state of strain uniquely as long as plastic deformation continues. This is identical to the nonlinear elastic stress-strain relation with no unloading and is theoretically valid only for loading paths that are proportional. The second formulation uses incremental or flow theory in the form of an incremental stress-strain relation. This theory relates the increment of plastic strain components to the state of stress and the stress increment. It is more general than deformation theory and can be applied to a wide variety of loading conditions, including non-proportional and cyclic loads. For a typical monotonic pipe test under combined bending and tension, or for a pipe in service, the tensile force is usually held constant due to constant internal pressure, but the bending moment is changed. During the progression of load increments, the load factor, which is defined as the ratio of bending moment and tension, also increases, thus violating load-proportionality, which is the essential condition for the validity of deformation theory of plasticity. However, the typical values of service pressure in a pipe is 15.51 MPa (2,250 psi) for primary PWR piping and 7.24 MPa

(1,050 psi) for BWR piping or secondary PWR piping. The pipe material behavior under these pressure loadings is mostly elastic with little or no plastic strain. Hence, both deformation and flow theories should be equally applicable to use with finite element analysis to determine the GE/EPRI influence functions.

Validation of Deformation Theory - To substantiate this claim of equal applicability, a verification study was conducted to determine the adequacy of results from the deformation theory of plasticity. As an example, consider a TWC pipe with $R_m/t=10$, $n=5$, and $\theta/\pi=1/8$, which is subjected to internal pressure of 15.51 MPa (2,250 psi) and increasing bending moment. It is assumed that the material stress-strain relation can be represented by the Ramberg-Osgood relation. Two finite element analyses were carried out for this pipe using deformation and incremental stress-strain formulations. The computer code used was ABAQUS with 20-noded, 3-D solid elements. Figure 2.1 shows the results of both analyses presented in terms of J-integral plots as a function of applied bending moment. They clearly indicate that the finite element results obtained using deformation theory provide accurate estimates of the crack driving force when compared with those obtained using flow or incremental theory. Figure 2.2 shows the percentage of error difference for various applied loads. The percentage of error difference is defined as the ratio of the difference between J from flow theory and J from deformation theory divided by J from flow theory, times 100. From this figure, it appears that prediction based on deformation theory is slightly conservative, with the maximum absolute error being less than 1 percent. Hence, the deformation theory can be used adequately for the rest of finite element analysis. This will allow significant savings of computational effort in determining the GE/EPRI functions.

Activity 1.4.3 Analyze Through-Wall Cracks in Welds

In this activity, efforts were undertaken to (1) conduct TWC pipe weld analysis of two pipe experiments from the past Degraded Piping Program (Ref. 2.3) and (2) compare predictive results with the available pipe fracture data.

Pipe Weld Experiments - Two circumferential through-wall-cracked (TWC) pipe experiments identified as Experiments 4141-1 and 4141-5 (Ref. 2.4) were considered. The stainless steel pipes were of 152 mm (6-inch) nominal pipe size and were subject to four-point bending at 288 C (550 F) without internal pressure. The crack lengths in both experiments were nearly 37 percent of the pipe circumference in the center of a SAW. Both welds were made at the same time. The only difference is that in Experiment 4141-5 the weld was solution-annealed. Table 2.1 provides exact dimensions of the pipe geometry and the results of welded pipe experiments.

J-Estimation Analyses - Five predictive J-estimation schemes were used to evaluate the load-carrying capacity of the TWC welded pipes in Experiments 4141-1 and 4141-5. They include:

(1) GE/EPRI method (Ref. 2.1),
(2) Paris/Tada method (Ref. 2.5),
(3) LBB.NRC method (Ref. 2.6),
(4) LBB.ENG2 method (Ref. 2.7), and
(5) LBB.ENG3 method (Ref. 2.8).

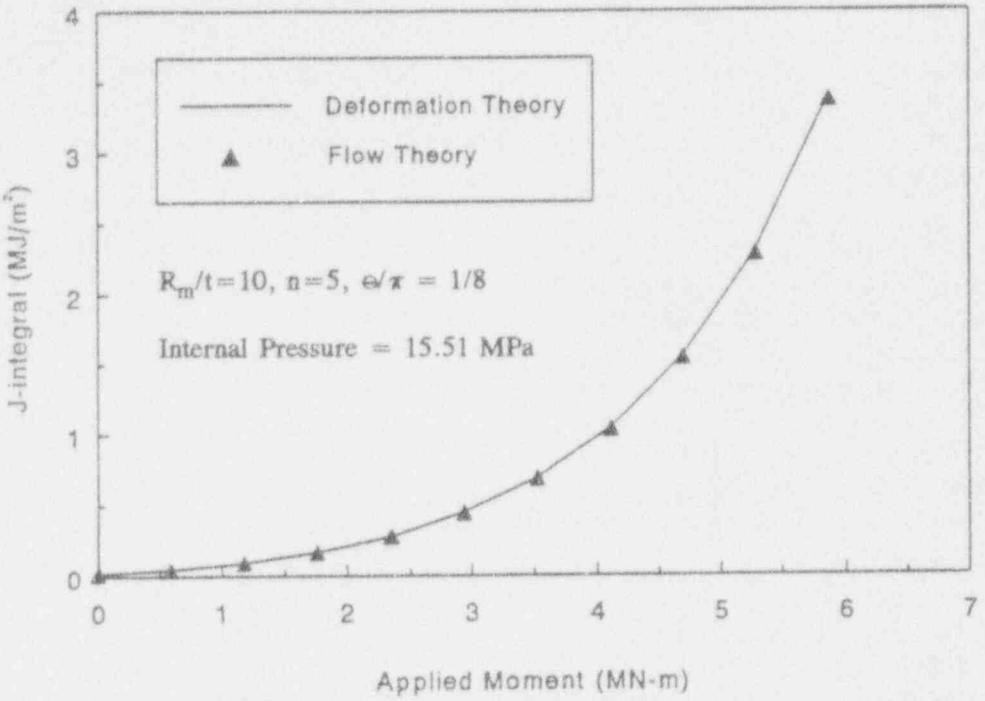

Figure 2.1 J-integral by deformation and flow theories as a function of applied bending moment

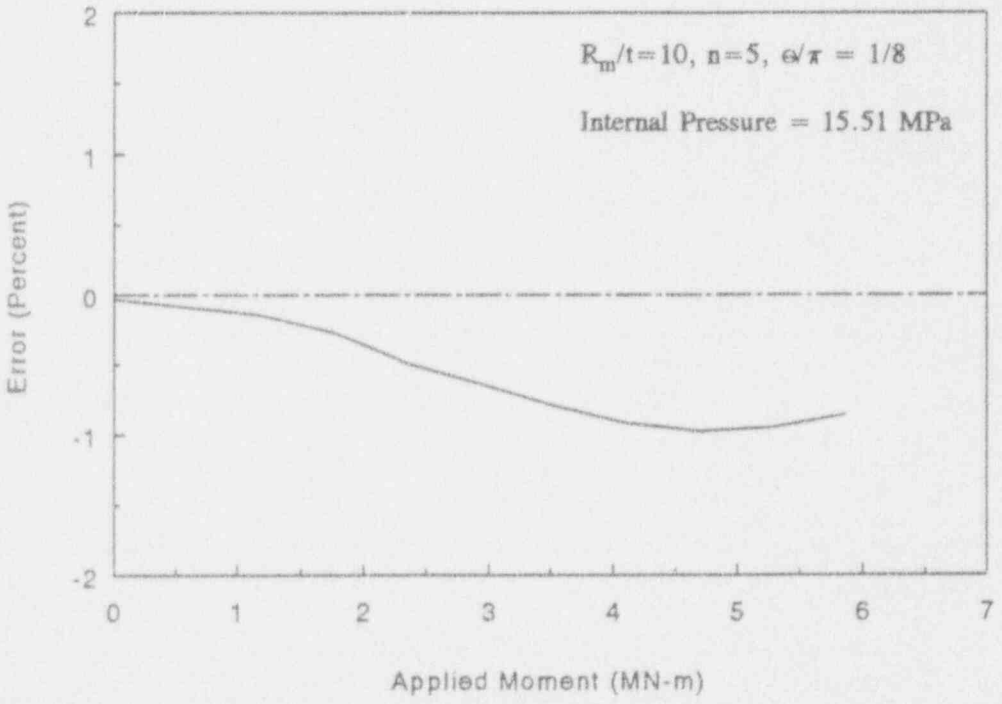

Figure 2.2 Percentage of error difference between J-integral estimates by deformation theory of plasticity

Table 2.1 Summary of pipe geometry and results for through-wall-cracked weld metal pipe experiments

	Experiment Number	
	4141-1	**4141-5**
Material	SA-376 TP304	SA-376 TP304
Weld Type	SAW	Solution-Annealed SAW
Average Outside Diameter, mm (in)	168.3[a] (6.625)	167.8 (6.605)
Average Measured Wall Thickness, mm (in)	14.3[a] (0.562)	14.1 (0.555)
Crack Length, percent circumference	37.1	38.3
Four-point Bending Inner Span, m (in)	1.2 (48)	1.2 (48)
Four-point Bending Outer Span, m (in)	3.25 (128)	3.25 (128)
Load at Crack, kN (lbs)	58.3 (13,100)	46.3 (10,400)
Maximum Load, kN (lbs)	73.8 (16,600)	60.5 (13,600)

[a]Nominal dimension

All estimation methods except LBB.ENG3 (this is a tentative acronym given here for the LBB.ENG2 method modified during this program to include the weld metal strength) are based on stress-strain properties of base metal and toughness properties of weld metals. The LBB.ENG3 method can account for strength properties of both base and weld metals in calculating the J-integral. Details of this method can be obtained from Reference 2.8. This method, which was developed during the course of this program, was also discussed in the second semiannual report from this program (Ref. 2.9).

In order to make the estimation methods applicable, it is assumed that the stress-strain curves of base or weld metals can be represented by the well-known Ramberg-Osgood model. Four samples of base metal stress-strain data and two samples of weld metal stress-stain data at test temperature were

Table 2.2 Material properties of base and weld metals in pipe Experiments 4141-1 and 4141-5

Material	Yield Stress, σ_y MPa	Ultimate Stress, σ_u MPa	α[(a)]	n
Base[(b)]	138.18	449.10	9.694	3.129
Weld (As-welded)	324.00	466.00	2.283	11.033
Weld (Solution-annealed)	194.00	465.00	3.420	4.838

(a) $\sigma_o = \sigma_y$, $\epsilon_o = \sigma_o/E$, E = 182.7 GPa (26,500 ksi).
(b) Base metal stress-strain curve unaffected by solution annealing.

available for pipe materials in each of these two experiments. A standard curve fit was developed to determine the corresponding Ramberg-Osgood parameters using the program ROFIT. Table 2.2 shows the mean values of the Ramberg-Osgood parameters for the base and the weld metals. The reference stress required for the Ramberg-Osgood fit was assumed to be the yield stress also given in the same table. The solution-annealing was found to not affect the base metal stress-strain curve. The J_D-resistance curves were obtained from compact tension, C(T), specimens and η-factor analysis based on pipe experimental load-displacement curves. Hence, two sets of analyses were performed. One was based on C(T) J_D-resistance curves and the other was based on pipe J_D-resistance curves. The C(T) specimens were from 25.4-mm (1.0-inch) thick plate welds, whereas the 6-inch nominal diameter pipe was much thinner. The fracture toughness curves for both cases are shown in Figure 2.3. Solution-annealing lowered the weld yield strength by 40 percent and slightly raised the toughness in C(T) specimen tests. However, comparison with fracture toughness values from η-factor analyses of TWC pipes indicates a lowering of J-resistance curves due to solution annealing; i.e., the opposite trend from the C(T) specimen J-R curves.

Results - An internal research version of the code NRCPIPE was used to compute crack initiation and maximum loads of the pipes in Experiment 4141-1 and 4141-5. This version of the code has recently been changed to incorporate the LBB.ENG3 method for welded pipe analysis. Figure 2.4 shows the initiation load ratio, defined as the ratio of the experimental crack initiation load to the predicted crack initiation load, for Experiments 4141-1 and 4141-5 obtained from five different J-estimation schemes using C(T) specimen J_D-resistance curves. From the results, it appears that all of the estimation methods except Paris/Tada significantly underestimate the crack initiation loads of both the as-welded pipe (Experiment 4141-1) and the solution-annealed pipe (Experiment 4141-5) when compared with test data. However, the underprediction of the initiation load becomes smaller for the solution-annealed pipe, in which case the strength properties of base and weld metals are not too different. The initiation load calculated by the Paris/Tada method is closer to the experimental value although the predictive error was made on the side of overpredicting loads.

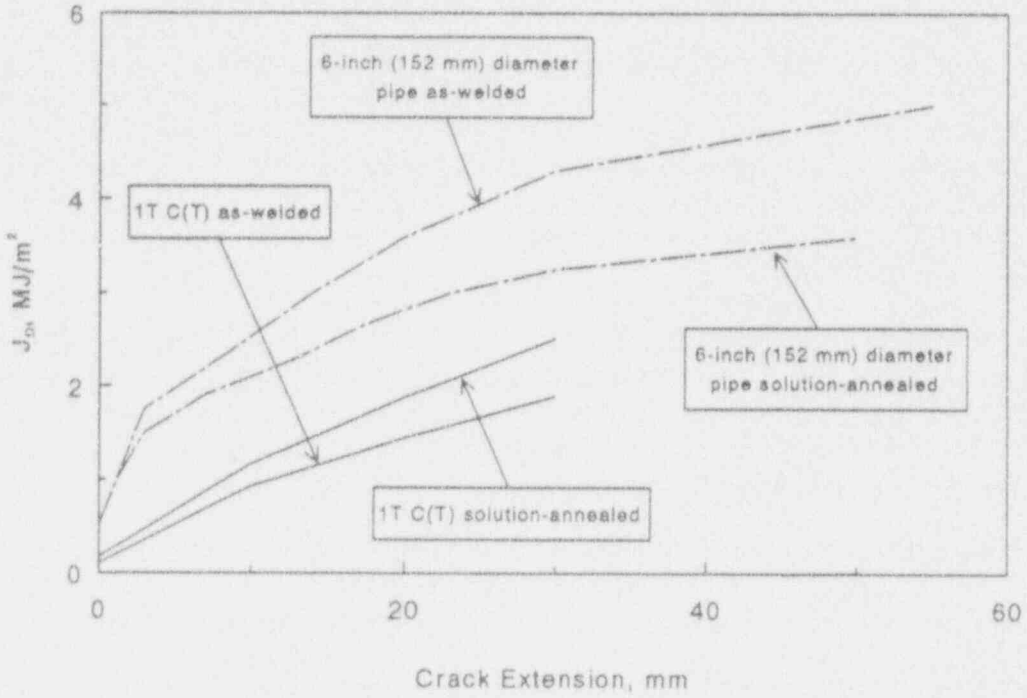

Figure 2.3 Comparison of pipe and C(T) specimen J_D-R curves from η-factor analysis

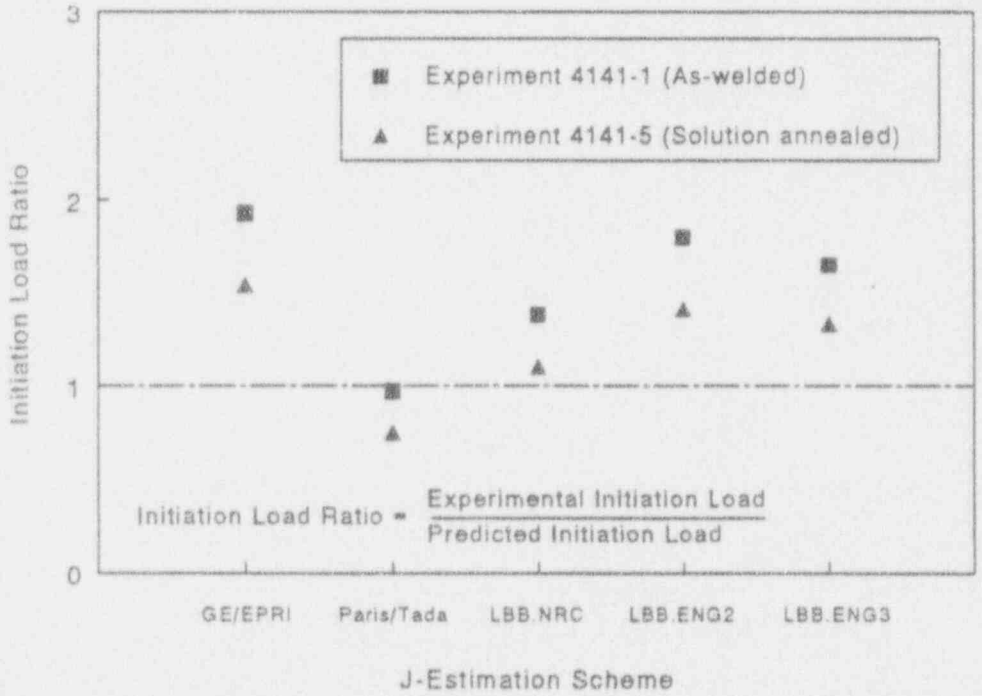

Figure 2.4 Initiation load prediction for the Experiments 4141-1 and 4141-5 using C(T) J_D-R curves

Similar results are also plotted for the same pipe experiments (Experiments 4141-1 and 4141-5) in Figure 2.5 in terms of the maximum load ratio, defined as the ratio of the experimental maximum load to the predicted maximum load as a function of the estimation methods. Results indicate that most estimation methods underpredict the experimental maximum load. As before, the degree of underprediction for the solution-annealed pipe is much less than that calculated for the as-welded pipe. The Paris/Tada method, which provided better results for the as-welded pipe, was found to overestimate load-carrying capacity for the solution-annealed pipe.

The LBB.ENG3 method, which uses strength properties of both base and weld metals, did not provide the anticipated accuracy in calculating initiation and maximum loads. However, in both experiments, the degree of conservatism by LBB.ENG3 lies between that calculated by LBB.ENG2 and GE/EPRI and that calculated by Paris/TADA and LBB.NRC. All these results were predicted by using C(T) specimen J_D-resistance curves.

In order to evaluate the adequacy of C(T) specimen data for J_D-resistance curves, standard η-factor analyses were conducted by using the load-displacement record from actual pipe experiments. The η-factor analysis is described in a topical report (Ref. 2.4) and will not be repeated here. From the

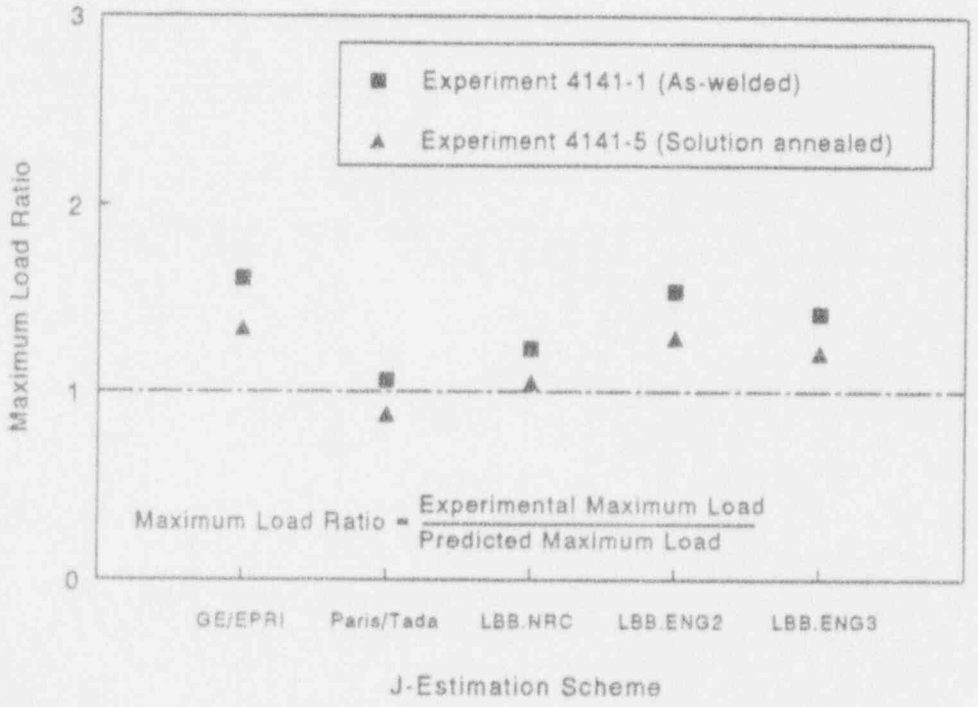

Figure 2.5 Maximum load prediction for the Experiments 4141-1 and 4141-5 using C(T) J_D-R curves

same report, the pipe J_D-resistance curves were obtained for both as-welded and solution-annealed pipes (see Figure 2.3). Using these pipe J_D-resistance curves, the estimation analyses were conducted again to determine the initiation and maximum load ratios in Experiments 4141-1 and 4141-5. They are shown in Figures 2.6 and 2.7, respectively.

Comparisons of the results clearly show that (1) most estimation methods provide reasonably accurate load predictions and (2), among the five estimation methods considered here, LBB.ENG3 is the most accurate method to compute both the initiation and maximum loads of as-welded and solution-annealed pipes when the fracture toughness properties are generated from large-scale pipe tests. Note Discrepancies between the pipe and C(T) specimen J-R curve arise in part because the C(T) specimens came from 25.4-mm (1-inch) thick plate and the pipes were 14.2 mm (0.56 inches) thick. Both welds had two layers of TIG weld metal (a tough weld) and the balance being SAW (low toughness). Hence the thicker weld used for the C(T) specimens had a higher percentage of low-toughness weld metal than the nominal 6-inch diameter pipe test welds.

Activity 1.4.4 Develop New GE/EPRI Functions

Short Through-Wall-Cracked Pipe Under Tension

This activity involves three-dimensional finite element analyses to define the GE/EPRI F, V, and h functions for short through-wall cracked (θ/π = 1/8 and θ/π = 1/16) pipe subjected to remote tension.

During this reporting period, all analyses required in this activity were completed. Table 2.3 shows the matrix of finite element calculations that were performed. See Reference 2.1 for all appropriate definitions for the GE/EPRI method. For the far-field displacement due to the crack (V_2, h_3), the displacement is defined at the center of the uncracked pipe. The precise definition of the displacement is not clear in Reference 2.1, and our results for displacement are quite different from those given in Reference 2.1.

Table 2.4 shows the F and V functions obtained from the ABAQUS analysis (tension-elastic). Tables 2.5, 2.6, and 2.7 show the fully plastic h functions (tension) for several n values.

2.4 Plans for Next Year of the Program

2.4.1 Subtask 1.4 Analyses for Short Through-Wall Cracks in Pipes

There are four activities in this subtask. The current status and future plans for these activities are given below.

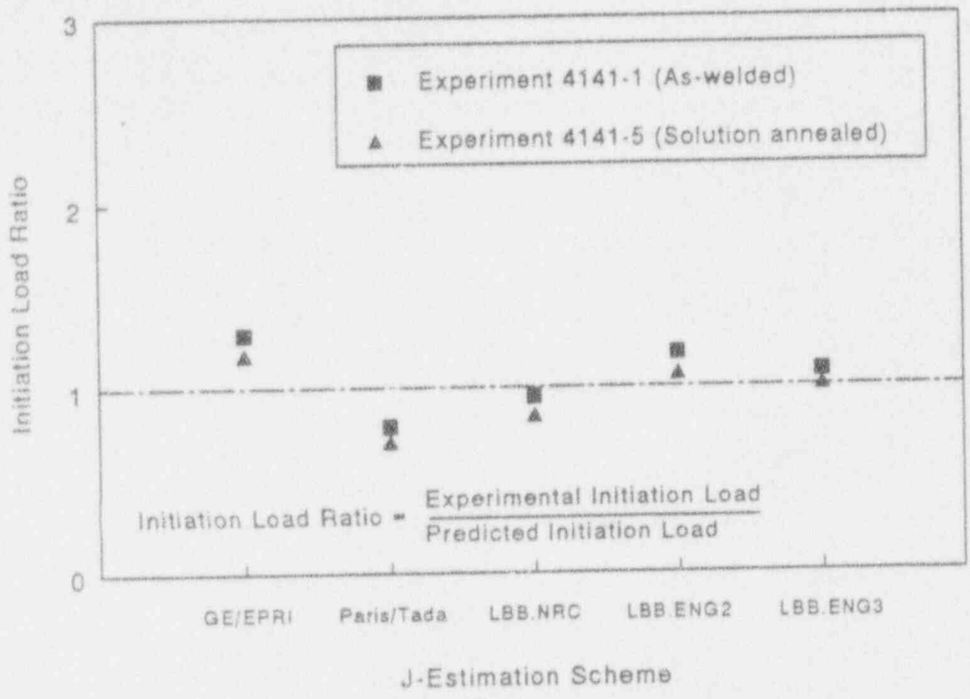

Figure 2.6 Initiation load prediction for Experiments 4141-1 and 4141-5 using pipe J_D-R curves from η-factor analyses

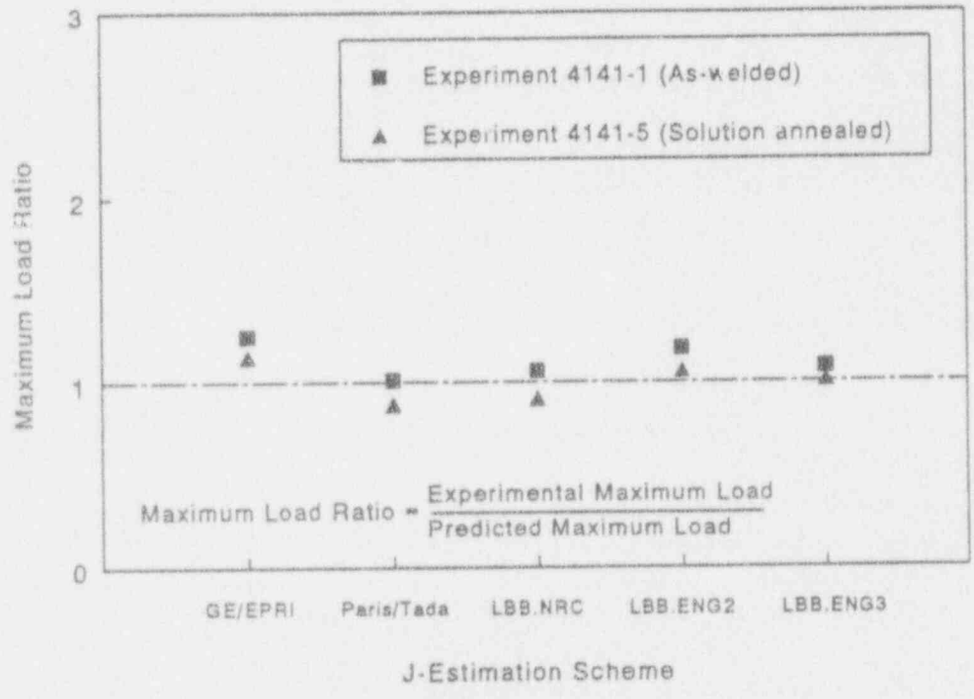

Figure 2.7 Maximum load prediction for Experiments 4141-1 and 4141-5 using pipe J_D-R curves from η-factor analyses

Table 2.3 Matrix of finite element calculations for circumferentially through-wall-cracked pipe under tension

Model No.	Model Name	R_m/t	n[(a)]	θ/π	Remarks
1	CASE1A3DTN	5	1,2,3,5,7,10	0.0625	6 runs
2	CASE1B3DTN	5	1,2,3,5,7,10	0.125	6 runs
3	CASE2A3DTN	10	1,2,3,5,7,10	0.0625	6 runs
4	CASE2B3DTN	10	1,2,3,5,7,10	0.125	6 runs
5	CASE3A3DTN	20	1,2,3,5,7,10	0.0625	6 runs
6	CASE3B3DTN	20	1,2,3,5,7,10	0.125	6 runs

(a) n is the power-law hardening exponent and n = 1 for the elastic case.

Table 2.4 ABAQUS calculated values for F, V_1, V_2, and V_3 for a circumferentially through-wall-cracked cylinder in tension

		θ/π = 0.0625	θ/π = 0.125
R_m/t = 5	F	1.027	1.139
	V_1	1.178	1.359
	V_2	0.164	0.363
	V_3	0.021	0.086
R_m/t = 10	F	1.053	1.250
	V_1	1.186	1.482
	V_2	0.186	0.436
	V_3	0.020	0.099
R_m/t = 20	F	1.107	1.469
	V_1	1.258	1.719
	V_2	0.229	0.591
	V_3	0.023	0.116

Table 2.5 ABAQUS calculated values for h_1, h_2, h_3, and h_4 for a circumferentially through-wall-cracked cylinder in tension ($R_m/t = 5$)

		n = 1	n = 2	n = 3	n = 5	n = 7	n = 10
$\theta/\pi = 1/16$	h_1	2.707	3.385	3.825	4.301	4.332	4.093
	h_2	4.125	4.775	5.068	5.307	5.124	4.664
	h_3	0.564	2.608	3.166	4.187	3.035	2.983
	h_4	0.072	0.126	0.181	0.273	0.332	0.368
$\theta/\pi = 1/8$	h_1	2.638	3.087	3.269	3.210	2.817	2.159
	h_2	4.092	4.376	4.351	3.990	3.368	2.495
	h_3	1.092	2.248	2.648	3.041	2.622	2.157
	h_4	0.259	0.402	0.505	0.597	0.569	0.455

Table 2.6 ABAQUS calculated values for h_1, h_2, h_3, and h_4 for a circumferentially through-wall-cracked cylinder in tension ($R_m/t = 10$)

		n = 1	n = 2	n = 3	n = 5	n = 7	n = 10
$\theta/\pi = 1/16$	h_1	2.849	3.624	4.162	4.827	5.003	4.902
	h_2	4.152	4.896	5.313	5.776	5.762	5.471
	h_3	0.650	2.697	3.249	4.290	3.188	3.244
	h_4	0.069	0.123	0.175	0.271	0.337	0.392
$\theta/\pi = 1/8$	h_1	3.176	3.809	4.130	4.223	3.836	3.062
	h_2	4.459	4.931	5.065	4.893	4.309	3.349
	h_3	1.314	2.512	2.961	3.477	3.151	2.737
	h_4	0.298	0.462	0.587	0.722	0.720	0.605

Table 2.7. ABAQUS calculated values for h_1, h_2, h_3, and h_4 for a circumferentially through-wall-cracked cylinder in tension ($R_m/t = 20$)

		n = 1	n = 2	n = 3	n = 5	n = 7	n = 10
$\theta/\pi = 1/16$	h_1	3.148	4.119	4.843	5.848	6.263	6.399
	h_2	4.406	5.341	5.949	6.765	6.998	6.934
	h_3	0.802	2.958	3.607	4.815	3.806	3.983
	h_4	0.074	0.141	0.202	0.317	0.399	0.484
$\theta/\pi = 1/8$	h_1	4.384	5.394	5.983	6.300	5.784	3.485
	h_2	5.173	5.999	6.412	6.547	5.941	4.749
	h_3	1.778	3.242	3.912	4.738	4.428	3.911
	h_4	0.350	0.570	0.743	0.953	0.976	0.852

Activity 1.4.1(a) - Numerically assess the effect of plastic ovalization on the validity of J. This activity is essentially complete and writing the final topical report will be the only activity next year.

Activity 1.4.1(c) - Improve F, V, and h functions. The efforts for calculating GE/EPRI functions for TWC pipe under combined bending and tension have been started. They will be completed in the next year of the program.

Activity 1.4.2 - The new GE/EPRI functions developed in this program will be used to analyze large-diameter TWC pipe tests. The analysis will be completed in the next year of this program.

Activity 1.4.3 - Analyze through-wall cracks in welds. The efforts in analyzing welded pipe experiments from the Degraded Piping Program have been completed. The weld experiments conducted in this program will be analyzed in the next year.

Activity 1.4.4 - The GE/EPRI functions for the following cases will be completed in the next period:

(i) Short Through-Wall-Cracked Pipe Under Tension and Bending

(ii) Long Through-Wall-Cracked Pipe Under Bending

All work planned in this subtask will be completed. The first draft of the topical report will be written and submitted to the NRC for review.

2.5 References

2.1 Kumar, V., German, M. D., and Shih, C. F., "An Engineering Approach to Elastic-Plastic Fracture Analysis," Electric Power Research Institute Report, NP-1931, 1981.

2.2 ABAQUS, User's Guide and Manual, Version 5.0, Hibbit, Karlsson & Sorensen, 1993.

2.3 Wilkowski, G. M., and others, "Degraded Piping Program-Phase II," Summary of Technical Results and Their Significance to Leak-Before-Break and In-Service Flaw Acceptance Criteria, March 1984 - January 1989, Battelle, NUREG/CR-4082, Vols. 1-8, 1985-1989.

2.4 Wilkowski, G. M., and others, "Analysis of Experiments on Stainless Steel Flux Welds," Topical Report, NUREG/CR-4878, April 1987.

2.5 Paris, P. C. and Tada, H., "The Application of Fracture Proof Design Methods Using Tearing Instability Theory to Nuclear Piping Postulating Circumferential Through-Wall Cracks," NUREG/CR-3464, September 1983.

2.6 Klecker, R., and others, "NRC Leak-Before-Break (LBB.NRC) Analysis Method for Circumferentially Through-Wall-Cracked Pipes Under Axial Plus Bending Loads," NUREG/CR-4572, February 1987.

2.7 Brust, F. W., "Approximate Methods for Fracture Analyses of Through-Wall Cracked Pipes," Topical Report, NUREG/CR-4853, February 1987.

2.8 Rahman, S. and Brust, F. W., "An Approximate Method for Evaluating Energy Release Rates of Circumferential Through-Wall Cracked Pipe Welds," *Engineering Fracture Mechanics*, Vol. 43, No. 3, pp 417-430, 1992.

2.9 Wilkowski, G. M., and others, "Short Cracks in Piping and Piping Welds," Second Semiannual Report by Battelle, NUREG/CR-4599, Vol. 1, No. 2, April 1992.

3. TASK 2 SHORT SC PIPE EVALUATIONS

3.1 Task Objective

The objective of this task is to modify and verify analyses for short surface-cracked (SC) pipe using existing and new data on large-diameter pipe.

3.2 Task Rationale

These results will verify and may be used to refine analyses that have been used for pragmatic in-service flaw evaluations such as those in ASME Section XI.

3.3 Task Approach

The five subtasks in this task are:

Subtask 2.1	Material characterization for surface-cracked pipe experiments
Subtask 2.2	Small-diameter pipe fracture experiments in pure bending for limit-load ovalization correction
Subtask 2.3	Large-diameter surface-cracked pipe fracture experiments under combined bending and tension (pressure)
Subtask 2.4	Analysis of short surface cracks in pipes
Subtask 2.5	Topical report.

During the last reporting period, Subtasks 2.1, 2.3, and 2.4 were active. Subtask 2.2 is complete and results are in prior semiannual reports. Progress in the active subtasks is described below.

3.3.1 Subtask 2.1 Material Characterization for Surface-Cracked Pipe Experiments

3.3.1.1 Objective

The objective of this activity is to generate the data necessary to document material strength and toughness for analysis of the Subtask 2.3 Pipe Fracture Experiments.

3.3.1.2 Rationale

The material property data needed for the analysis procedures in Subtask 2.4 need to be determined for each pipe and weld subjected to a pipe fracture experiment. These data are also to be included in the NRC PIFRAC database (Ref. 3.1).

3.3.1.3 Approach

With several exceptions, material property data for pipes tested within the Short Crack Program, i.e., Charpy, chemical analyses, tensile, and J-R curves, are already available from the Degraded Piping Program.

One exception is a nominal 16-inch-diameter Schedule 30 stainless steel pipe that replaced the pipe damaged in the accident associated with the IPIRG-1 Experiment 1.3-7. This replacement pipe has been designated DP2-A52.

Another exception is a nominal 24-inch-diameter carbon-steel pipe weld used in Subtask 2.3. Instead of having tests conducted on specimens machined from the welded pipe, material characterization tests have been performed on welds prepared in A516 Grade 70 carbon steel plate material, using welding procedures nominally identical to those used in welding the pipe.

The data are recorded digitally and reduced to a format identical to that used in past Degraded Piping Program Data Record Book entries. These data will also be available for input into the NRC PIFRAC database (Ref. 3.1).

3.3.1.4 Progress

Plate Weld DP2-F49W. Characterization of Pipe DP2-F49W was completed. This weld was made using a C-Mn-Mo weld procedure. Babcock and Wilcox used it in most of their carbon steel plant piping. The weld wire designation was EA3 and SFA 5.23. The flux was Linde 80. Figure 3.1 is a composite J-R curve graph showing the results for all compact specimens. This figure shows the significant effect of test temperature on fracture resistance of the weld. The room temperature specimens had about 0.5 mm (0.02 inch) of stable ductile crack growth prior to cleavage fracture. The average value of J_i at 288 C (550 F) was approximately sixty percent of the room temperature average, while dJ/da averaged one quarter or one third of the room temperature values, depending on side grooving. Side grooving decreased J_i by approximately five percent and decreased dJ/da by approximately 30 percent in this material.

Pipe DP2-A52. Fracture toughness and tensile experiments on Pipe DP2-A52 were also completed. Figure 3.2 shows the J-resistance curves for material from this pipe. There is a small decrease in both J_i and dJ/da between 20 C and 93 C. However, both quantities decrease significantly between 93 C and 288 C.

3.3.2 Subtask 2.3 Large-Diameter Surface-Cracked Pipe Fracture Experiments Under Combined Bending and Tension (Pressure)

3.3.2.1 Objective

The objective of this subtask is to develop experimental data for internally surface-cracked large-diameter pipe under more typical combined pressure and bending loading conditions for the purpose of making a critical assessment of the ASME Section XI and J-estimation scheme analyses.

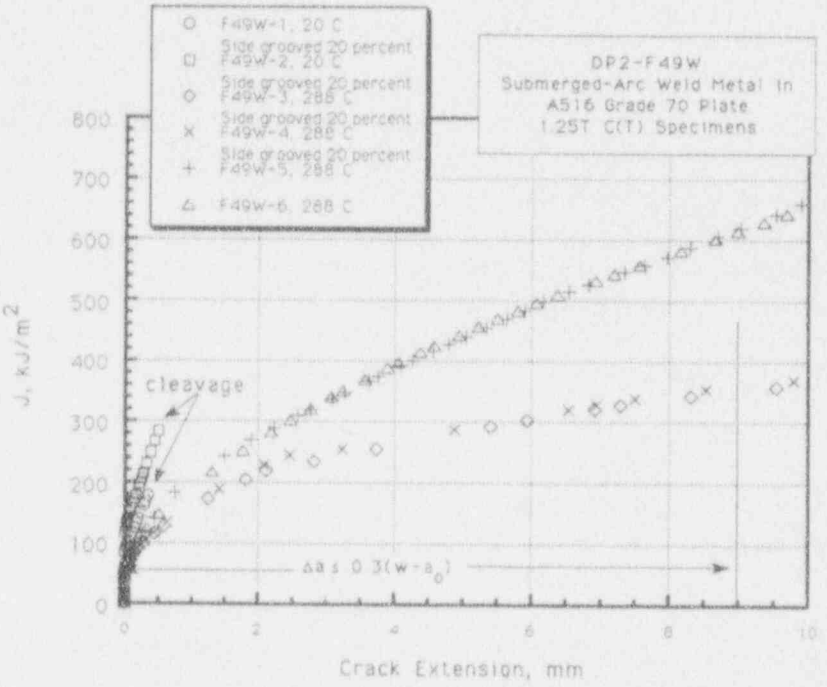

Figure 3.1 Composite plot of J-resistance curves for Plate Weld DP2-F49W tests (Data with $\Delta a \leq 0.3(w-a_0)$ are believed to be valid as per Ref. 3.2)

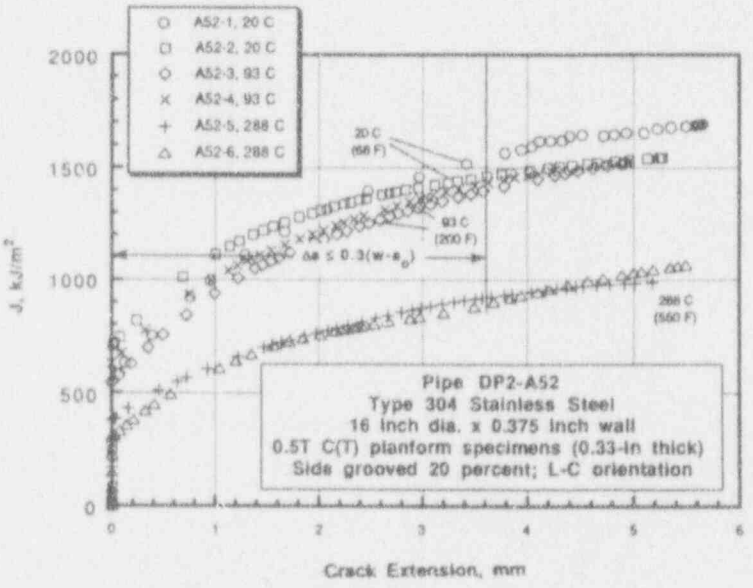

Figure 3.2 Composite plot of J-resistance curves for Plate Weld DP2-A52 (Data with $\Delta a \leq 0.3(w-a_0)$ are believed to be valid as per Ref. 3.2)

3.3.2.2 Rationale

With one exception, the largest surface-cracked pipe experiments conducted as part of the Degraded Piping (Ref. 3.3), IPIRG (Ref. 3.4), and EPRI NP-2347 (Ref. 3.5) programs were 16-inch diameter. The one exception was a 30-inch-diameter carbon steel surface-cracked pipe experiment conducted as part of the IPIRG program. Consequently, a definite void exists in the pipe fracture experimental data base. Since pipe diameter is an important governing parameter in assessing failure mode, i.e., limit-load or elastic-plastic, it seems prudent to fill this void. The effects of larger diameter on the fracture behavior of surface-cracked pipe needs to be evaluated in order to make a critical evaluation of the ASME Section XI and J-estimation scheme analyses.

3.3.2.3 Approach

To satisfy the data requirement for verifying the analysis methods, three large-diameter surface-cracked pipe fracture experiments will be conducted, see Table 3.1.

Table 3.1 Test matrix for large-diameter surface-cracked pipe experiments

Expt. No.	Nominal Diameter	Schedule	Material	Test Temp.	Test Pressure	$2c/\pi D_m$	d/t
1.2.3.15	28-inch	60	A515 Gr 60	288 C (550 F)	9.56 MPa (1,387 psi)	0.25	0.5
1.2.3.16	28-inch	80	TP316L SAW	288 C (550 F)	10.14 MPa (1,470 psi)	0.25	0.5
1.2.3.17	24-inch	100	A106B SAW	288 C (550 F)	TBD	0.25	0.5

TBD = To be determined.

3.3.2.4 Progress

During the last reporting period efforts were initiated to prepare the test specimen for the nominal 24-inch diameter, carbon steel weld, short surface-cracked pipe experiment (Experiment 1.2.3.17). The test pipe for this experiment was from a length of A106 Grade B carbon steel pipe tested in a previous Battelle program in the late 1960's for the Atomic Energy Commission (AEC) (Ref. 3.6). Data are already available from this AEC program for three elevated temperature, axially flawed, pipe burst tests. In addition, material characterization data are available; i.e., circumferential tensile (yield and ultimate strength values), transverse Charpy, and chemical analyses. The wall thickness of this pipe is approximately 43 mm (1.7 inch). This wall thickness is greater than that for any pipe

tested to date with a short surface crack. The test weld to be used is the same Babcock and Wilcox (B&W) low toughness C-Mn-Mo weld procedure used in Experiment 1.1.1.24 of this program, see Section 3.3.1 of this report.

3.3.3 Subtask 2.4 Analysis of Short Surface Cracks in Pipes

The objective of this subtask is to develop, improve, and verify the engineering analyses for short circumferential surface-cracked large-diameter pipe where elastic-plastic fracture is expected.

3.3.3.2 Rationale

The short surface-cracked (SC) pipe analysis improvements are aimed at assessing and improving the ASME Section XI flaw evaluation criteria (Refs. 3.7 and 3.8).

3.3.3.3 Approach

The ten activities in this subtask are:

Activity 2.4.1 Uncracked pipe analysis
Activity 2.4.2 Improve SC.TNP and SC.TKP analyses
Activity 2.4.3 Compare improved limit-load solutions with short surface-cracked small-diameter pipe data
Activity 2.4.4 Analyze large-diameter surface-cracked pipe test data
Activity 2.4.5 Evaluate procedures in J-estimation schemes for surface cracks in welds.
Activity 2.4.6 Extend SC.TNP and SC.TKP for external surface-crack geometries under combined loading
Activity 2.4.7 Uncracked SS pipe mesh refinement
Activity 2.4.8 Surface-cracked mesh refinement study
Activity 2.4.9 SC J-estimation verification.
Activity 2.4.10 New GE-EPRI function for 360-degree surface cracked pipe

3.3.3.4 Progress

During the last reporting period, Activities 2.4.2, 2.4.7, 2.4.8, and 2.4.10 were active. The progress in these activities is reported below.

Activity 2.4.2 Improve SC.TNP and SC.TKP Analyses

In this activity, several different η-factor analyses on surface-cracked pipe were independently reviewed and re-derived. Several discrepancies between these analyses were found. Once these are resolved, the analysis of the SC pipe experiments will be completed and included in the next semiannual report.

Activity 2.4.7 Uncracked Pipe Mesh Refinement

Since the efforts in Activities 2.4.1 and 2.4.6 are related, progress in the two are reported together.

The FE analysis of JAERI pipe Experiment S-17, Ref. 3.9, showed that a full 3-D analysis rather than mesh refinement resolved the descrepancy between the experiment data and FE analysis conducted earlier. A comparison of the predicted to the experimental load-displacement curve is shown in Figure 3.3 In light of this result, it is not necessary to pursue further mesh refinement studies. The objectives of this subtask are, therefore, accomplished. These results will be included in the topical report for Task 2.

Subtasks 2.4.1 and 2.4.7 are therefore completed, and no further work is planned.

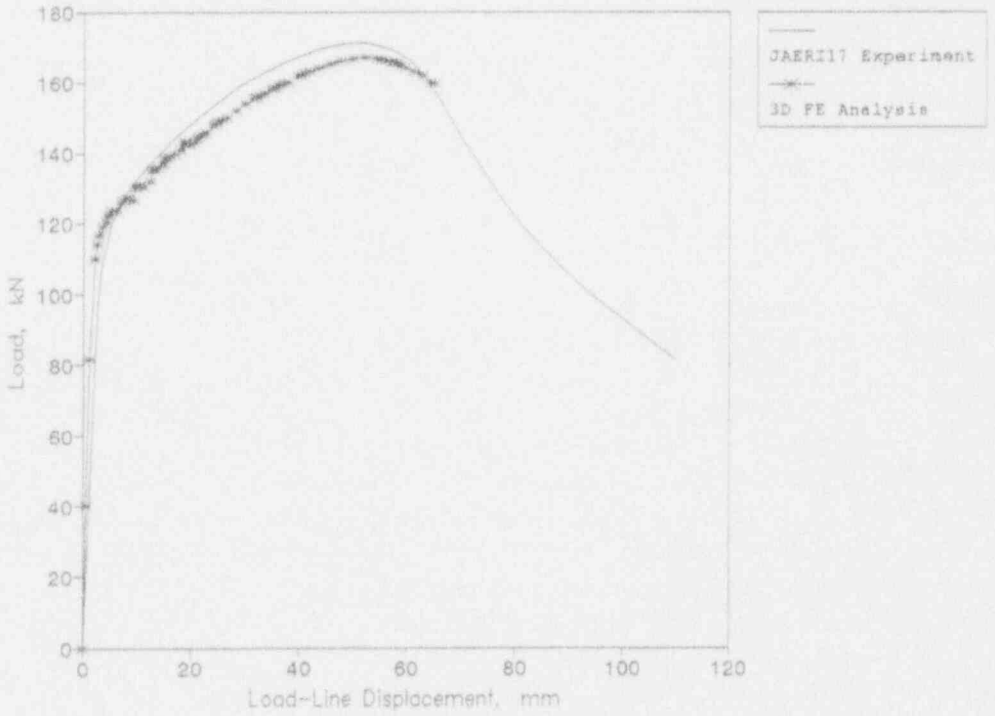

Figure 3.3 Uncracked pipe FE analysis

Activity 2.4.8 Surface-Cracked Mesh Refinement Study

To accurately compute the crack tip fields and J-integral values for surface-cracked pipes using finite element analyses, sufficient care must be taken to ensure adequate refinement of the mesh. Recent work by Shimakawa and Yagawa (Ref. 3.10) has shown that mesh refinement, load increments and material modeling can strongly influence the finite element solutions. In the following, a critical examination of the effect of mesh refinement on finite element solutions for circumferentially surface-cracked pipe loaded under 4-point bending is made using the commercially available software program ABAQUS. A fan-like mesh focussed at the crack-tip is employed in all cases, since this yields more accurate solutions for quasi-static crack problems. There are three levels of mesh refinement which may be examined, namely, refinement along the thickness direction of the cracked and uncracked ligaments, refinement along the crack front direction, and refinement along the

circumferential direction of the fan-like mesh focussed at the crack tip. Since the most critical location in circumferentially surface-cracked pipes is at the deepest point of the flaw, the mesh refinement examined in this task was confined to the thickness direction of the crack and remaining ligament of the pipe.*

Mesh refinement in circumferentially surface-cracked pipes loaded under 4-point bending was examined using three 3-D finite element meshes. All of these meshes used 8-noded brick elements and had the same refinement along the crack front, which was modeled with 13 elements. Mesh 1 consists of eight elements along the crack and seven elements along the ligament. Figure 3.4(a) shows Mesh 1 and Figure 3.4(b) shows a magnified view of the cracked region. The detail of the crack tip region at the center of the crack front is shown in Figure 3.4(c). The size of the smallest element at the crack tip in Mesh 1 is 0.0508 mm (0.002 inch). Mesh 1 may be considered as a moderately refined model. Mesh 2 was a coarser model than Mesh 1, consisting of only five elements along the crack and four along the ligament. Details of the crack tip region at the center of the crack front for Mesh 2 are shown in Figure 3.5. Mesh 3 was a more refined model than Mesh 1, consisting of 14 elements along the crack and 13 elements along the ligament; details of the crack tip for Mesh 3 are shown in Figure 3.6.

Elasto-plastic simulations of a surface-cracked pipe experiment (4112-8) have been carried out using the aforementioned three 3-D finite element models and a shell finite-element model with the crack being modeled with line-spring elements. The stress-strain behavior of the material is shown in Figure 3.7. The predicted variation of load versus load-line displacement using all the models is compared with the experimentally measured variation in Figure 3.8. The difference between the predictions of various models is negligible. This is not surprising since the load point, being sufficiently far away from the crack, is relatively unaffected by details of crack-tip refinement. The difference between the predicted and measured values increases beyond a load-line displacement of 95.25 mm (3.75 inches). The predicted load at crack initiation is more than 9 percent higher than the measured load.

The calculated J-integral versus load-point displacement is shown in Figure 3.9. Although, the various models showed little difference in the variation of load versus load-point displacement (see Figure 3.8), they exhibit notable difference in the variation of J-integral values with load-point displacement. The calculated values of J-integral for the three 3-D finite element meshes were almost path-independent. However, a ± 10 percent variation of J-integral values between various contours was observed in the case of Mesh 2 (coarser mesh), while a ± 5 percent variation of J-integral values between various contours was observed for Meshes 1 and 3. This is expected in light of more refinement of the crack tip region in Meshes 1 and 3. The applied load-line displacement was achieved in eight time steps (moderate increments) for Meshes 1 through 3. The analysis was repeated with more time steps (fine increments) for Meshes 2 and 3. The reason for this will be explained later.

*In all the cases the crack was modeled with a fan-like mesh with uniform grading in the circumferential direction (giving an angular resolution of 22.5 degrees and with geometrically increasing radial grading with varying number of rings for each mesh).

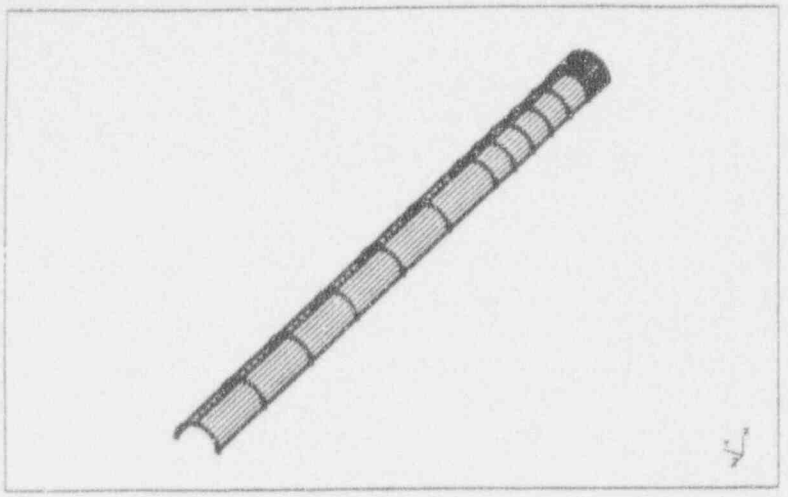

(a)

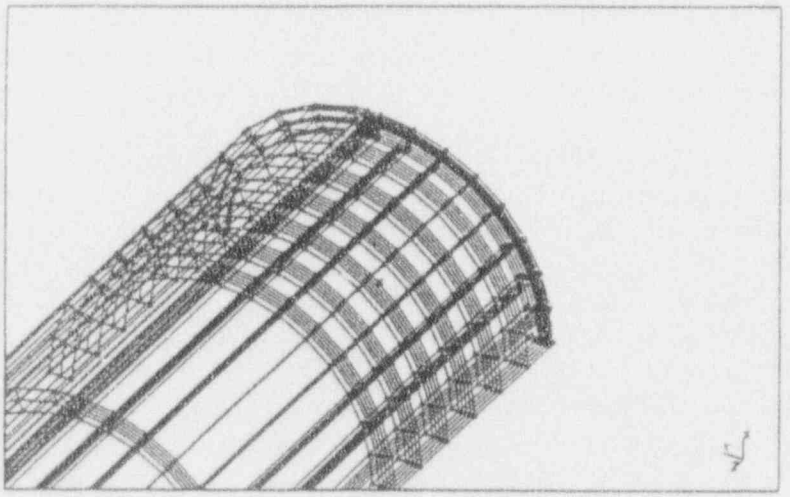

(b)

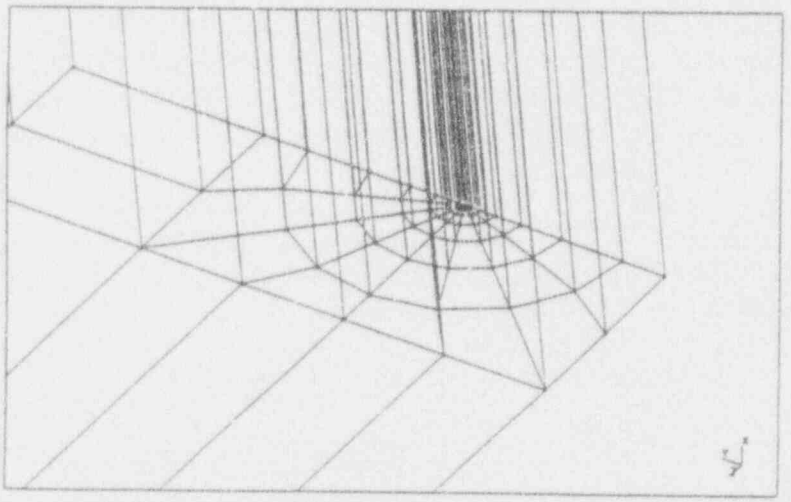

(c)

Figure 3.4 Finite element model (Mesh 1) of surface-cracked pipe (intermediate mesh size)

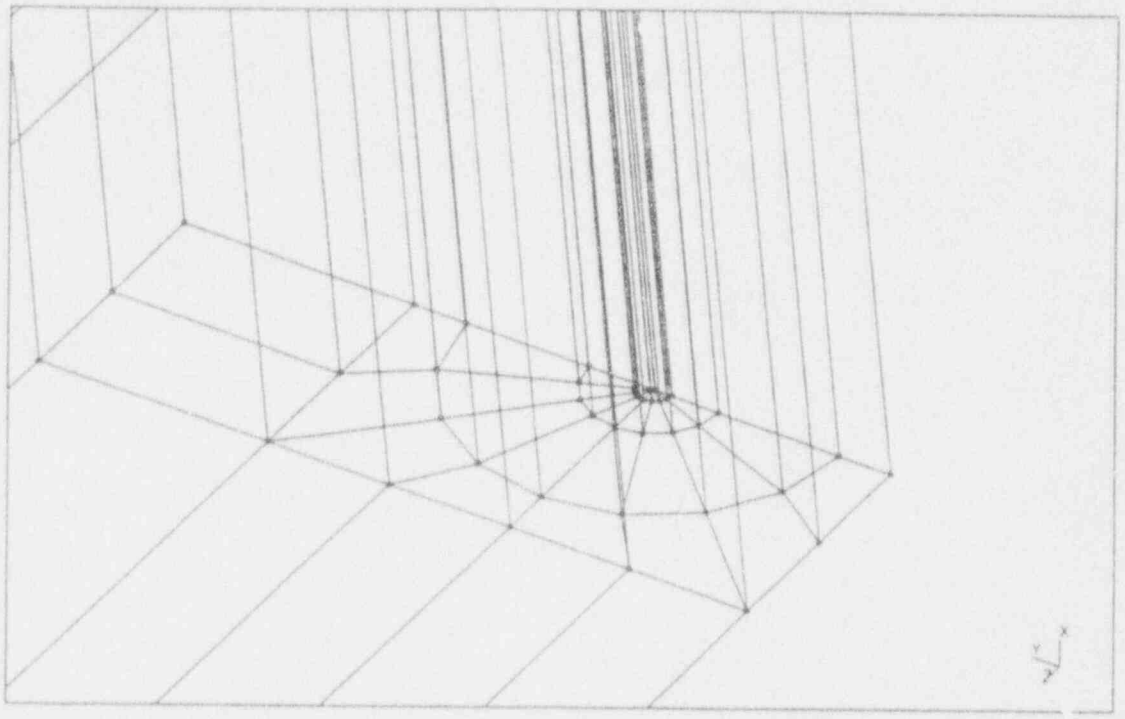

Figure 3.5 Detail of the crack-tip region at the center of the crack front for Mesh 2 (coarsest mesh size)

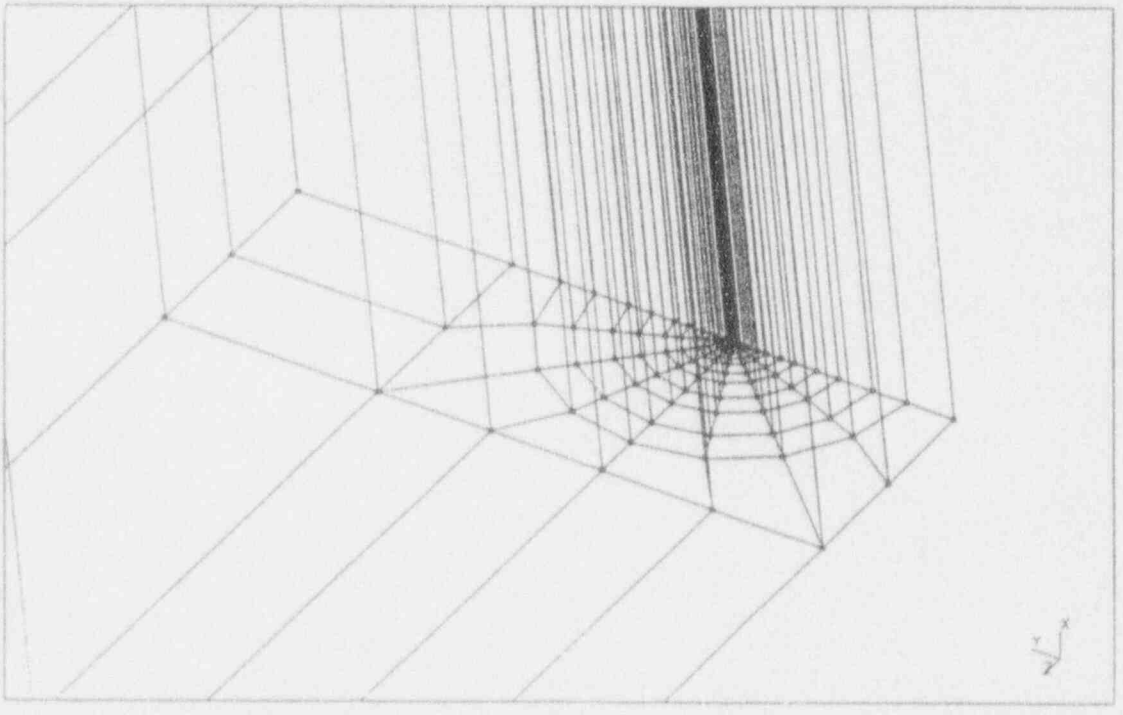

Figure 3.6 Detail of the crack-tip region at the center of the crack fron for Mesh 3 (finest mesh size)

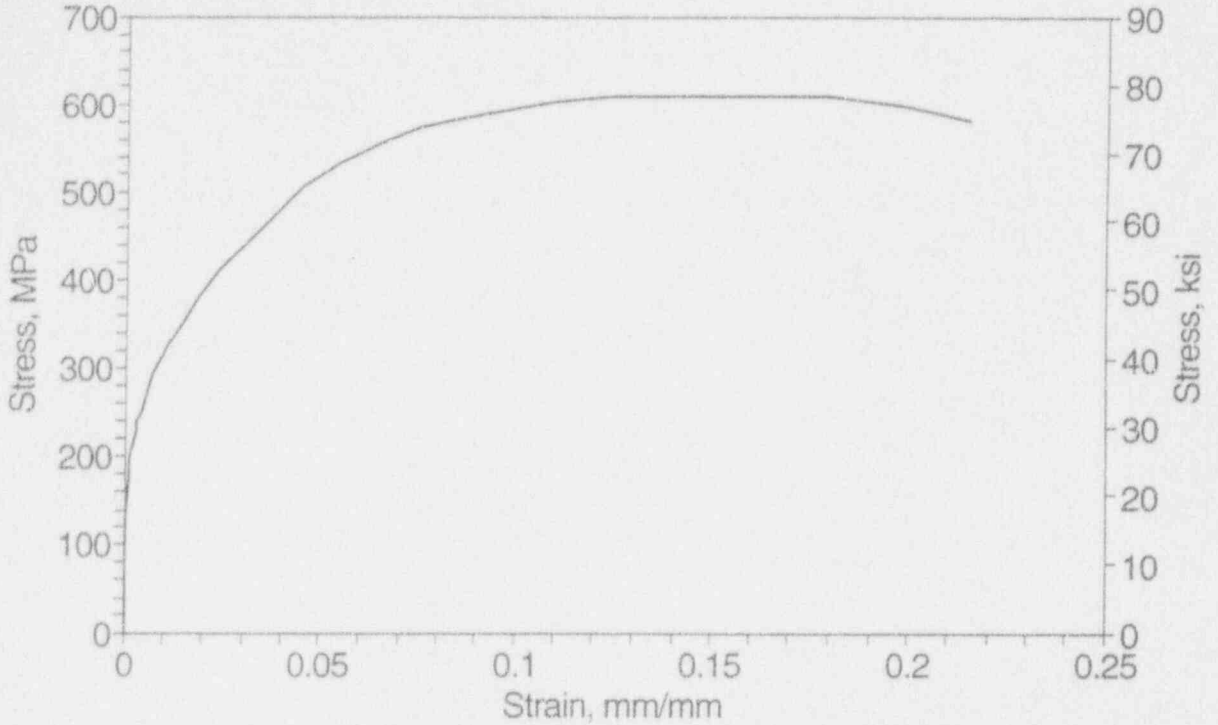

Figure 3.7 Stress-strain behavior of the material (average of data from Specimens F29-5 and F29-6)

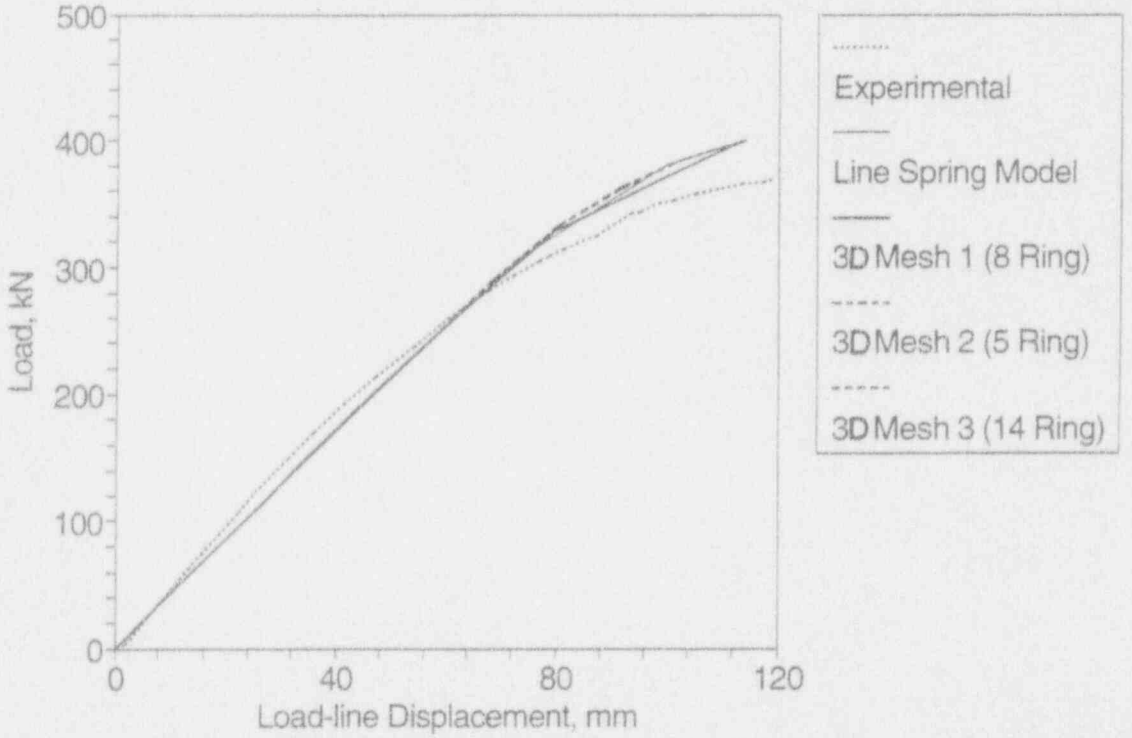

Figure 3.8 Predicted and experimentally measured variation of load versus load-line displacement of surface-cracked pipe

Several conclusions may be inferred from Figure 3.9. Below load-line displacement values of 95.25 mm (3.75 inch) the difference in predicted values of J-integral is less than 6 percent between various models. However, the differences become more noticeable beyond this value of load-line displacement. The line-spring model predicts the highest values of J-integral and, hence, is more conservative in its estimate of loads for a given J. The coarse mesh (Mesh 2) with moderate time increments predicts lower values of J-integral compared with Meshes 1 and 3. Interestingly enough, Meshes 1 and 3 predict similar J-integral values, implying that Mesh 1 is optimum for this analyses. To further investigate this, finer displacement increments were used for Meshes 2 and 3. The reason for using finer displacement increments for Mesh 2 was to explore whether the predicted J-integral values would be closer to the predictions of Mesh 1. If this were true, then a coarser mesh such as Mesh 2 with fine displacement increments would be adequate for the analysis. However, the predicted values of J with finer increments using Mesh 2 still diverged from the solution obtained from Mesh 1. Thus, using only five elements along the crack is not adequate for analysis of surface-cracked pipe.

To further reinforce our argument that the solutions obtained with Meshes 1 and 3 are indeed convergent solutions, Mesh 3 was used to analyze this problem with finer displacement increments. The predicted variation of J-integral values with load-line displacement using finer increments with Mesh 3 yielded similar results as Mesh 1. Thus, using at least eight elements along the crack and at least seven elements along the ligament is necessary for analyzing surface-cracked pipe subjected to 4-point bending.

This conclusion is further supported by the effect of mesh refinement on the crack-mouth-opening displacement, CMOD. Figure 3.10 shows the variation of CMOD with applied load-line displacement. As is evident from the figure, nearly identical variations are obtained for Meshes 1 and 3. As expected, the variation obtained using the coarser mesh (Mesh 2) deviates from those obtained by the other two meshes, especially at higher values of applied load-line displacement. The crack-mouth-opening configuration at the center of the crack front corresponding to a load-line displacement of 114.3 mm (4.5 inches) obtained using the various finite element meshes is shown in Figure 3.11. The prediction of the coarser mesh is less conservative than those of the other two meshes.

3.4 Plans for Next Year of the Program

3.4.1 Subtask 2.1 Material Characterization for Surface-Cracked Pipe Experiments

The material characterization data for Plate Weld F49W will be completed and submitted for inclusion in the NRC PIFRAC database (Ref. 3.1) in order to complete this task.

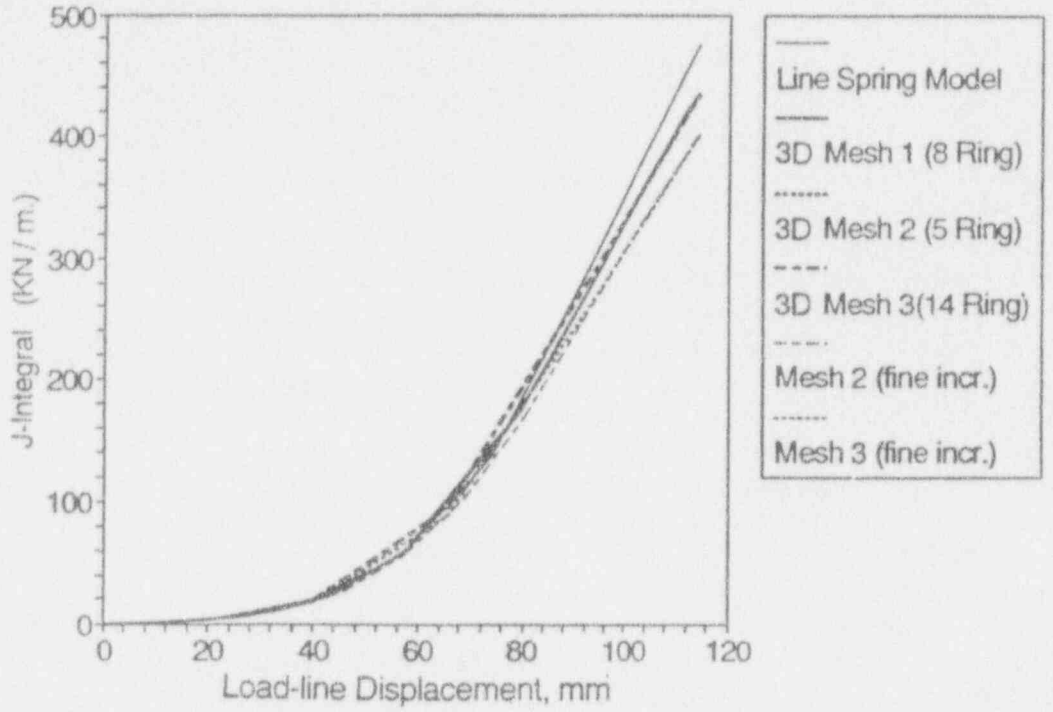

Figure 3.9 Variation of calculated J-integral values versus load-line displacement for the various models studied

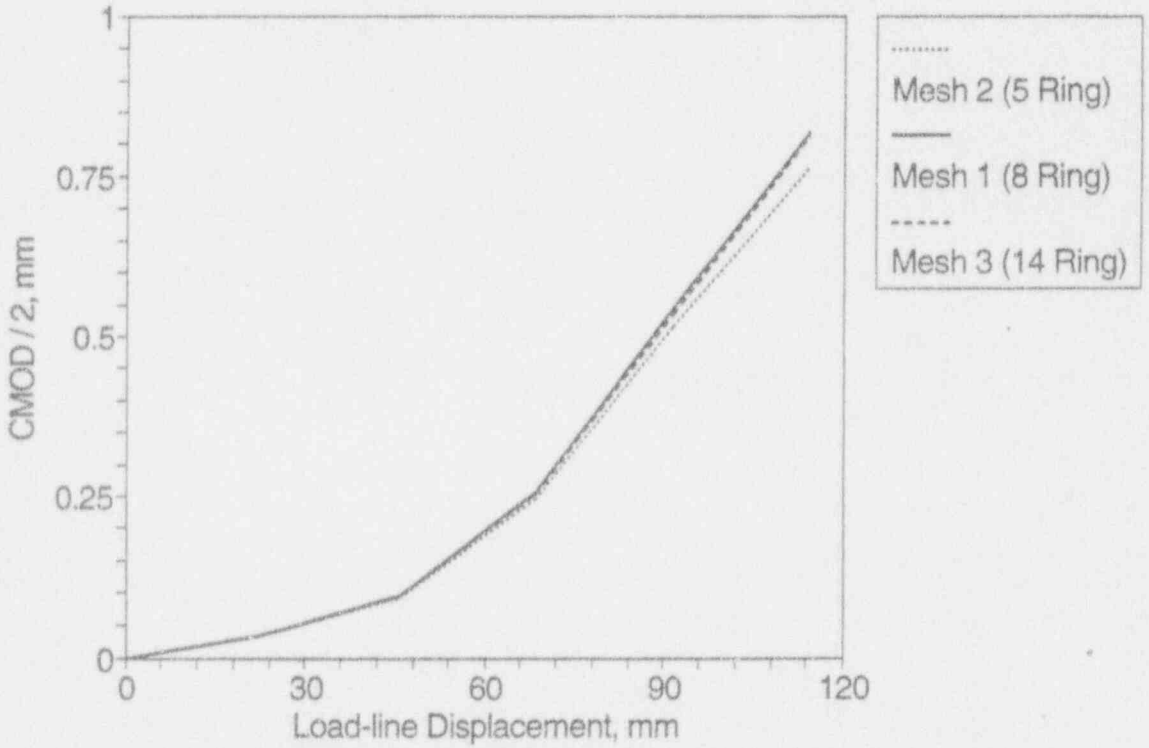

Figure 3.10 Variation of crack-mouth-opening displacement with applied load-line displacement for the various models studied

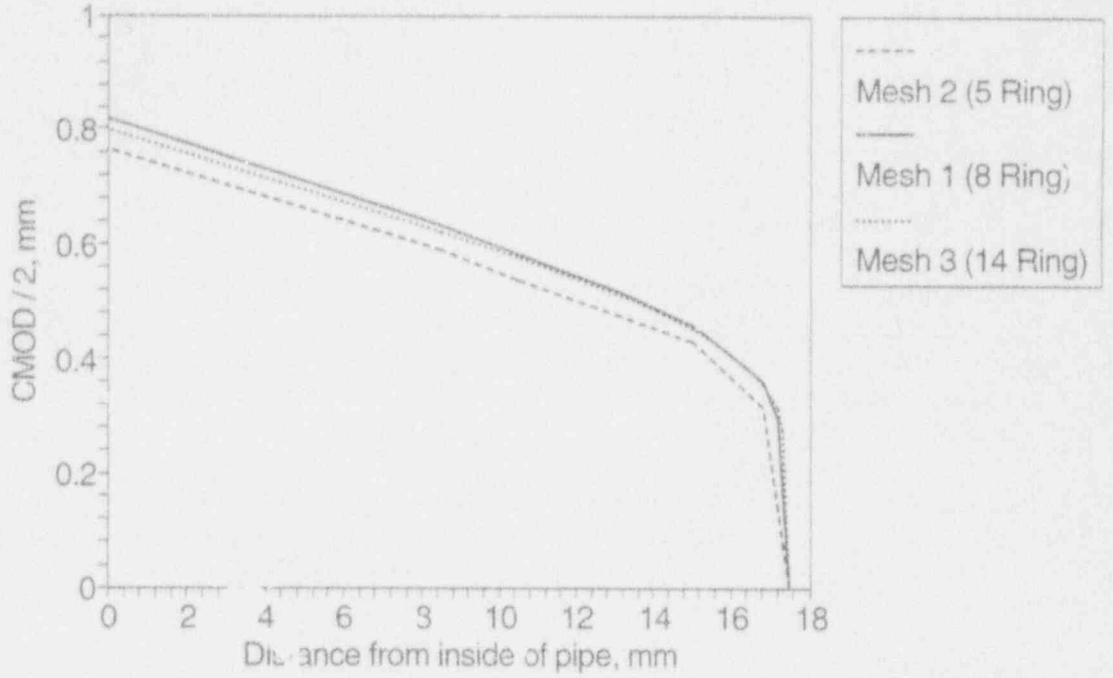

Figure 3.11 Crack-opening configuration at the center of the crack front corresponding to a load-line displacement of 114.3 mm (4.5 inches)

3.4.2 Subtask 2.3 Large-Diameter Surface-Cracked Pipe Fracture Experiments Under Combined Bending and Tension (Pressure)

During the next reporting period work will continue towards preparing the test specimen for the 24-inch diameter, carbon steel weld, short surface crack pipe experiment (Experiment 1.2.3.17). The initial machine flaw will be introduced into the center of the low toughness C-Mn-Mo weld and precracked using pressure cycling techniques. The internal surface crack will be instrumented with crack opening displacement gages and electric potential probes. Once the internal instrumentation is in place, lengths of moment arm pipe will be welded onto the test specimen in preparation for testing.

3.4.3 Subtask 2.4 Analysis of Short Surface Cracks in Pipes

Activities 2.4.1, 2.4.6, 2.4.7 and 2.4.10 have been completed. Plans for other activities will involve the following.

Activity 2.4.2 Improve SC.TNP and SC.TKP Analyses

Once the η-factor analysis discrepancy is resolved, the η factor solutions will be compared to the 3-D FEM J values from the virtual crack extension method, and the η factor solution will be used to determine J values from several of the pipe experiments.

Activity 2.4.8 SC Mesh Refinement

This subtask has been completed. Input to the topical report will be prepared to summarize the findings of this study.

Activity 2.4.9 Verification of J-estimation Schemes

Work will be initiated on this subtask. Based on the work performed under the subtask on "SC Pipe Analysis - Mesh Refinement," results obtained using the line-spring model for surface-cracked pipes appeared accurate and adequate for comparison with J-estimation schemes. To further examine this, the analyses using line-spring and 3-D models of the surface-cracked pipe reported in Activity 2.4.7 will be extended to higher applied load levels.

If the line-spring model should prove to be adequate and accurate enough, all the following analyses would use this model. The following flaw geometries of circumferentially surface-cracked pipes loaded under bending, tension, and a combination of these two would be analyzed and compared with the SC.TNP and SC.TKP J-estimation scheme analyses.

Internal Surface Flaws

length/circumference	-	1/16 and 1/4
depth/thickness	-	1/2
strain-hardening exponent	-	3 and 10

External Surface Flaws

length/circumference	-	1/4
depth/thickness	-	1/2
strain-hardening exponent	-	3 and 10

3.5 References

3.1 Hiser, A. L. and Callahan, G. M., "A User's Guide to the NRC's Piping Fracture Mechanics Database (PIFRAC)," NUREG/CR-4894, May 1987.

3.2 G. M. Wilkowski, C. W. Marschall, and M. Landow, "Extrapolations of C(T) Specimens J-R Curves for Use in Pipe Flaw Evaluations", ASTM STP 1074, 1990, pp 56-84.

3.3 Wilkowski, G. M., and others, "Degraded Piping Program - Phase II," Summary of Technical Results and Their Significance to Leak-Before-Break and In-Service Flaw Acceptance Criteria, March 1984-January 1989, by Battelle Columbus Division, NUREG/CR-4082, Vol. 8, March 1989.

3.4 Schmidt, R. A., Wilkowski, G. M., and Mayfield, M. E., "The International Piping Integrity Research Group (IPIRG) Program - An Overview," SMiRT-11, Paper G12/1, August 1991.

3.5 Kanninen, M. F. and others, "Instability Predictions for Circumferentially Cracked Type 304 Stainless Steel Pipes under Dynamic Loadings," EPRI Report NP-2347, April 1982.

3.6 Eiber, R. J., Maxey, W. A., and Duffey, A. R., "Investigation of the Initiation and Extent of Ductile Pipe Rupture", Battelle Memorial Institute Report, BMI-1908, 1971.

3.7 "Evaluation of Flaws in Austenitic Steel Piping" (Technical basis document for ASME IWB-3640 analysis procedure), prepared by Section XI Task Group for Piping Flaw Evaluation, EPRI Report NP-4690-SR, April 1986.

3.8 American Society of Mechanical Engineers Boiler and Pressure Vessel Code, Section XI, Article IWB-3650, 1992 Edition, July 1, 1992. Published by American Society of Mechanical Engineers, New York, N.Y. 10017.

3.9 Yasuda, Y., et al., "Investigations on Ducitle Fracture Behavior of 3-Inch Diameter Type 304 Stainless Steel Pipe with a Circumferential Through-Wall Crack," JAERI-87-068, 1987.

3.10 Shimakawa, T., and Yagawa, G., "The Influences of Mesh Subdivision on Nonlinear Fracture Analyses for Surface-Cracked Structures," International Journal of Pressure Vessels and Piping, Vol. 45, 1991.

4. TASK 3 BIMETALLIC WELD EVALUATION

4.1 Task Objective

The objective of this task is to develop material property data and develop pipe fracture data necessary to assess current analytical engineering estimation schemes to assess the behavior of through-wall cracks in bimetallic welded pipe under bending.

4.2 Task Rationale

In nuclear piping systems, several bimetallic welds are used. Examples from Westinghouse reactors are hot and cold legs to the reactor pressure vessel and steam generators. In C.E. and B&W reactors, such welds include ferritic piping to cast stainless steel pump housings, as well as at several nozzle locations, and stainless steel pipe to BWR reactor pressure vessel nozzles. Such welds are difficult to fabricate and inspect. Because of differential thermal expansion stresses, these welds are subjected to additional service loads that welds between similar metals do not experience. Consequently, a more thorough evaluation of the fracture behavior of such welds is warranted.

4.3 Task Approach

There are four subtasks in this task. These are:

Subtask 3.1 Material characterization of a bimetallic weld
Subtask 3.2 Conduct pipe experiment
Subtask 3.3 Analysis of pipe test
Subtask 3.4 Topical report.

Only Subtasks 3.1 and 3.3 were active during this reporting period.

4.3.1. Subtask 3.1 Material Characterization for Bimetallic Weld Evaluation

4.3.1.1 Objective

The objective of this subtask is to conduct experiments characterizing material in the bimetallic welded pipe designated DP2-F33.

4.3.1.2 Rationale

A more thorough evaluation is required of the components of bimetallic welds because such welds are known to exist in nuclear piping systems and their fundamental fracture behavior is poorly characterized.

4.3.1.3 Approach

Test specimens are fabricated from the bimetallic weld in DP2-F33, a 36-inch diameter, cold-leg, carbon steel pipe that included a Type 316 stainless steel safe end that was welded using stainless steel filler metal. Tensile specimens for 288 C (550 F) tests were prepared from the stainless steel weld metal and both Charpy V-notch impact specimens and 2T compact tension specimens for 288 C (550 F) tests were prepared so that the crack would grow circumferentially along the carbon steel/weld metal fusion line. A total of four compact specimens will be tested; two will be fatigue precracked and two will contain a sharp-machined notch, the latter to simulate the notch that is expected to be used in a subsequent pipe test.

Compact tension specimens (1T) also are being machined from the Type 316 stainless steel portion of the bimetallic weld in Pipe DP2-F33. In addition to their use for characterizing the stainless steel portion of the bimetallic weld, the J-R curves from this material will be used for comparison with slant-notch C(T) specimens that are to be tested in Subtask 8.2 of Task 8.

4.3.1.4 Progress

Microhardness traverses were made on the bimetallic weld in Pipe DP2-F33. The weld metal was found to be harder by 15 to 20 Rockwell B points than the carbon steel base metal. In terms of ultimate tensile strength, the weld metal is approximately 160 to 240 MPa (23 to 35 ksi) stronger than the carbon steel. Knoop microhardness traverses near the carbon steel/weld metal fusion line were made in order to obtain higher resolution of distance and revealed that the hardness of the carbon steel increases as the fusion line is approached but then shows a slight decrease just before reaching the fusion line. The narrow region of decreased hardness is associated with the heat-affected zone of the weld, which extends from the fusion line approximately 1 to 2 mm (0.04 to 0.08 inch) into the carbon steel.

In the process of fabricating the Charpy specimens from the bimetal weld fusion line, it was discovered that one of the longitudinal slices from which the specimens were to be machined contained a repair weld. Figure 4.1 is a photograph that illustrates the repair weld. From the etching pattern on the surface of the cross section, it is evident that the weldment was gouged from both the inside and outside and additional filler metal added. Because the repair welds were not immediately adjacent to the carbon steel/weld metal fusion line, it was assumed that the properties at the bimetal fusion line were not affected by the repair welds.

The Charpy V-notch impact specimen results are shown in Table 4.1. Only one of the six specimens (Specimen No. 3) fractured completely and it displayed the lowest energy absorption value. Each of the five remaining specimens exhibited pronounced splitting in which the crack turned away from the fusion line and grew into the carbon steel nearly perpendicular to the intended crack growth direction. This splitting precluded complete fracture and resulted in the unusually high energy absorption values shown in Table 4.1. Splitting is evident in the scanning electron photographs of the surface shown in Figures 4.2 and 4.3 for Specimen No. 4. Figure 4.2 shows that the crack initially grew in the carbon steel immediately adjacent to the fusion line from Arrow 1 to Arrow 2. It is also evident in

Table 4.1 Results of Charpy V-notch impact tests[a] at 288 C (550 F) on specimens from the bimetallic weld (DP2-F33W)

Specimen Number	Energy Absorbed, J (ft-lb)
1	220 (162)
2	259 (191)
3	178 (131)
4	301 (222)
5	266 (196)
6	256 (189)
Mean	247 (182)
Standard Deviation	42 (31)

(a) The notch was located in the heat-affected zone of the carbon steel, immediately adjacent to the fusion line; it was oriented such that the crack would grow circumferentially, i.e., the L-C orientation.

Figure 4.2 that the carbon steel was deformed more than the far-stronger weld metal, as indicated by the distinct step at the fusion line. Figure 4.3 shows that the crack turned away from the fusion line at Arrow 2 and grew toward Arrow 3. Several other splits can be seen as well in Figure 4.3. Charpy Specimen No. 4 was then sectioned along its midplane and etched to reveal the microstructure. Figure 4.4 shows the tip of one of the cracks, with no apparent preferred orientation that would cause the crack to travel along the path it took.

4.4 Plans for Next Year of the Program

4.4.1 Subtask 3.1 Material Characterization on Bimetallic Weld Evaluation

Data from the 1T C(T) stainless steel specimens will be reduced. In addition, the notched and precracked specimens with crack paths along the carbon-steel/weld fusion line will be tested and the data reduced. A topical report on bimetallic weld effects will be prepared at the conclusion of this task.

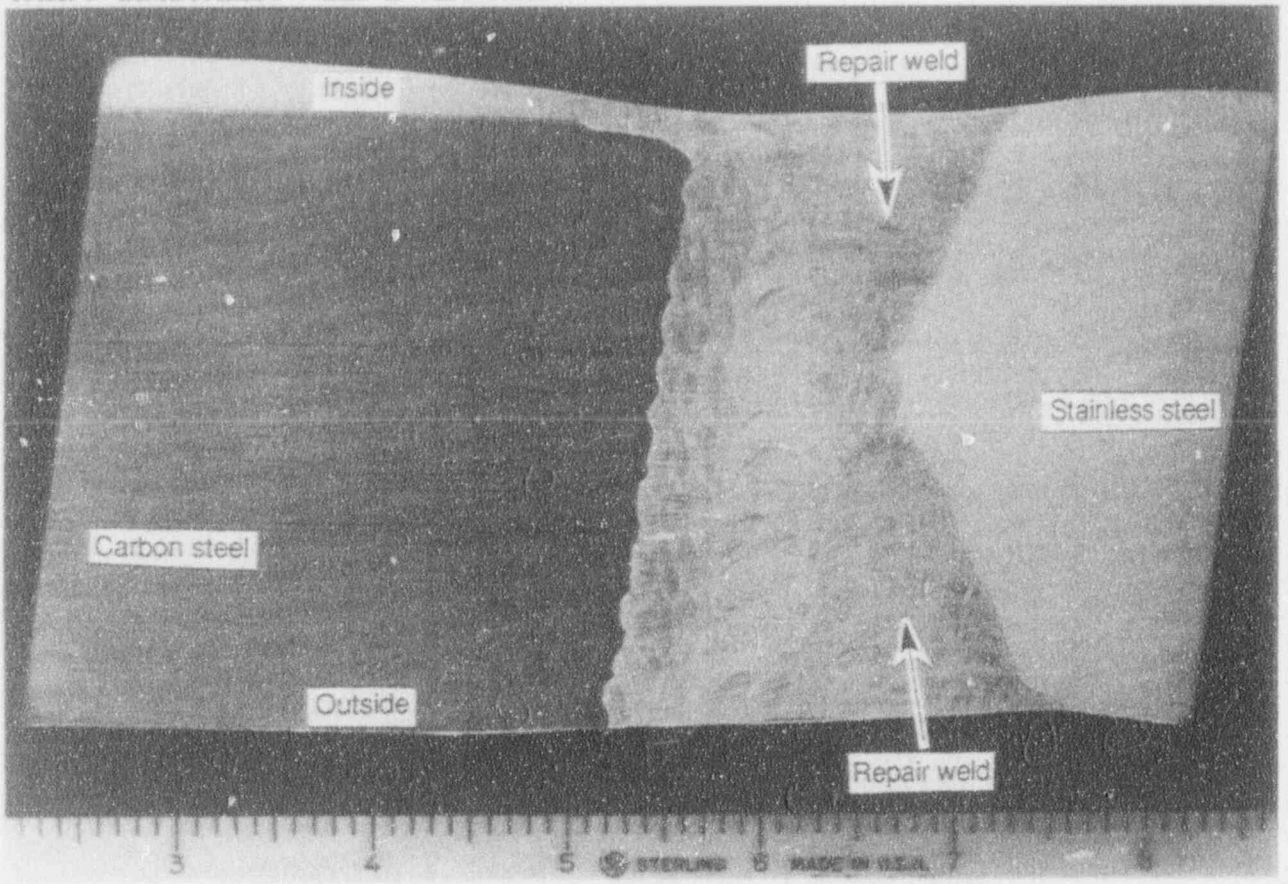

Figure 4.1 Photograph of bimetallic weld DP2-F33W

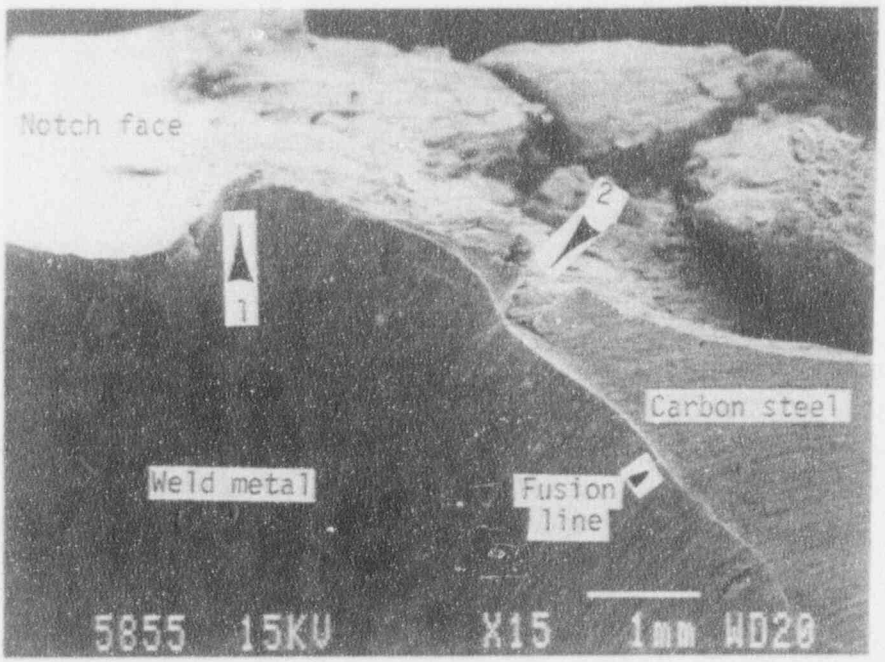

Figure 4.2 Photograph of tested SEM Charpy Specimen No. 4 showing first part of the fracture path in the carbon steel immediately adjacent to the weld

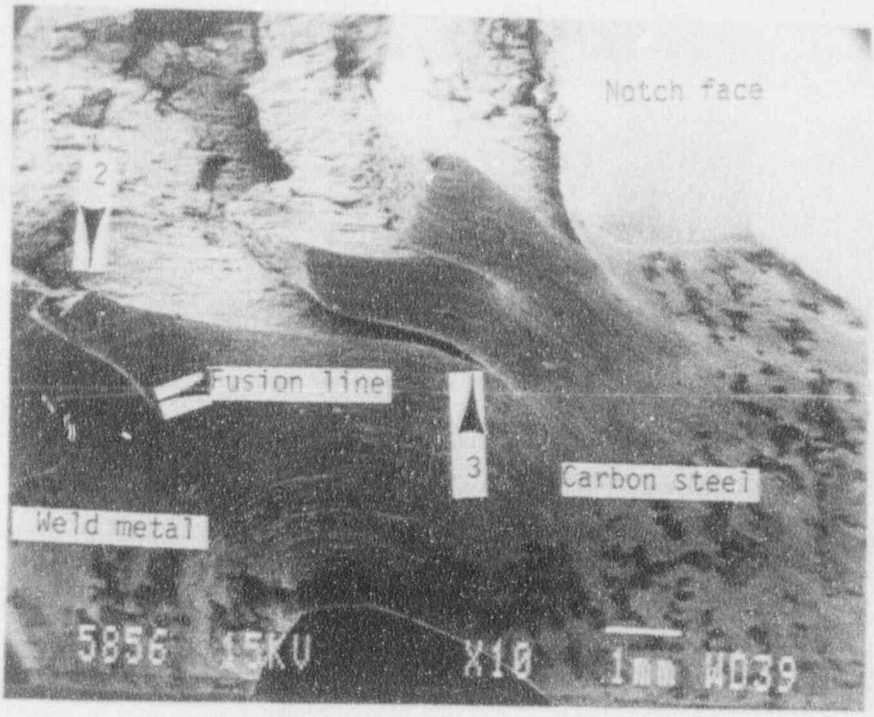

Figure 4.3 Photograph of SEM Charpy Specimen No. 4 showing crack veering away from the fusion line and into the carbon steel

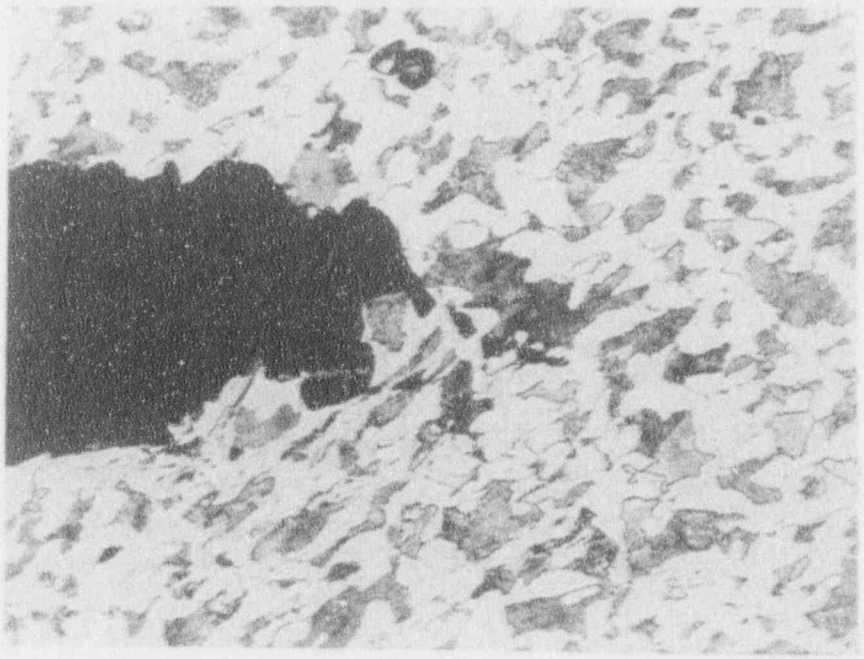

Figure 4.4 Photomicrograph of tip of crack in delamination of Charpy specimen of bimetallic weld DP2-F33

4.4.2 Subtask 3.2 Bimetallic Weld Pipe Experiments

During the next reporting period, the nominal 36-inch diameter, bimetallic weld, through-wall-cracked pipe experiment will be conducted. The initial through-wall crack will be 37 percent of the pipe circumference in length. This is the same flaw length as used in the Degraded Piping Program through-wall-cracked pipe experiments. The crack will be introduced at the fusion line of the ferritic base metal to the austenitic weld metal. Once the initial through-wall crack is introduced at the fusion line, the test specimen will be welded to the moment arm pipes, instrumented, and set up in Battelle's large pipe bend facility.

4.4.3 Subtask 3.3 Analysis of Pipe Test

Once the material property data are complete, the pipe test results will be predicted using the various J-estimation schemes with the carbon steel pipe and stainless steel safe-end base metal stress-strain curves, and the fusion line J-R curve.

5. TASK 4 DYNAMIC STRAIN AGING

5.1 Task Objective

The objective of this task is to evaluate and predict the effects of crack instabilities, believed to be due to dynamic strain aging (DSA), on the fracture behavior of pipe. Specific objectives are (1) to establish a simple screening criterion to predict which ferritic steels may be susceptible to unstable crack jumps, and (2) to evaluate the ability of current J-based analysis methodologies to assess the effect of unstable crack jumps on the fracture behavior of ferritic steel pipe. If necessary, alternative procedures for predicting pipe behavior in the presence of crack jumps will be derived.

5.2 Task Rationale

The methodology developed here will be applicable to both LBB and in-service flaw evaluations. It will also be valuable for selecting materials for future advanced reactor designs.

5.3 Task Approach

The four subtasks and two optional subtasks in this task are:

Subtask 4.1	Establish a screening criterion to predict unstable crack jumps in ferritic steels
Subtask 4.2	Evaluate procedures for characterizing fracture resistance during crack jumps in laboratory specimens
Subtask 4.3	Assess current procedures for predicting crack jump magnitudes in pipes
Subtask 4.4	Prepare interim and topical reports on dynamic strain aging induced crack instabilities in ferritic nuclear piping steels at LWR temperatures
Subtask 4.5	(Optional Subtask) Refine procedures for characterizing fracture resistance during crack jumps in laboratory specimens
Subtask 4.6	(Optional Subtask) Refine procedures for predicting crack jump magnitudes in pipes

Only Subtask 4.1 was active during the last reporting period. Progress in this subtask is described below.

5.3.1 Subtask 4.1 Establishment of a Screening Criterion to Predict Unstable Crack Jumps in Ferritic Steels

5.3.1.1 Objective

The objective of this activity is to evaluate the relation between dynamic strain aging and crack instabilities in ferritic pipes.

5.3.1.2 Rationale

The significance of crack instabilities in flawed-pipe safety analyses has already been demonstrated in at least one 288 C (550 F) low compliance pipe test conducted at David Taylor Research Center. In that experiment, a crack jump of approximately one-fourth of the pipe circumference was observed for a circumferential through-wall crack. Obviously, such an instability in a nuclear plant would lead to a large loss of cooling water. Therefore, it is important to determine how to predict the occurrence and magnitude of crack instabilities. This task represents an attempt to tackle these issues in a logical manner.

5.3.1.3 Approach

The approach in Task 4 is based on experimental data obtained in the Degraded Piping Program (Ref. 5.1). In several pipe steels tested at 288 C (550 F), both in laboratory and pipe specimens, crack instabilities were observed, interspersed between periods of stable, ductile tearing. These instabilities have been assumed to be related to a steel's susceptibility to DSA (Ref. 5.2). Dynamic strain aging results from interactions between dislocations and free nitrogen and/or carbon atoms during plastic straining, thereby increasing the strength during plastic straining and reducing the ductility. However, no firm proof of that tie between DSA and crack instabilities presently exists.

A limited number of laboratory experiments are being conducted in Subtask 4.1. The results of those experiments, when combined with existing data, will be examined for a direct link between crack instabilities and DSA. If that link can be established, it should be possible to assess a steel's propensity for crack jumps by conducting a few tensile tests or, even better, a few hardness tests. Hardness tests would be especially attractive in nondestructive, in-plant testing of pipes for which no archival material exists, or as a simple mill quality control test.

5.3.1.4 Progress

Testing was completed on C(T) specimens from a carbon steel weld (DP2-F29W). This weld was made using a Babcock and Wilcox C-Mn-Mo-Ni weld procedure used in some piping applications and in their pressure vessel welds. Previous tensile and hardness tests had indicated that the DSA temperature range for this weld was significantly higher than that for the several carbon steel base metals tested. Several of the base metals displayed significant crack jumps in C(T) tests at 288 C (550 F), but the weld metal did not. The purpose of these tests was to see whether the weld metal would display significant crack jumps when tested at temperatures higher than 288 C (550 F). The test temperatures selected for these additional tests were 316, 332, 349, and 371 C (600, 630, 660, and 700 F).

Load-displacement curves for four C(T) specimen tests are shown in Figure 5.1. At the lowest of the four temperatures, the crack jumps were small and numerous, as indicated by the sudden small load drops (see arrows). As the test temperature was increased, the crack jumps tended to become larger in magnitude and less numerous. These findings support the hypothesis that the occurrence of crack instabilities is closely related to a steel's susceptibility to dynamic strain aging, and that either hardness tests or tensile tests conducted over a range of temperatures can be used to estimate the temperature range in which crack instabilities will occur.

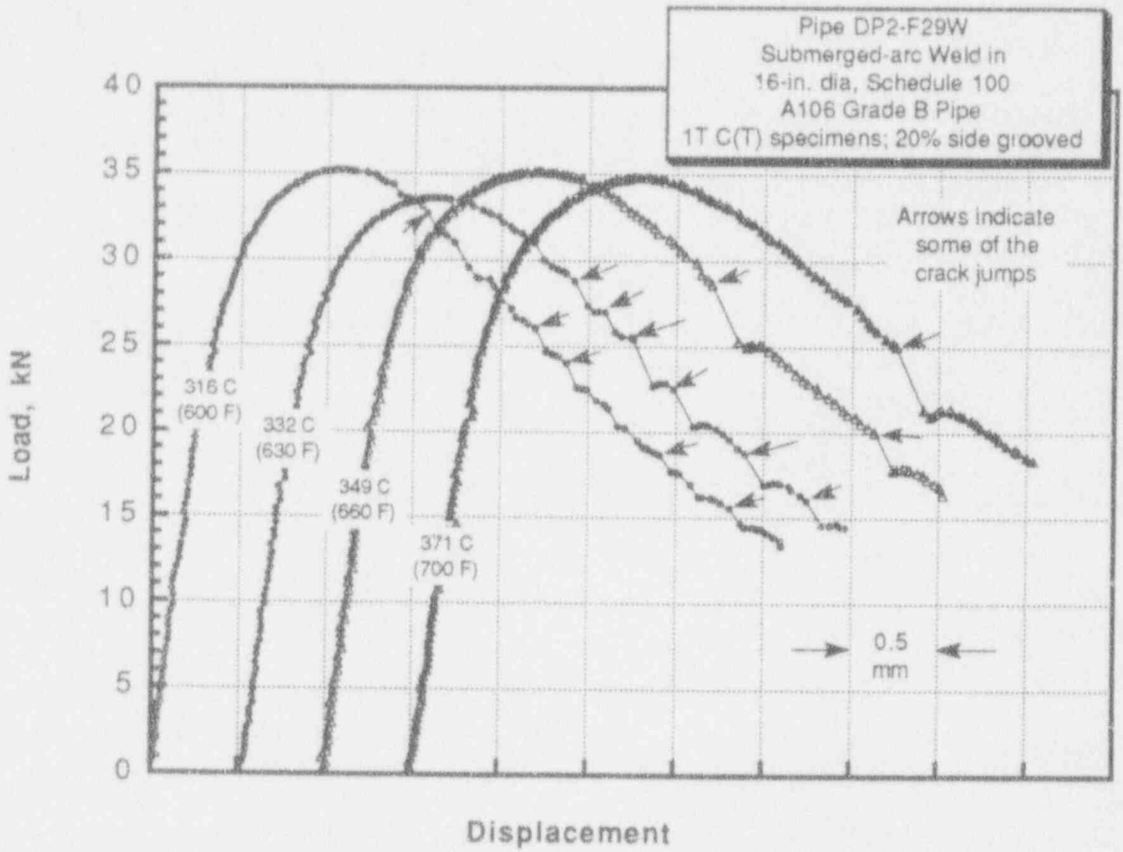

Figure 5.1 Load-displacement curves for C(T) specimen tests

5.4 Plans for Next Year

Subtask 4.1 will be completed with the submission of a topical report. Plans for Subtask 4.2 and 4.3 are as follows.

5.4.1 Subtask 4.2 Evaluate Procedures for Assessing Fracture Resistance During Crack Jumps in Laboratory Specimens

One finite element analysis of a C(T) specimen experiment showing crack jumps will be undertaken in the next year. The experimental load-displacement and crack-growth load-line displacement curves will be used in the FE analysis. The behavior of the J-integral as well as other fracture parameters such as the crack tip opening angle (CTOA) will be investigated during the crack-jump phenomenon.

5.4.2 Subtask 4.3 Assess Current Procedures for Predicting Crack Jump Magnitudes in Pipes

During the next year, the objectives for this subtask will be re-evaluated in light of the findings to date in this task. The phenomenon of crack jumps in pipe experiments due to dynamic strain aging appears to be random. Hence, predicting this phenomenon using deterministic models may not be possible, although the susceptibility of various carbon steels can be determined using a screening criterion. We suggest that this subtask be eliminated in the next year.

5.4.3 Subtask 4.4 Prepare Interim and Topical Reports on Dynamic Strain Aging-Induced Crack Instabilities in Ferritic Nuclear Piping Steels at LWR Temperatures

Once the analysis work in Subtask 4.2 is completed, the topical report on these efforts will be written. At this time, we see no need for Subtask 4.3 or Optional Subtask 4.6.

5.5 References

5.1 Wilkowski, G. M. and others, "Degraded Piping Program - Phase II," Summary of Technical Results and Their Significance to Leak-Before-Break and In-Service Flaw Acceptance Criteria, March 1984 - January 1989, Battelle, NUREG/CR-4082, Vol. 8, March 1989.

5.2 Marschall, C. W., Landow, M. P. and Wilkowski, G. M., "Effect of Dynamic Strain Aging on Fracture Resistance of Carbon Steels Operating at Light-Water-Reactor Temperatures," pp. 339-360, ASTM STP 1074, 1990.

6. TASK 5 FRACTURE EVALUATIONS OF PIPE ANISOTROPY

6.1 Task Objective

The objective of this subtask is to assess whether anisotropic fracture properties (in which the toughness is typically lower in a helical direction or the axial direction for ferritic seamless pipe) together with the occurrence of high principal stresses in a helical direction can cause a lower failure stress than that calculated using the toughness in the L-C orientation and using only the longitudinal stresses.

6.2 Task Rationale

The rationale for this task is to assess whether the source equations in the current LBB and ASME flaw evaluation procedures could overpredict the maximum loads for out-of-plane crack growth under certain service loading conditions. If current procedures are found to significantly overpredict the load, modifications to existing fracture analysis methods will be made.

6.3 Task Approach

Five subtasks will be conducted in this task. Two of them are optional subtasks that would be started only with NRC approval after an interim report is completed. The subtasks are:

Subtask 5.1	Assess the effect of toughness anisotropy on pipe fracture under combined loads
Subtask 5.2	Determine the magnitude of toughness anisotropy and establish a screening criterion to predict out-of-plane crack growth
Subtask 5.3	Prepare interim and topical reports on anisotropy and mixed-mode studies
Subtask 5.4	Establish ductile crack growth resistance under mixed-mode loading (optional subtask)
Subtask 5.5	Refine J-estimation scheme analyses for pipes (optional subtask).

All the subtasks were inactive during the last reporting period; hence, there is no progress to report.

6.4 Plans for Next Year of the Program

This subtask was put on hold during the last reporting period. All experiments have been completed. A topical report on screening for toughness anisotropy in Subtask 5.2 will be prepared. The FE analysis of a stationary angled crack to determine the crack-driving force will be addressed during the next year.

7. TASK 6 CRACK-OPENING-AREA EVALUATIONS

7.1 Task Objective

The objective of this subtask is to make improvements in the crack-opening-area predictions for circumferentially cracked pipe, with particular attention to cracks in welds. The crack-opening-area analyses will be incorporated into the SQUIRT code.

7.2 Task Rationale

From past efforts in the Degraded Piping Program, IPIRG, and ASME Section XI round-robin efforts, it has been found that leakage area predictions are reasonably consistent for circumferential through-wall cracked (TWC) pipe in bending (with the cracks in the base metal). For the case of a crack in the center of a weld, the predictions showed more error in the intermediate to higher bending load levels. For the case of a crack in base metal, but with the pipe in combined bending and tension, the error in the results was significantly greater. If the crack had been in a weld under combined loading, the scatter might have increased even more. The accuracy of the solutions for a crack in a weld and for cracked pipe under combined loading needs verification and improvement for LBB analyses.

7.3 Task Approach

The five specific subtasks are:

Subtask 6.1	Create combined loading improvements
Subtask 6.2	Implement short TWC crack-opening improvements
Subtask 6.3	Improve weld crack evaluations
Subtask 6.4	Modify SQUIRT Code
Subtask 6.5	Prepare topical report on crack-opening-area improvements
Subtask 6.6	Quantify leak rates.

Work was conducted only in Subtask 6.6 during this reporting period. Progress in this subtask is described below.

7.3.1 Subtask 6.6 Quantify Leak Rates

This is a subtask created during the course of this program. Its objective, rationale, and approach are given below.

7.3.1.1 Objective

The objective of this effort is to perform analyses to support potential changes to the NRC's current Regulatory Guide 1.45, "Reactor Coolant Pressure Boundary Leakage Detection Systems."

7.3.1.2 Rationale

Regulatory Guide 1.45, "Reactor Coolant Pressure Boundary Leakage Detection Systems," was published in May 1973, and its revision is being considered. The Nuclear Regulatory Commission (NRC) currently wants to update this procedure taking into account the current leak-detection instrumentation capabilities, experience from the accuracy of leak-detection systems in the past, and current analysis methods to assess the significance of the detectable leakage relative to the structural integrity of the plant. Of the different potential sources of leakage that challenge the structural integrity of the pressure boundary in containment, circumferential cracks in piping have been of much greater significance than any other source. Cracks in steam generator tubing were excluded due to other leakage detection requirements for them. Furthermore, few axial cracks occur in piping, but numerous cases of circumferential crack have been reported. Consequently, the analysis in this study keyed on circumferential cracks in piping to evaluate potential changes in NRC Regulatory Guide 1.45.

7.3.1.3 Approach

The analyses to be performed shall build on other work being done in Task 6. The specific work to be performed includes the following activities.

Activity 6.6.1	Develop the technical background information for verification of analyses
Activity 6.6.2	Develop SQUIRT4 and SQUIRT5 codes
Activity 6.6.3	Evaluate the proposed changes in leak detection requirements in terms of the potential impact on LBB analyses
Activity 6.6.4	Evaluate the proposed changes on leak rate for "non-LBB" piping systems
Activity 6.6.5	Coordinate with NRC-RES and NRC-NRR staff
Activity 6.6.6	Prepare NUREG/CR report

Progress to be reported is limited to the efforts under Activities 6.6.5 and 6.6.6. The details of these efforts are described below.

7.3.1.4 Progress

Activity 6.6.5 Coordinate with NRC-RES and NRC-NRR Staff

By request from NRC staff, additional efforts were undertaken to develop statistics (mean and standard deviation) of J-resistance curves for stainless steel base metals. The statistical analysis was similar to the one conducted earlier in the probabilistic leak-before-break study.

Definition of Toughness Parameters - Let J_R denote the J-resistance from the compact tension [C(T)] specimen, which is assumed to be adequately characterized by a power-law equation of the form

$$J_R(\Delta a) = J_{Ic} + C' \frac{(\Delta a)^m}{r} \quad (7\text{-}1)$$

where Δa is extension of crack length (mm), J_{Ic} is the J-resistance at crack initiation (kJ/m^2), r is a normalizing constant equal to 1 mm, and C′ and m are power-law parameters from a best fit of experimental data. Samples of raw data for J-resistance curves were obtained from the actual experiments. These tests were conducted on the side-grooved, fatigue pre-cracked, C(T) specimens at 288 C (550 F). Results from each of these tests were then fitted with Equation 7-1 to obtain the corresponding values of the toughness parameters, J_{Ic}, C′, and m. Table 7.1 shows the sample values of the above parameters for the base metal (TP304) of the stainless steel pipe. Further details can be obtained from the draft topical report, "Probabilistic Pipe Fracture Evaluations for Leak-Rate Detection Applications" (NUREG/CR-6004) by Rahman, S., Ghadiali, N., Paul, D., and Wilkowski, G., which will be published in the next year of this program, and Ref. 7.1.

Statistical Analysis - The lower bound curves for the toughness properties of the material were obtained from the statistical analysis of the experimental data. For example, for a given Δa, the samples of $J_R(\Delta a)$ were generated by using Equation 7-1 and the sample values of toughness parameters listed in Table 7.1. From standard statistical analyses, the mean, μ, and the standard deviations, s, of $J_R(\Delta a)$ were estimated. By repeating the same steps for different values of Δa, the statistics of the whole J_R curve were obtained. The method is approximate only because the basic toughness parameters, J_{Ic}, C′, and m were obtained from a finite number of samples. The statistics of the J_R curve were obtained in a digitized form.

Figure 7.1 shows the experimental J_R curves of stainless steel base metal (TP304) with the values of the toughness parameters listed in Table 7.1. Significant variability is exhibited in the toughness properties, specially when the crack extension becomes larger. The lower bound data was from Specimen A8-54 in Table 7.1. We carefully examined that data set, as well as the rest of the data to confirm the quality of the data. For Specimen A8-54, there was an inclusion in the base metal of the ligament causing the low crack growth resistance. Hence, this was an unusual data set, but such natural inclusions could (and obviously did) occur, hence it was deemed as valid. Figure 7.2 shows the mean (μ curve) and standard deviation (s curve) of the J_R curve as a function of Δa for the stainless steel base metal. From these curves, a lower-bound curve defined by μ-is for a given value of i can be generated. Two such curves, such as μ-s (i=1) and μ-2s (i=2), are shown in Figure 7.2. Discretized values of μ, s, and μ-2s curves for several crack growth extensions are also given in Table 7.2.

Activity 6.6.6 Prepare NUREG Report

During the previous year of the program, considerable effort was spent on preparing a topical report for the leak rate quantification subtask. The report is titled "Probabilistic Pipe Fracture Evaluations

Table 7.1 Experimental values of the toughness parameters of stainless steel base metal (TP304)

Spec Code	J_{Ic}, kJ/m^2	C′, kJ/m^2	m	Net Thickness, mm
A23-10	1090	213.3	0.6144	10.414
A35-9	573	353.6	0.7667	13.030
A8-43	623	459.3	0.7953	18.212
A8-54	910	232.2	0.3121	4.064
A8-55	924	272.8	0.672	8.636
A8-56	962	287.8	0.6104	8.255
A8-57	2230	284.0	0.4907	16.256
A8-71	1500	374.7	0.7236	18.288
A8-12A	854	451.5	0.7691	15.519
A23-113	646	232.6	0.8345	9.639

Table 7.2 Statistics of the J_R curve for stainless steel base metal (TP304)

Δ a, mm	J_R, kJ/m^2		
	μ	s	μ - 2s
0.00	1031.2	474.1	82.9
1.25	1399.4	463.6	472.0
2.5	1625.6	456.9	711.8
3.75	1820.6	469.5	881.6
5.00	1998.3	498.6	1001.2
6.25	2164.1	540.2	1083.7
7.50	2321.2	590.9	1139.4
8.75	2471.3	647.9	1175.6
10.00	2615.9	709.2	1197.5
11.25	2755.7	773.4	1208.9
12.5	2891.4	839.5	1212.4

μ = mean value of J_R; s = standard deviation of J_R

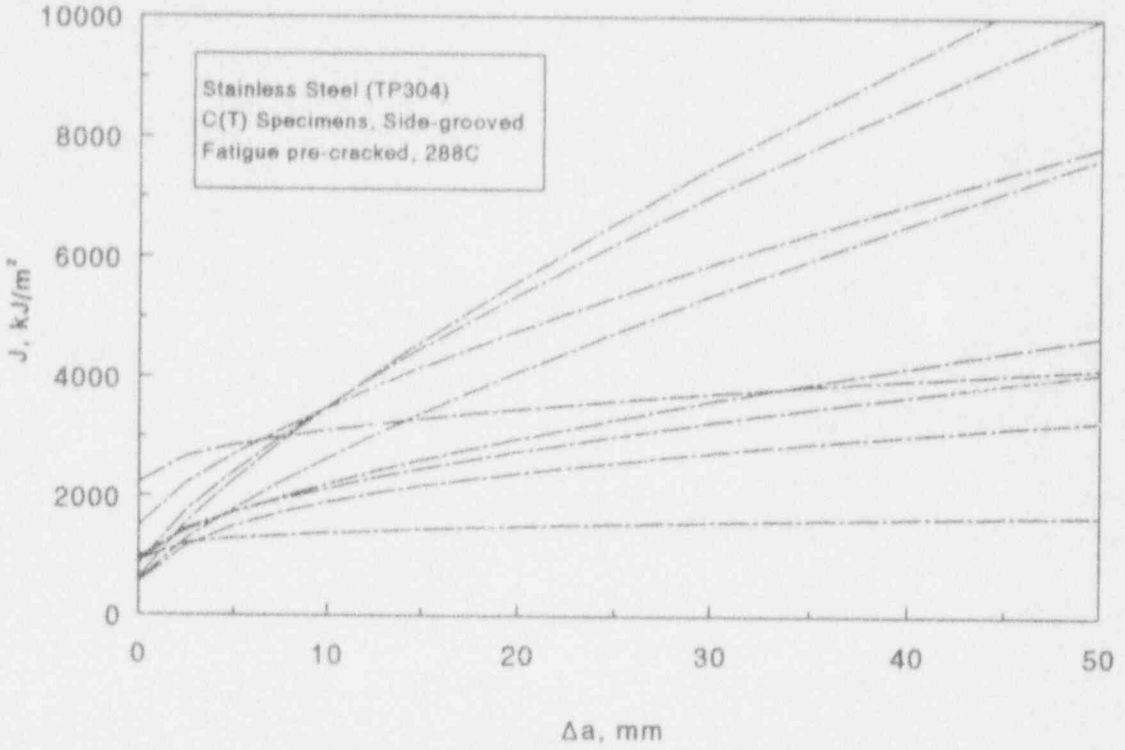

Figure 7.1 Experimental J_R curves of stainless steel base metals (TP304)

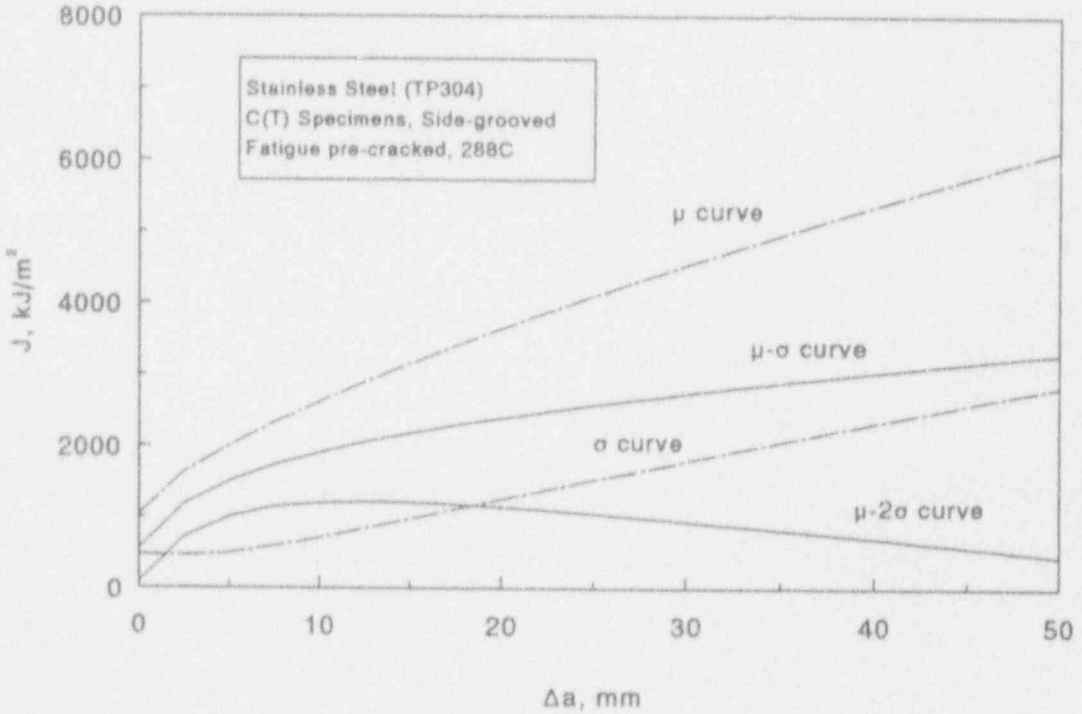

Figure 7.2 Statistical properties of J_R curve of stainless steel base metals (TP304)

for Leak-Rate Detection Applications," NUREG/CR-6004, by S. Rahman, N. Ghadiali, D. Paul, and G. Wilkowski. Draft copies of this report were sent to the NRC and other independent reviewers. The paper for Reference 7.1 was prepared and presented during the last reporting period. It is expected that the NUREG/CR report will be finalized in the next year of the program.

The above statistical analysis of the stainless steel base metal J-R curves was conducted after the draft NUREG/CR-6004 report and Reference 7.1 were written. The careful review of the data resulted in finding that the statistics for the J-R curve in the draft NUREG/CR and Reference 7.1 had higher scatter than they should have due to the data reduction scheme. Hence, this effect on the probabilistic calculations needs to be assessed.

7.4 Plans for Next Year of Program

The plans for efforts in the next year are summarized below.

7.4.1 Subtask 6.1 Create Combined Loading Improvements

There are three activities in this subtask. Activities 6.1.1 and 6.1.3 have been completed. The remaining Activity 6.1.2 (Account for Pressure on the Crack Face) will be started in next year of the program.

7.4.2 Subtask 6.2 Implement Short TWC Crack-Opening Improvements

The two activities in this subtask will be started in the next year of the program.

7.4.3 Subtask 6.3 Improve Weld Crack Evaluations

There are two activities in this subtask. Activity 6.3.1 was completed. Activity 6.3.2 (Compare with Recent DP^{3}II and Task 1 Data) has started and will continue as data become available. It will .e completed in the next year of the program.

7.4.4 Subtask 6.4 Modify SQUIRT Code

This subtask has started in this fiscal year. Work will continue in the next year of the program.

7.4.5 Subtask 6.5 Prepare Topical Report on Crack-Opening-Area Improvements

This subtask was not scheduled to start in this fiscal year. It will begin in the next year of the program.

7.4.6 Subtask 6.6 Quantify Leak Rates

A final review of the topical report is in progress.

7.5 References

7.1 S. Rahman, G. Wilkowski, and N. Ghadiali, "Probabilistic Pipe Fracture Evaluations for Applications to Leak-Rate Detection", proceedings of CSNI International Workshop on Reactor Coolant System Leakage and Failure Probability, Köln, Germany, December 1992.

8. TASK 7 NRCPIPE

8.1 Task Objective

The main objective of this task is to incorporate the analysis improvements from Subtasks 1.4 and 2.4 into the NRCPIPE code. A secondary objective is to make the NRCPIPE code more efficient and also to restructure the code to allow for ease of implementation of the activities described below.

8.2 Task Rationale

In the Degraded Piping Program, the computer code NRCPIPE was developed for circumferential through-wall-cracked pipe fracture analyses. A VAX version of the code also contained the circumferential internal surface-wall-cracked pipe J-estimation schemes. The PC version was made specifically for the through-wall-cracked analyses. Numerous J-estimation schemes were developed or modified. The improvements developed in the current program need to be incorporated into this code to take advantage of technology developments as well as to facilitate comparisons with the experimental results.

8.3 Task Approach

The progress in each of these subtasks is discussed below.

Subtask 7.1 Improve Efficiency of Current Version of NRCPIPE
Subtask 7.2 TWC Improvement
Subtask 7.3 Surface Crack Code
Subtask 7.4 User's Manual

8.3.1 Subtask 7.1 Improve Efficiency of Current Version of NRCPIPE

A revised version of the NRCPIPE code (Version 1.4g) was developed during this reporting period. The NRCPIPE code was made more user friendly; e.g., the output file includes a problem title and the version number of the code. Additional information regarding limitations and definitions of certain terms were put on the interactive screens. Several minor bugs were also fixed. A revised User's Manual, along with the code, were delivered to the NRC.

8.3.2 Subtask 7.2 TWC Improvement

During this reporting period, the weld metal algorithm for LBB.ENG3 was incorporated into NRCPIPE. Also, the implementation of the new GE/EPRI functions was initiated.

8.3.3 Subtask 7.3 Surface Crack Code

The NRCPIPES surface crack code was revised to be more user friendly in a manner similar to the NRCPIPE code.

8.3.4 Subtask 7.4 User's Manual

A revised User's Manual for NRCPIPE Version 1.4g was prepared.

8.4 Plans for Next Year of the Program

Efforts scheduled for the next year of the program are discussed below.

8.4.1 Subtask 7.2 Incorporate TWC Improvements in NRCPIPE

All of the new GE/EPRI functions developed including those for tension and bendings will be incorporated in NRCPIPE. This, along with the weld crack algorithm, will form the basis of Version 2.0 of the program.

8.4.2 Subtask 7.3 Surface Crack Version of NRCPIPE

The PC Version of the NRCPIPES code will be debugged and the 360-degree-deep crack GE/EPRI functions will be implemented. Implementation of the combined bending and pressure algorithm will also be performed.

8.4.3 Subtask 7.4 Provide New User's Manual

The user's manual for both the NRCPIPE and NRCPIPES code will be updated.

9. TASK 8 ADDITIONAL EFFORTS

9.1 Task Objective

The objective of this task is to undertake analyses or experiments needed to clarify issues that develop during the course of this program. To date, five subtasks have been initiated.

9.2 Task Rationale

When the program was initiated, it was realized that the results obtained during the course of the tasks may require additional efforts to be undertaken. This task was, therefore, created. All work in this task is as a result of contract modifications to the original program.

9.3 Task Approach

The six subtasks involving additional efforts are:

Subtask 8.1 Validity Limits on J-R Curve Determination
Subtask 8.2 Stainless Steel SAW Fusion-Line Toughness
Subtask 8.3 Update PIFRAC Data Files
Subtask 8.4 Develop Database for Circumferential Pipe Fracture Experiments
Subtask 8.5 Data File Conversion from HP to IBM Format
Subtask 8.6 ASME Section III S_m Limits Allowable Stress Limits

Progress in Subtasks 8.1 through 8.5 is discussed below.

9.3.1 Subtask 8.1 Validity Limits on J-R Curve Determination

9.3.1.1 Objective

The objective of this subtask is to carry out a theoretical and computational study of the limits of validity of J-R curve data from bend-type specimens under contained and fully yielded conditions. The results of the study should make it possible to validate if J_D or J_M resistance curves can be used. This work is being performed under a subcontract to Professor F. Shih at Brown University.

9.3.1.2 Rationale

The results will have direct bearing on the problem of determining J-R curves from small-bend-type specimens where it is desired to obtain valid data to characterize large amounts of crack growth for pipe and pressure vessel applications.

9.3.1.3 Approach

Through extensive and systematic numerical analyses of crack growth under small-scale yielding conditions, as well as for finite crack geometries, the parameters which characterize the validity limits for the determination of J-R curves will be identified. The effect of crack tip constraint on the crack growth behavior also will be examined in detail. A critical assessment of the several definitions of J that are used in the analysis of crack growth will be made.

9.3.1.4 Progress

Many metals which fail by a void growth mechanism display a single fracture plane on which voids have grown and coalesced. This fracture process involves localization of plastic flow in a planar zone of essentially one void spacing in thickness as evidenced by the fact that voids away from the planar zone display little or no growth. We idealized this process by assuming that void growth and coalescence occur in a layer of initial thickness. The response of the material in this layer of material is governed by Gurson's constitutive equation for a rate-sensitive elastic-plastic material containing voids (Ref. 9.1). Unlike the conventional flow theory of plasticity, in which hydrostatic stress plays no role, the Gurson constitutive equation is highly sensitive to the hydrostatic stress level, a critical feature for our studies. Thus, our model, which has a physically based length scale, is quite well suited for exploring the effects of near-tip constraint and crack geometry on fracture initiation toughness and crack growth resistance behavior.

We have incorporated the above model of ductile failure into a computational finite element model and have completed studies for the small-scale yielding problem in which the remote loading is specified by K_I and T. The remote loading is applied by gradually increasing the stress intensity factor K_I and keeping T/σ_y fixed to correspond to a certain level of near-tip constraint. As the load increases, the process of ductile crack growth occurs naturally in the layer of Gurson material, assigned an initial porosity f_{int} ahead of the crack tip.

First, we consider these material conditions: the critical microstructure controlling cleavage is unchanging; the microstructure controlling ductile crack growth is varied in a systematic manner. When the initial porosity is high, say $f_{int} = 0.01$, the crack growth occurs in a purely ductile mode and the tearing resistance is small. Lowering the initial porosity to say 0.001, raises the initiation fracture toughness slightly; however, the tearing resistance increases by a substantial factor. The tearing modulus exhibits a strong dependence on the T-stress (or the effect of geometry); negative T-stresses increase the tearing resistance while positive T-stresses have negligible effect. The initiation toughness is slightly dependent on T-stress.

9.3.2 Subtask 8.2 Stainless Steel SAW Fusion-Line Toughness

9.3.2.1 Objective

The objective of this effort is to determine the fracture toughness associated with a crack growing along the fusion line in an austenitic stainless steel submerged-arc weldment.

9.3.2.2 Rationale

During the conduct of Pipe Experiment 1.2.3.16 (surface crack test of a stainless steel submerged-arc weld, SAW) and previous pipe tests in the Degraded Piping Program with cracks centered in stainless steel welds, the cracks have tended in many cases to propagate from the center of the weld to the fusion line of the weld. This indicates that the fusion line may often be the least fracture resistant, whereas previously the weld metal has been thought to be the lowest toughness crack location. If the findings confirm the indications described above, then flaw assessment criteria should be based on the fusion-line toughness rather than on the weld-metal toughness. That result could affect the IWB-3640 flaw evaluation criterion and possibly LBB analyses for wrought and cast stainless steel pipes.

9.3.2.3 Approach

A two-phase effort will be undertaken to accomplish this item. The first phase involves conducting basic verification-of-methodology experiments on a base metal, using compact specimens having either a straight (conventional) or a slant notch—the objective being to see if the J-R curve is the same for the two different orientations. This second phase involves testing of: (a) conventionally notched specimens from specially prepared welds having one fusion line perpendicular to the plate surfaces, and (b) slant notch specimens from typical single-arc welds. Other than a Charpy test, the slant-notch C(T) specimen is typical of the only type of specimen that could be tested for archival single-vee weldments for development of data in the future.

One of the difficulties in fusion-line toughness testing is the origination of the crack. Standard testing requires the crack to be perpendicular to the specimen surface. For standard single-vee welds from pipes, it is not possible to make standard C(T) specimens with fusion-line crack orientations because of the angle of the fusion line to the pipe or plate surface. Hence, we will make a slant-vee weld so the fusion line will be properly oriented for standard specimens. However, it may be desired also to test archival welds for plant specific applications. Here only a standard single-vee weld may exist. Hence, we will test slant notch C(T) specimens. Such specimens have a combined Mode I and Mode III component loading. If successful for fusion lines, the slant-notch specimen could be used for LBB requirements to assess the lowest toughness region of the material as required by NRC's S.R.P. 3.6.3.

The following tests will be performed.

a. Ten J-R curve tests at 288 C (550 F), with five each from the two weld fusion lines (one fusion line perpendicular to the plate thickness and the other along a typical 37-degree single-vee weld bevel). In each specimen, the notch will lie along the fusion line.
b. Six Charpy V-notch impact tests in the slant-vee weld, three at room temperature and three at 288 C (550 F); additionally three specimens will be tested at room temperature with the notch along the fusion line, which is perpendicular to the plate surfaces.
c. Six Charpy V-notch impact tests with slanted specimen orientations in the single-vee weld so the notch is in line with the fusion line, three at room temperature and three at 288 C (550 F) with the notch on the fusion line.
d. Chemical analysis of the welds.

9.3.2.4 Progress

Fabrication was completed by Uni-Facs of Columbus, Ohio, of a slant-vee submerged-arc weld, i.e., a specimen in which one of the fusion lines is perpendicular to the plate surface, in 25.4-mm (1-inch) thick TP304 stainless steel. This weld will be used to investigate toughness at the fusion line.

Testing of slant-notch C(T) specimens from the stainless steel base metal of Pipe DP2-F33, which contains a bimetallic weld, was initiated. A special technique was devised to monitor lateral displacement at the notch mouth as the slant crack extends. The results of these slant-n tests will be compared with results from ordinary C(T) specimens being conducted on the same material in Subtask 3.1 to determine the suitability of slant-notch specimens for evaluating fusion-line toughness.

9.3.3 Subtask 8.3 Update PIFRAC Data Files

9.3.3.1 Objective

The objective of this effort is to update the PIFRAC database, Ref. 9.2, to include data from NRC-sponsored programs and industry-funded programs to the extent that these data are readily available.

9.3.3.2 Rationale

PIFRAC, a computerized database for material properties of nuclear grade piping materials, which was developed under other NRC funding, was last updated in 1989. Since that time, considerable data have been developed from NRC-sponsored programs at Battelle and from a number of industry-funded programs. The NRC desires that the PIFRAC database be updated to include data from the NRC-sponsored programs and the industry-funded programs.

9.3.3.3 Approach

Battelle will update the PIFRAC database to include data from this program, from the IPIRG program (Ref. 9.3), and any data from the Degraded Piping Program Phase II (Ref. 9.4) that were not included in the 1989 update. Additionally, data from the Aging of Cast Stainless Steel program at Argonne National Laboratory (Ref. 9.5) will be obtained from Argonne and included in this update. Finally, any data known to Battelle, developed in industry-sponsored research programs and in which those data have been or will be supplied to Battelle in a format compatible with PIFRAC, will be included in this update. This includes data from the following programs:

- EPRI/Westinghouse (RP-1238-2) (Ref. 9.6)
- EPRI/GE stainless steel weld data (Project T303-3) (Ref. 9.7)
- EPRI/B&W carbon steel weld data (EPRI NP-6264) (Ref. 9.8)
- Ontario Hydro carbon steel pipe data (Ref. 9.9).

This effort specifically excludes literature searches or other surveys to identify such data. The effort will be limited to data from programs currently known to Battelle or the NRC where digital data exist.

9.3.3.4 Progress

During this reporting period, progress was made in the following areas:

1. Quality assurance of data already existing in Version 1.0 of PIFRAC was completed.

2. Version 2a of the PIFRAC database was completed. This included revising the structure and attributes of the PIFRAC database.

3. Implementation of data from the Degraded Piping Phase III program was started.

4. Additional material data were obtained from DTRC in a form different than the standard method. Implementation of a typical data set was performed to check the required effort of implementing this data.

5. In order to incorporate the data from NRC-sponsored programs and industry-funded programs, contacts were made and data obtained from some companies.

9.3.4 Subtask 8.4 Develop Database for Circumferential Pipe Fracture Experiments

9.3.4.1 Objectives

The objective of this task is to expand the database of circumferentially cracked pipe fracture experiments.

9.3.4.2 Rationale

In addition to Battelle, a number of other organizations worldwide have conducted, and are conducting, pipe fracture experiments on circumferentially cracked pipe. To date there is no single reference, or database, which lists the test conditions and results for these experiments. Such a database would be useful to those individuals assessing the validity of analytical or code approaches in that the appropriate experiments necessary for confirming the approaches would be readily identified. Also such a database would be helpful in eliminating any redundancy in efforts between organizations.

9.3.4.3 Approach

As part of our ASME Section XI Code Committee efforts we have developed a database of circumferentially cracked pipe fracture experiments. This database, in its current form, includes the test conditions, experimental results, and applicable material property data from

- the Degraded Piping Program - Phase II (Ref. 9.4),
- the IPIRG-1 Program (Ref. 9.3),
- the Short Cracks in Piping and Piping Welds Program (Ref. 9.10),
- two David Taylor Research Center (DTRC) programs on A106 Grade B pipe (Ref. 9.11) and welded Type 304 stainless steel pipe (Ref. 9.12), and

— two Battelle programs conducted for EPRI on small-diameter stainless steel pipe (Ref. 9.13, 9.14).

Currently the database has entries for over 140 circumferentially cracked-pipe fracture experiments. As part of this task we will expand the database to include data from a number of other organizations/programs. Table 9.1 is a comprehensive list of programs for which we will include data. Some of the data represented in Table 9.1 already exist in referenced journals while some of the data will need to be obtained from the appropriate organization. Table 9.2 is a list of the test parameters (i.e., test conditions, experimental results, and material property data) that will be included in the database for each of the experiments. As part of this effort, we envision that the size of the database will expand from approximately 140 experiments to over 400 experiments.

9.3.4.4 Progress

During this reporting period we began the process of soliciting data from other laboratories for inclusion into the database of previously conducted, circumferentially cracked, pipe fracture experiments (CIRCUMCK.WK1). Currently the database includes data from pipe fracture programs conducted at David Taylor Research Center in the United States and L'Energia Nucleare e delle Energie Alternative (ENEA) in Italy, as well as the Battelle data. In the future we plan to add data from such organizations as MPA-Stuttgart in Germany; Japan Atomic Energy Research Institute (JAERI), Hitachi, and the National Research Center for Disaster Prevention in Japan; Electricite de France (EDF); Nuclear Electric in the United Kingdom; and Westinghouse in the United States.

9.3.5 Subtask 8.5 Data File Conversion from HP to IBM Format

9.3.5.1 Objective

The objective of this task is to convert all of the Degraded Piping Program data files that existed in HP9845 format to Lotus 1-2-3® format for IBM PC DOS compatible computers.

9.3.5.2 Rationale

The data acquisition system used in the Degraded Piping Program, Phase II (Ref. 9.4) was a Hewlett Packard (HP) HP3497A system controlled by an HP85 computer. After the experiment, the raw data were manipulated with software developed specifically for an individual experiment, or a series of experiments, and written in Basic on an HP9845 computer. With the advent of the personal computer (PC) and commercially available software, such as LOTUS 1-2-3®, this technology is now obsolete. The old HP data files and floppy disks in their present format are incompatible with PCs and commercially available software packages. However, even though the file format technology is obsolete, the data from these experiments are still of great value. The data are still frequently used in the verification of new pipe fracture analyses. Consequently, there is a need to convert these data into a universally used format; i.e., IBM PC format using Lotus 1-2-3® software.

Table 9.1 List of programs for which circumferentially cracked pipe fracture data will be included

Sponsoring Agency	Laboratory	Program or Report Number	Scope of Experiments
USNRC	Battelle	Degraded Piping	Through-wall Crack (TWC), Surface Crack (SC), Complex Crack (CC); Pressure (P), Bend (B), Pressure and Bend (P&B); 4-42"
USNRC	Battelle	IPIRG-1	TWC and SC; B, P&B; 6", 16", 30" diameter
USNRC	Battelle	Short Cracks	Large diameter, short cracks, TWC and SC
AEC	Battelle	BMI-1908	Carbon steel (CS), pressure tests, SC
EPRI	Battelle	NP-192	Small diameter, stainless steel, TWC
EPRI	Battelle	NP-2347	stainless steel, TWC and SC
AGA-NG18	Battelle	Battelle Files	CS, TWC, line pipe pressure
AGA-WSC	Battelle	Battelle Report	Girth weld defects
AGA-WSC	Battelle	Battelle Report	Repair grooves
Offshore Program	Battelle	Battelle Files	4" diameter, bending, carbon steel base metal
EPRI	GE	NP-2472	4" diameter, axial tension
AEC	GE	GEAP-10023	Small diameter, A106
USNRC	DTRC	NUREG/CR-3740	8" A106B carbon steel
USNRC	DTRC	NUREG/CR-4538	Stainless TIG weld
USNRC	DTRC	Unpublished	4" Stainless base metal
USNRC	DTRC	Unpublished	Carbon steel MIG weld
STA	JAERI	NED Paper	Stainless steel, 6" and 16" diameter, TWC, SC
STA	JAERI	JAERI Reports	Carbon steel, 6" and 16" diameter, TWC, SC
ENEA	CISE	LBB [illegible]	Carbon steel, small diameter, TWC
ENEA	CISE	NED paper	Stainless steel, small diameter, TWC
Westinghouse Owner's Group	Westinghouse	ASME PVP-95	Cast stainless steel, small diameter, TWC
CEGB	CEGB	Technical paper	Thin wall, carbon steel tests
KWU	KWU	Technical paper	Carbon steel bend tests
MITI	NUPEC	NED paper	Stainless steel pipe in tension
MITI	NUPEC	NED paper	Carbon steel pipe, pressure and bend
STA	NRCDP	ASME PVP-150	Pipe system tests
BMFT	MPA	Phase I	Pressure to burst, LWR, large diameter
BMFT	MPA	Phase II	Pressure and bend
Hitachi	Hitachi	NED paper	Stainless steel pipe in tension

Table 9.2 List of test parameters, results, and material property data included in database

Test Parameters
Data Record Book Number
Experiment Number
Pipe Material Identification Number
Pipe Material
Outside Diameter
Schedule
Wall Thickness
Inner Span for Four-point Bending Experiments
Outer Span for Four-point Bending Experiments
Test Pressure
Crack Length
Crack Depth
Experimental Results
Load at Crack Initiation
Maximum Load
Moment at Crack Initiation
Maximum Moment
Material Property Data
Yield Strength
Ultimate Strength
Percent Elongation
Reduction in Area
Ramberg-Osgood Coefficients
J-value at Crack Initiation
dJ_D/da (initial slope of J-R curve)
Extrapolated J_D-R Curve Constants
Upper Shelf Charpy Energy
Room Temperature Charpy Energy
Room Temperature Shear Area Percent

9.3.5.3 Approach

As part of this effort Battelle will convert the experimental data files for 61 Degraded Piping Program - Phase II pipe fracture experiments from HP to IBM PC compatible format.

9.3.5.4 Progress

During this reporting period we began the process of converting the pipe fracture experimental data from the Degraded Piping Program from HP9845 format to IBM format. We have converted, or partially converted, the data files for 58 of the 61 pipe fracture experiments conducted as part of the Degraded Piping Program.

9.3.6 Subtask 8.6 ASME Section III Allowable Stress Limits

This is a new subtask in this program.

9.3.6.1 Objective

The objective of this effort is to determine the effect of changing the allowable stress value in the ASME Section III code from $3S_m$ to $7S_m$ on the critical flaw sizes in circumferentially surface-cracked pipe.

9.3.6.2 Rationale

One proposed change to the ASME Section III has been to increase the maximum allowable elastically calculated stress from $3S_m$ to $7S_m$. The higher stress limits would result in smaller critical flaw sizes. These allowable stresses are calculated assuming linear elastic behavior of the material. However, a value of $3S_m$ is above the flow stress of piping steels, and a value of $7S_m$ is more than twice that flow stress. Hence, a nonlinear correction to the actual values of stresses is needed to assess critical flaw sizes if the maximum allowable stress is raised to $7S_m$. Since stainless steels have considerably different strain-hardening behavior than ferritic nuclear pipe steels, both should be evaluated. Such a nonlinear correction for displacement-controlled stresses can be developed by conducting FE analyses of an uncracked pipe using the elastic-plastic stress-strain curve of typical carbon and stainless steels used in nuclear piping. Once this nonlinear correction is available, the critical surface-flaw sizes (crack depths for given circumferential crack length) corresponding to both $3S_m$ and $7S_m$ displacement-controlled stresses can readily be determined using Net-Section-Collapse analysis.

9.3.6.3 Approach

The first step in accomplishing the above objective involves conducting two finite element analyses of uncracked pipe with 20-noded, 3-D brick elements using both linear elastic and elastic-plastic material properties. Material properties for both stainless (Type 304) and ferritic (A106 Grade B) steels at 288C (550F) will be used in the analyses. For both cases, the same diameter (D) and radius-to-thickness ratio (R_m/t) will be selected and the loading will involve combined bending and internal pressure. An R_m/t ratio of 10 will be used as being typical of nuclear piping. The internal pressure

will correspond to one S_m axial stress for the $7S_m$ case, and $0.5S_m$ for the $3S_m$ case. An outside pipe diameter of 400 mm (16 inches) will be used.

Next, a comparison of the moment-rotation curve for the linear elastic and elastic-plastic analyses can be made to determine the moment corresponding to $3S_m$ and $7S_m$ as predicted by the two analyses. The two values of moment will then be used in the Net-Section-Collapse equation for a circumferentially surface-cracked pipe given as

$$M = 2\sigma_f R_m^2 t(2 \sin \beta - \frac{d}{t} \sin \theta) \quad (9.1)$$

where

$$\beta = \frac{1}{2}(\pi - \frac{d\theta}{t}) - \frac{\pi R_i^2 p}{4R_m t \sigma_f}$$

M	=	moment
R_i	=	internal radius
R_m	=	mean pipe radius
t	=	pipe wall thickness
d	=	surface crack depth
θ	=	half-crack angle
p	=	internal pressure
σ_f	=	flow stress

to determine the value of a/t for each value of θ/π. Since d/t cannot be obtained explicitly using Equation 9.1, it has to be solved for numerically using an iterative procedure. A plot of d/t versus θ/π can then be developed and used to define the fail and safe regions for the two values of allowable stresses $3S_m$ and $7S_m$.

9.3.6.4 Progress

This subtask was started late in the reporting period. Since progress during this period was very limited, the results will be included in the next semiannual report.

9.4 Plans for Next Year of the Program

The efforts described below will be undertaken during the next year.

9.4.1 Subtask 8.1 Validity Limits on J-R Curves Determination

We are continuing numerical simulations of crack growth in the three-point bend bar and the center-cracked panel. We are comparing R-curve results for the deformation J theory and Ernst's J_M. A detailed report will be prepared.

9.4.2 Subtask 8.2 Stainless Steel SAW Fusion-Line Toughness

Testing and data reduction of the stainless-steel base-metal slant notch specimens will be completed early in the year. Testing of the fusion-line specimens will then be initiated; these are scheduled for completion by the end of CY93.

9.4.3 Subtask 8.3 Update PIFRAC Data Files

The following efforts are scheduled for the next year:

1. Complete the implementation of DPII - Phase III data into PIFRAC.
2. Implement data from the IPIRG Program.
3. Implement data from the Short Cracks Program.
4. Collect data from various industrial companies on NRC-sponsored programs or industry-funded programs.

9.4.4 Subtask 8.4 Circumferential Cracked Pipe Database

During the next six months, we will continue with the process of soliciting experimental data from other organizations from previously conducted programs for inclusion into the circumferentially cracked pipe fracture database (CIRCUMCK.WK1).

9.4.5 Subtask 8.5 Degraded Piping Program Pipe Fracture Data File Conversion

During the next six months, we will continue with the process of converting the pipe fracture experimental data files from the HP9845 format to the Lotus 1-2-3® format.

9.4.6 Subtask 8.6 ASME Section III Allowable Stress Limits

Efforts in this subtask will be completed during the next year. The results will be included in the next semiannual report as well as in a separate letter to the NRC.

9.5 References

9.1 Gurson, A. L., "Continuum Theory of Ductile Rupture by Void Nucleation and Growth: Part 1 - Yield Criteria and Flow Rules for Porous Ductile Media," Journal of Engineering Material Technology, ASME, 99, 2-15 (1977).

9.2 Hiser, A. L. and Callahan, G. M., "A User's Guide to the NRC's Piping Fracture Mechanics Database (PIFRAC)," NUREG/CR-4894, May 1987.

9.3 Schmidt, R. A., and others, "The International Piping Integrity Research Group (IPIRG) Program - An Overview," SMiRT-11, Paper G12/1, August 1991.

9.4 Wilkowski, G. M., and others, "Degraded Piping Program -- Phase II," Summary of Technical Results and Their Significance to Leak-Before-Break and In-Service Flaw Acceptance Criteria: March 1984 - January 1989, NUREG/CR-4082, Vol. 8, March 1989.

9.5 Chopra, O. K., Sather, A., Bush, L. Y., "Long-Term Embrittlement of Cast Duplex Stainless Steels in LWR Systems," NUREG/CR-4744 Vol. 4, No., 2, June 1991.

9.6 Landes, J. D., McCabe, D. E., and Ernst, H. A., "Elastic-Plastic Methodology to Establish R Curves and Instability Criteria", Eighth Semiannual Report to EPRI on Contract No. RP1238-2, July 1, 1983 to December 31, 1983, by Westinghouse R&D Center, July 24, 1984.

9.7 Horn, R. M., Methta, H. S., Andrews, W. R., Ranganath, S., "Evaluation of the Toughness of Austenitic Stainless Steel Pipe Weldments," GE San Jose, Ca. report to EPRI on Contract T303-3,April 1985.

9.8 Van der Sluys, W. A., "Toughness of Ferritic Piping Steels," EPRI NP-6264, October 1988.

9.9 Manning, B. W., "Fracture Mechanics Leak-Before-Break Material Test Program," Ontario Hydro Design and Development Division - Generation, Report No. 85120, September 1986 (Rev. 2).

9.10 Wilkowski, G. M., et al., "Short Cracks in Piping and Piping Welds," Semiannual Report, October 1991 - March 1992, NUREG/CR-4599, Vol. 2, No. 2, February 1993.

9.11 Vassilaros, M. G., and others, "J-Integral Testing Instability Analysis for 8-Inch-Diameter ASTM A106 Steel Pipe," NUREG/CR-2347, April 1984.

9.12 Hays, R. A., and others, "Fracture Analysis of Welded Type 304 Stainless Steel Pipe," NUREG/CR-4538, Vol. 1, May 1986.

9.13 Kanninen, M. F., and others, "Mechanical Fracture Predictions for Sensitized Stainless Steel Piping with Circumferential Cracks," EPRI Report NP-192, September 1976.

9.14 Kanninen, M. F., and others, "Instability Predictions for Circumferentially Cracked Type 304 Stainless Steel Pipes Under Dynamic Loadings," Final Report on EPRI Project T118-2, by Battelle Columbus Laboratories, EPRI Project Number NP-2347, 1982.

10. TASK 9 INTERPROGRAM COOPERATION AND PROGRAM MANAGEMENT

10.1 Task Objective

The objectives of this task are to develop and maintain national and international cooperation through sharing data and analysis procedures and to maintain program administration.

10.2 Task Rationale

One of the most important elements of this program is the transfer of the technology developments into ASME Section XI flaw evaluation procedures and LBB analysis procedures for the NRC. The results of this program will be presented to the ASME Section XI Pipe Flaw Evaluation Task Group. This will help implement the results into U.S. Codes and Standards. Additionally, if appropriate, results will be presented to the ASTM E8 (formerly E24) fracture committee. Finally, the scope of this task includes incorporation of ongoing efforts from programs conducted elsewhere in the world that enhance the results from this program.

10.3 Task Approach

The seven subtasks are:

Subtask 9.1 Technical Exchange and Information Meetings
Subtask 9.2 Internal Program Coordination
Subtask 9.3 Reports
Subtask 9.4 Review Meetings
Subtask 9.5 Travel
Subtask 9.6 Quality Assurance and Control
Subtask 9.7 Task Management

Only technical progress in Subtask 9.1 is discussed in semiannual reports.

10.3.1 Subtask 9.1 Technical Exchange and Information Meetings

10.3.1.1 Objective

The objective of this subtask is to enhance the program's technical efforts by developing a forum to exchange technical information both nationally and internationally. Specifically, this involves transferring technical aspects from this program that may be helpful to ASME code or NRC criteria to the appropriate organizations.

10.3.1.2 Rationale

The timely exchange of technical developments offers the opportunity for peer review and acceptance of the results of this program, and enhances implementation of the results into regulatory or code criteria.

10.3.1.3 Approach

There are four activities within this subtask:

Activity 9.1.1	ASME Section XI meetings
Activity 9.1.2	ASTM meetings
Activity 9.1.3	Other technical meeting coordination
Activity 9.1.4	Coordination with Japanese Elastic-Plastic Fracture in Inhomogeneous Materials program.

Only progress in Activity 9.1.1 is reported here.

10.3.1.4 Progress

Activity 9.1.1 ASME Section XI Meetings

Battelle has conducted a number of activities as part of its involvement with the Pipe Flaw Evaluation Task Group of the Section XI Committee for the ASME Pressure Vessel and Piping Code. These activities are discussed below.

Charpy Energy Based Elastic-Plastic Fracture Mechanics (EPFM) Criterion for Axial Cracks

An axial crack elastic-plastic fracture mechanics (EPFM) analysis using a Charpy energy approach was prepared and presented to the ASME Section XI Pipe Flaw Evaluation Group and documented in our last semiannual report, Ref. 10.1. The analysis method uses the semi-empirical failure assessment equations developed by Maxey (Ref. 10.2) to establish the allowable flaw depths that satisfy the EPFM criteria in Appendix H. The detailed equations are given in Section 10 of Ref. 10.1.

Currently, in the ASME ferritic pipe flaw evaluation criteria in Appendix H of Section XI, EPFM analyses exist only in tabular form for materials with $J_{Ic} > 105$ kJ/m^2 (600 in-lb/in^2) as given in Tables H-6410-1 and H-6410-2. For comparison purposes, the Charpy energy criteria given in Ref. 10.1 was compared with some critical values for Table H-6410-1 and the experimental data of Maxey (Ref. 10.2). Since the Table H-6410-1 values are for J_{Ic}, an equivalent Charpy energy had to be calculated. From past Charpy versus J_{Ic} data, the mean and upper bound correlations are given by Equations 10.1a and 10.1b. These correlations were used to correlate the Charpy data.

The mean fit to the data is given by

$$J_{Ic} = 10CVP \tag{10.1a}$$

and an upper bound fit to the data is given by

$$J_{Ic} = 20CVP \tag{10.1b}$$

where

CVP = Charpy V-notch upper-shelf energy.

Equation 10.1b underestimates the CVP values from J_{Ic} data.

The ranges of Charpy values are indicated by the bar connecting the data points in Figure 10.1 for the Table H-6410 values. The comparisons in Figure 10.1 show that the method used to create the Table H-6410-1 values significantly underpredicted the experimental failure loads; furthermore, table values should have been limit-load failures rather than EPFM failures.

Charpy Energy Based Elastic-Plastic Fracture Mechanics (EPFM) Criterion for Circumferential Cracks

A Charpy energy based EPFM criterion for circumferential cracks was created similar to the axial crack criteria described above. With the existing Z-factor method in IWB-3650, a step change occurs in going from limit-load to EPFM analysis. Therefore, as a result of a discussion in the ASME Section XI meeting, this effort was initiated to eliminate this step change.

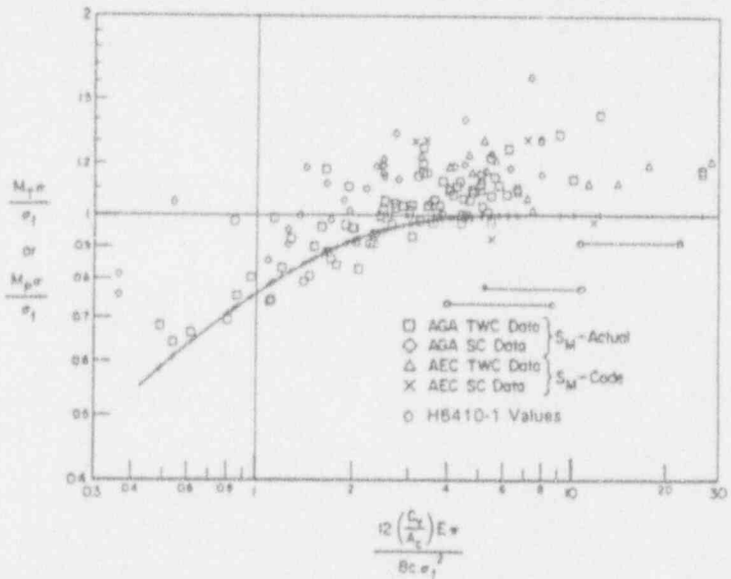

Figure 10.1 Comparison of axial cracked pipe burst data to Maxey analysis with $\sigma_f = 2.4\ S_m$ and ASME Table H-6410 values

Several factors contribute to step changes and the degree of conservatism in the current IWB-3650 Z-factor approach. These factors are briefly summarized below.

(1) The type of crack used in developing the Z factors: the analysis is based on through-wall-cracked pipe data, whereas surface-cracked pipe typically fail closer to limit-load than through-wall-cracked pipe for the same toughness material.

To eliminate this source of conservatism, the flaw evaluation criteria should base the Z factor on a surface-crack analysis.

(2) Crack size: the current Z-factor analysis is based on the most sensitive through-wall-crack length (i.e., about 30% of circumference), which results in the largest Z.

To eliminate this source of conservatism, having a Z-factor as a function of crack size would be helpful, i.e., as crack depth or crack length approaches 0, then Z should approach 1.

(3) Use of a minimum toughness: if the Charpy energy is known and there is a case where the toughness is in the EPFM range and just below limit-load analysis conditions, then the lower bound toughness inherent in the creation of the Z-factors must be used. This can cause step changes from the limit-load to the EPFM allowable flaw sizes.

To eliminate this source of conservatism, a Z factor as a function of Charpy energy would be useful.

(4) Anisotropy and constraint effects on toughness: the toughness for a surface-cracked pipe may be higher than from typical L-C oriented Charpy or C(T) specimen data for two reasons. First, anisotropy of the toughness is well documented to occur for carbon steel base metals. The toughness in the L-R direction for base metals is typically much higher than in the L-C direction. Figure 10.2 is one such example from WRC Bulletin 175 (Ref. 10.3). The L-R to L-C toughness ratio using Charpy upper-shelf energy is frequently a factor of 2.5.

Second, recent work on constraint has shown that the lower the constraint the higher the effective toughness of the material. Work in progress in this program and elsewhere has shown that a circumferential surface-cracked pipe in bending will have much lower constraint than a crack in a C(T) specimen. Hence, C(T) specimen toughness data should be conservative compared to the effective toughness of a circumferential surface-cracked pipe. These two aspects may be the main reasons for surface-cracked pipe failing closer to limit load than through-wall-cracked pipe.

To eliminate this source of conservatism, this higher toughness in base metals in the radial crack growth direction due to anisotropy and constraint, and in weld methods due to constraint needs to be accounted for. (There are no significant data that we are aware of to document the anisotropy of nuclear pipe welds.)

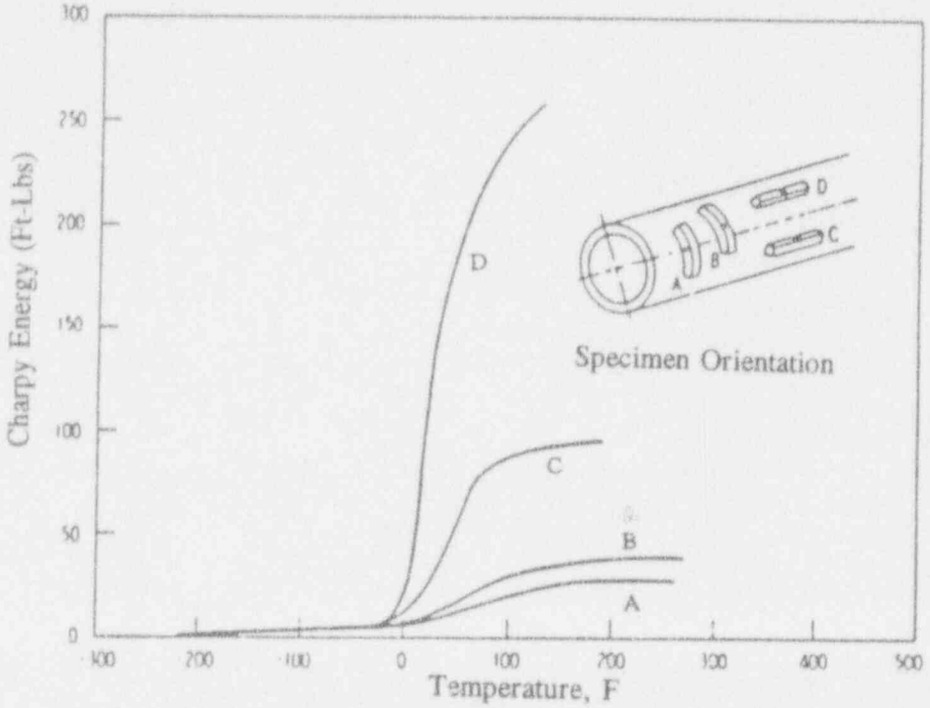

Figure 10.2 Toughness anisotropy of ASTM A106 B pipe (From WRC Bulletin 175)

(5) Inconsistency of including the thermal expansion stress term (P_e): P_e is used in the screening criterion, but not in the limit-load analysis. This can contribute to step changes from limit-load to EPFM analyses.

The IPIRG pipe system experiments (Ref. 10.4) with large circumferential surface cracks demonstrate that P_e should be included in the limit-load solution even for the stainless steel base metal. This is consistent with the R6 analysis which would consider P_e and seismic anchor motion (SAM) stresses as primary stresses. This is illustrated in Figure 10.3, which shows that if the thermal expansion and SAM stresses are not included, then the pipe system failure stresses are only about half of the failure stresses for the quasi-static pipe tests. These quasi-static pipe tests were used to qualify the source equations for IWB-3640 and IWB-3650. Hence, the P_e and SAM stresses should be included as primary stresses in limit-load and EPFM analyses for both austenitic and ferritic pipe.

Some additional desirable aspects for a Charpy Energy-Based EPFM criterion for circumferential cracks are:

(a) Extend the stainless steel flux weld criteria in IWB-3640 to a/t values of 0.75 instead of the current limit of 0.60.

(b) Examine the database for stainless steel submerge-arc weld (SAW) and shielded-metal-arc weld (SMAW) J-R curves and assess if only one Z factor is needed. (Note, the weld metal J-R curve used for developing the SAW Z factor in IWB-3640 was actually a SMAW.)

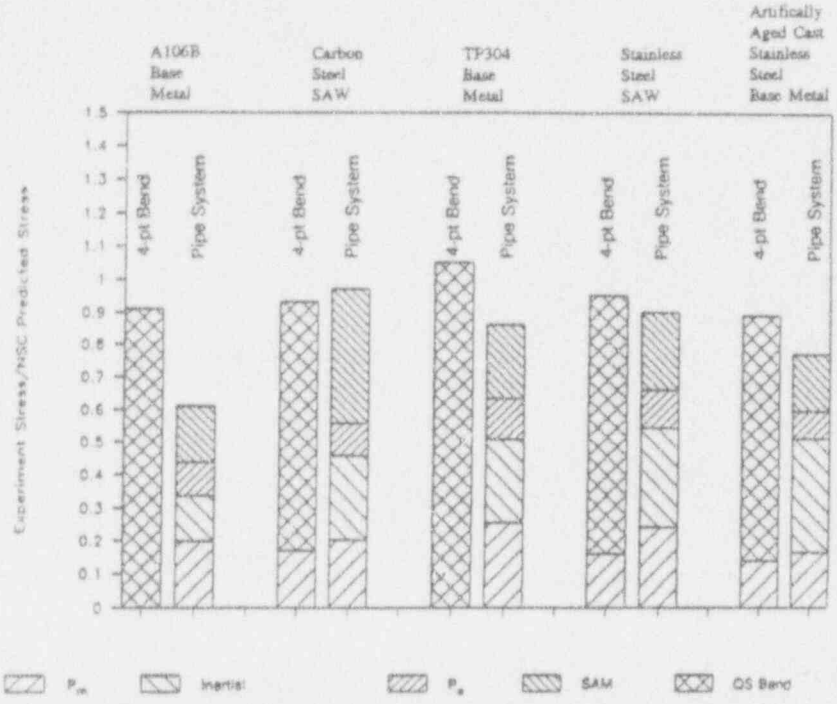

Figure 10.3 Comparison of quasi-static pipe test loads at failure with IPIRG-1 pipe system test failure loads on identical pipes with same crack size

(c) Have a simplified criterion using a Z-factor type approach, but note that a more detailed evaluation could be made if there is difficulty meeting the single criterion (i.e., using the approach in ASME Code Case 494-1).

(d) Any new approach should be applicable to Class 2 and 3 piping as well as stainless and ferritic pipe.

To address some of these needs, we reevaluated the Dimensionless Plastic-Zone-Parameter (DPZP) analysis (Ref. 10.5). This method would allow using available Charpy energy for any material to calculate what the Z factor would be, rather than having to use the current Z factors for the Code minimum toughness values for base or weld metals. Also since this is an empirical analysis for surface-cracked pipe, it will then be possible to address the concerns in Items (1), (3), and (4). Item (2) can be addressed by use of the SC.TNP J-estimation scheme in the NRCPIPES PC code developed as part of Task 2 of this program. This approach also addresses Items (c) and (d). Item (d) is addressed by using a flow stress definition of the average of the Code yield and ultimate strength values rather than using S_m to define the flow stress.

The DPZP analysis was reassessed by examining all the surface-cracked pipe data we have to date. The basic equation is

$$\sigma/\sigma_{nsc} = (2/\pi)\{\arccos[e^{-C(DPZP)}]\} = Z^{-1} \quad (10.2)$$

where

$$DPZP = 2EJ_i/(\pi^2 D\sigma_f^2) \quad (10.3)$$

and,

- σ = predicted failure stress
- σ_{nsc} = Net-Section-Collapse analysis predicted failure stress
- E = elastic modulus
- J_i = J at crack initiation
- D = nominal outside pipe diameter
- σ_f = flow stress
- C = Empirical constant

The flow stress, σ_f, was found to be statistically equal to 1.16 times the average of the yield and ultimate strengths, but a mean minus 1.96 standard deviation value (95-percent reliability) was found to give a flow stress equal to the average of the yield and ultimate strengths. Hence, the following equation is suggested

$$\sigma_f = (\sigma_y + \sigma_u)/2 \quad \text{or} \quad (S_y+S_u)/2 \quad (10.4)$$

where,

- σ_y = actual yield strength
- σ_u = actual ultimate strength
- S_y = Code value of yield strength
- S_u = Code value of ultimate strength

The DPZP C factor in the past was 21.8 for the best fit through the surface-cracked pipe data. This was reassessed using all the data in the CIRCUMCK.WK1 database, from Subtask 8.4 of this program. Figure 10.4 shows that the C value for the best fit of all the data is 32, and for the ferritic pipe data only, it is 34. The difference between the curves using values of 32 or 34 is imperceptible in Figure 10.4 and is reproduced in Figure 10.5 using a reduced x-axis scale.

Also note that there are two 95-percent confidence curves shown in Figure 10.4. One has a C value of 8.9 while the other has a value of C of 3.0. The curve with a C value of 8.9 used only data with the DPZP less than one, where EPFM is expected, while the curve with C of 3.0 is biased by the data with DPZP values greater than one. Where limit-load failure should govern, we believe the C = 8.9 value is the most appropriate for the 95-percent confidence curve.

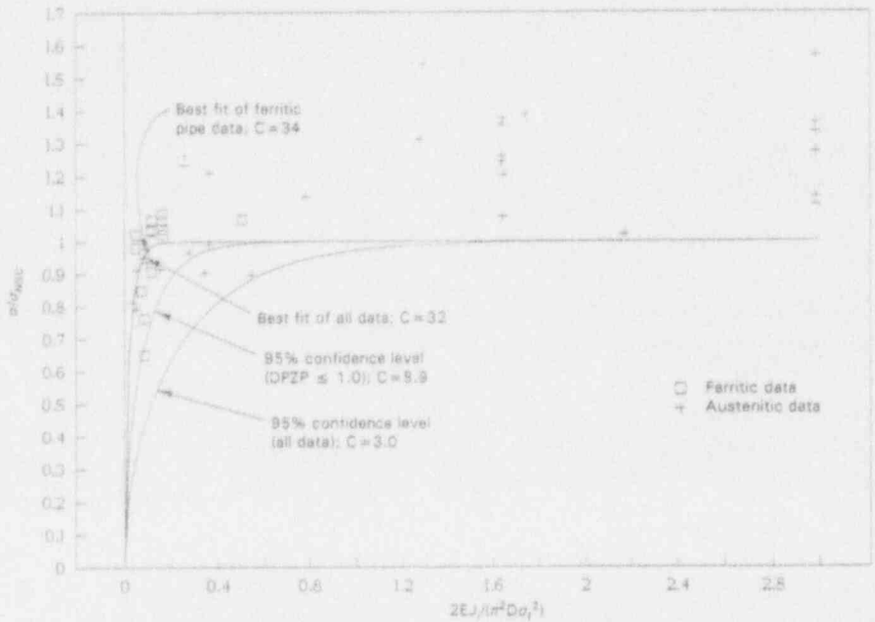

Figure 10.4 Redefining of DPZP analysis C factors using all current surface-cracked pipe data

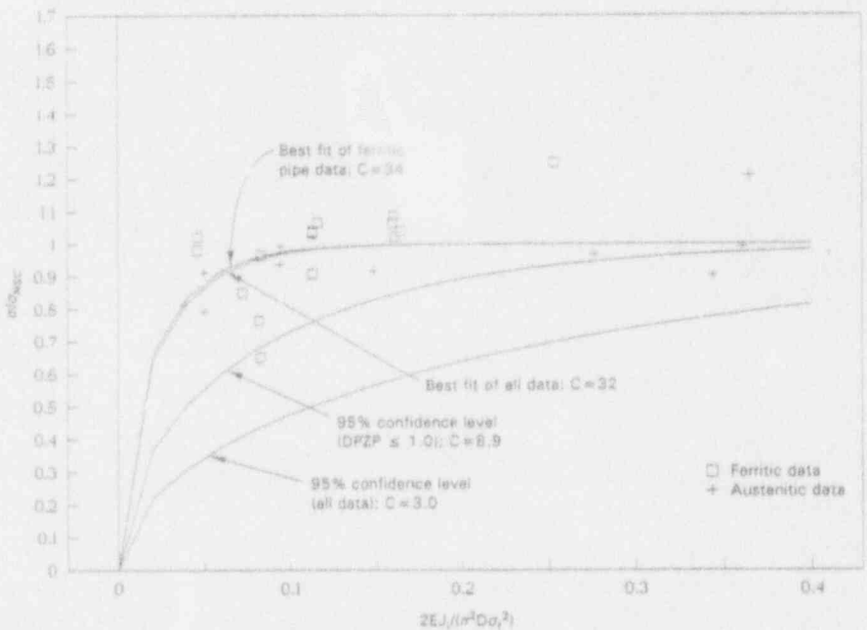

Figure 10.5 Redefining of DPZP analysis C factors using all current surface-cracked-pipe data (expanded scale of Figure 10.4)

Next, we assessed if the Charpy energy could be used in place of the J_i value. It is well known that the Charpy upper-shelf energy is proportional to J_{Ic}. The proportional constant varies from 6 to 10 depending on the degree of conservatism desired. (Note: the values of 10 and 20 previously given are mean and upper bound values rather than lower bound values.) This proportional constant was determined empirically using the experimental pipe data and the DPZP analysis. Using the experimental Charpy upper-shelf data values, the data were replotted and solved for the Charpy energy constant by forcing the value of C to be 34. This gave

$$J_i = 7.5(CVP) \tag{10.5}$$

Furthermore, the 95-percent confidence curve through the data set using the Charpy energy gave a C value of 10, see Figure 10.6.

Hence, Equations (10.2) and (10.3) can be rewritten in terms of Charpy energy data to solve for the Z-factor as shown below:

$$Z = \pi/(2 \text{ arc } \cos[e^{-C(2 E 7.5 CVP/\pi^2 D\sigma_f^2)}]) \tag{10.6}$$

or where

$$Z = \pi/(2 \text{ arc } \cos[e^{-1.52C E CVP/D\sigma_f^2)}]) \tag{10.7}$$

C = 34 for the best-fit curve, and
C = 10 for the 95-percent confidence curve.

To see how the DPZP calculated Z factors compared with the current ASME Code Z factors, the material properties used to develop the current ASME Z factors in the ferritic and austenitic pipe criteria were used to calculate the DPZP-based Z factors.

For the ferritic pipe IWB-3650 Z factors, there are two ASME Code Z-factor equations. One is for base metal and shielded-metal-arc welds with a lower bound J_{Ic} of 105 kJ/m^2 (600 in-lb/in^2). The other is for submerged-arc welds with a J_{Ic} of 61 kJ/m^2 (350 in-lb/in^2). This criterion is limited to pipe larger than a nominal pipe diameter of 102 mm (4 inches).

Using a flow-stress definition for A106B at 288 C (550 F) as the average of code specified yield and ultimate, i.e., $(S_y + S_u)/2$, which is less than one percent different than the ASME flow stress of $2.4S_m$, the Z factors by Equations 10.6 and 10.7 were calculated. These are shown in Figure 10.7 for both the best-fit and the 95-percent confidence-level curves. The best-fit curves for the DPZP analysis Z factors are significantly below the ASME Z-factor curves. The 95-percent confidence curve for Material 1 [J_{Ic} = 105 kJ/m^2 (600 in-lb/in^2)] is below the ASME Z-factor curve. For Material 2 the ASME and DPZP Z-factors are approximately the same, except for diameters less than 406 mm (16 inches).

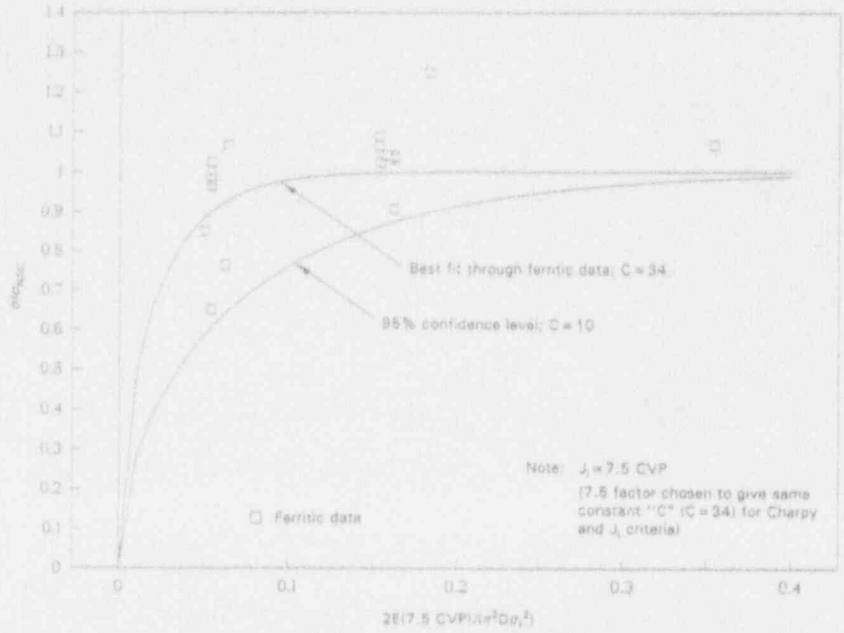

Figure 10.6 Fit of surface-cracked ferritic steel pipe data to define J_i versus CVP constant and 95 percent confidence of C factor

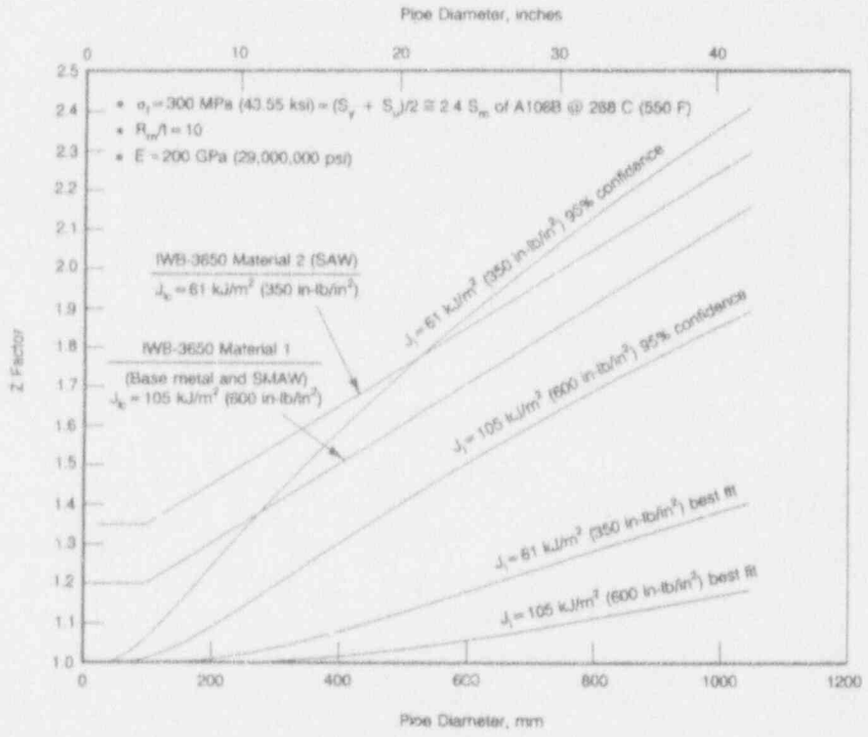

Figure 10.7 Comparisons of Z factors from DPZP analysis and ASME IWB-3650 analysis for ferritic steels

For the austenitic pipe, the calculated Z factors shown in Figure 10.8 used the ASME Code definition of flow stress of $3S_m$, whereas Figure 10.9 shows the DPZP results using the average of the code specified yield and ultimate strengths of TP304 stainless steel at 288 C (550 F). Here if the pipe is smaller than 610 mm (24 inches), then the Z factor for a 610-mm (24-inch) diameter pipe is used.

In Figures 10.8 and 10.9, it can be seen that the DPZP best-fit curves are well below the ASME Z-factor curves. However, for the case where the flow stress is $3S_m$, Figure 10.8, the DPZP based Z-factor curve, using the 95 percent confidence level, is higher than the ASME Z-factor curve, except for pipe diameter less than 457 mm (18 inches). The 95-percent confidence DPZP based Z-factor curve for the SMAW is approximately the same as the current ASME Z factors for diameters larger than 610 mm (24 inches).

If the flow stress for stainless steel is changed to the average of the yield and ultimate strength, i.e., $(S_y + S_u)/2$, then the curves in Figure 10.9 should be used. Here the 95-percent-confidence DPZP-based Z-factor curve for SAW is approximately the same as the ASME Z-factor curve for pipe diameters larger than 610 mm (24 inches). The 95-percent confidence DPZP based SMAW Z-factor curve is well below the ASME Z-factor curve as shown in Figure 10.9.

Finally, we examined how the Z factors change with Charpy upper shelf energy. Hence, the user is not required to use a single Z-factor curve regardless of the actual toughness of the material. Instead there is a smooth transition from limit load to EPFM using this approach. This smooth transition is show in Figure 10.10 where the DPZP based Z factor is calculated as a function of the Charpy energy for a 406-mm (16-inch) diameter A106 Grade B pipe at 288 C (550 F). The flow stress chosen was the average of the yield and ultimate strength [i.e., $(S_y + S_u)/2$], which was almost identical to $2.4S_m$ in this case. As can be seen in Figure 10.10, the ASME Z-factor curves are significantly greater than the 95-percent confidence DPZP curve when the Charpy upper-shelf energy is greater than approximately 54 Joules (40 ft-lbs).

Assessment of α-Modified GE/EPRI Analysis

The Zahoor α-modification of the GE/EPRI method for predicting loads (or moments) and crack opening areas, Ref. 10.6., was assessed. The α-modification for the relation of J to moment changes the α in Equation 10.8 from the original GE/EPRI method (Ref. 10.7) to $\alpha^{[1/(n+1)]}$ as shown in Equation 10.9.

$$J_p = \alpha\sigma_o\epsilon_o C_1(a/b)h_1(P/P_o)^{n+1} \qquad (10.8)$$

$$J_p = \alpha^{[1/(n+1)]}\sigma_o\epsilon_o C_1(a/b)h_1(P/P_o)^{n+1} \qquad (10.9)$$

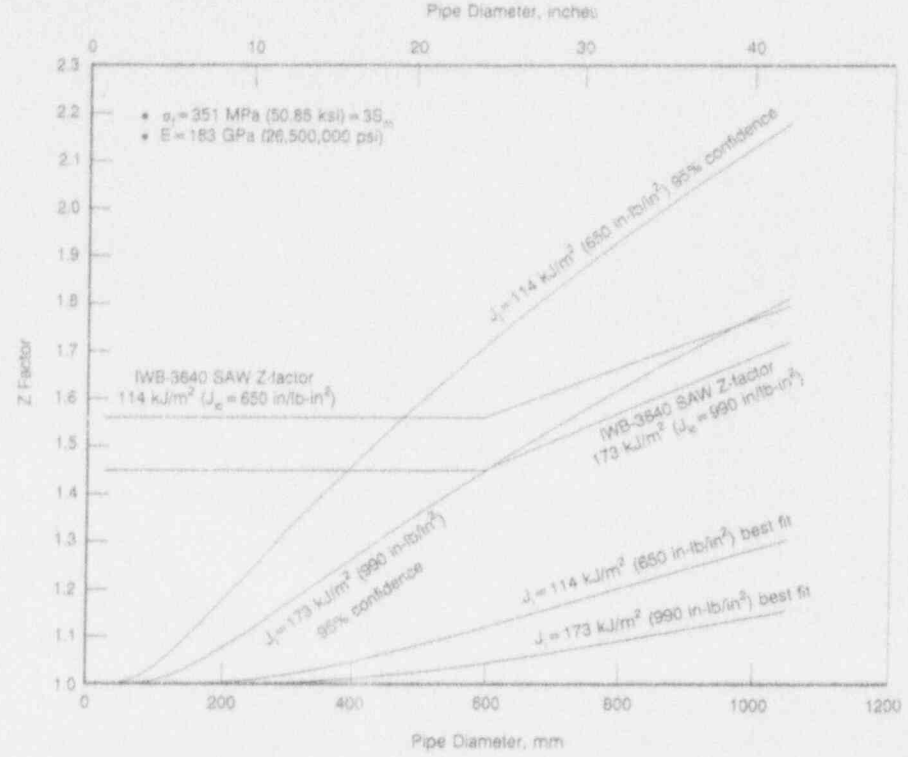

Figure 10.8 Comparison of Z factors from DPZP analysis with ASME IWB-3640 analysis using $\sigma_f = 3S_M$

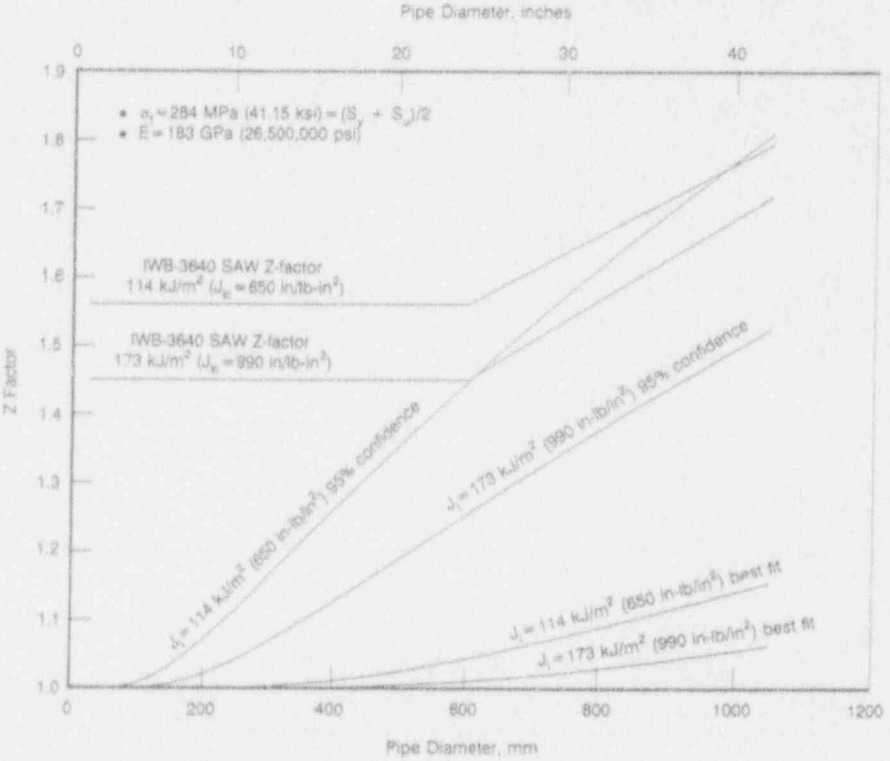

Figure 10.9 Comparison of Z factors from DPZP analysis with ASME IWB-3640 analysis using $\sigma_f = (S_y + S_u)/2$

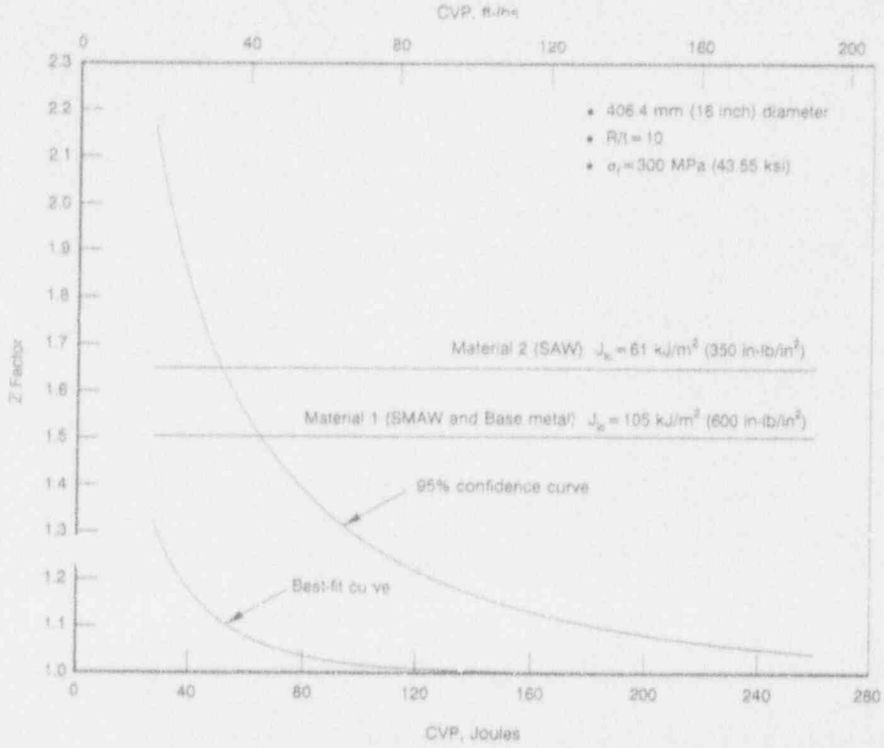

Figure 10.10 DPZP Z factors as a function of Charpy energy for 406-mm (16-inch) diameter pipe and comparison to ASME IWB-3650 values

Similarly for crack-opening displacement predictions, one might change α in Equation 10.10 to $\alpha^{[1/(n+1)]}$ as shown in Equation 10.11.

$$\delta_p = \alpha\epsilon_o a h_2 (P/P_o)^n \tag{10.10}$$

$$\delta_p = \alpha^{[1/(1+n)]}\epsilon_o a h_2 (P/P_o)^n \tag{10.11}$$

As has been previously been pointed out, see Section 6.1.3 of Reference 10.8, Equation 10.9 gives nonunique analytical solutions for the prediction of moments for a given stress-strain and J-R curve. This is because for the normalized Ramberg-Osgood relation

$$\epsilon/\epsilon_o = \sigma/\sigma_o + \alpha(\sigma/\sigma_o)^n \tag{10.12}$$

the reference stress, σ_o, and reference strain, ϵ_o, are relatively recent parameters used for normalizing fracture analyses, whereas the original Ramberg-Osgood relation is

$$\epsilon = \sigma/E + F'\sigma^n \tag{10.13}$$

Hence, for the same stress-strain curve, α can take on any value as long as the reference stress and reference strain are changed to satisfy Equations 10.14 and 10.15.

$$\alpha = \sigma_o^n/(\epsilon_o F') \tag{10.14}$$

$$E = \sigma_o/\epsilon_o \qquad (10.15)$$

Figures 10.11a and 10.11b show sample calculations for a 406-mm (16-inch) diameter 25.4-mm (1.0-inch) thick carbon steel pipe (using the stress-strain data from Battelle A106 Grade B Pipe Number F29) with two different crack lengths. Note that the original GE/EPRI estimation scheme is independent of the choice of the reference stress, σ_o, for both moment and crack-mouth-opening displacement. However, the α-modified equations gave increasing moment and decreasing crack-mouth-opening displacement as σ_o increases. Hence, for LBB applications, as the reference stress in the α-modified approach is increased, the crack-opening-displacement predictions become conservative (smaller than the GE/EPRI which means a longer crack size calculated for a given leak rate), but the load predictions become nonconservative (larger loads predicted than by the GE/EPRI method for the same size crack). Other estimation schemes such as the LBB.ENG and LBB.NRC methods are also independent of the choice of σ_o. Hence, we do not recommend using the α-modification GE/EPRI approach for LBB applications because of this nonuniqueness.

10.4 Plans for Next Year of the Program

10.4.1 Subtask 9.1 Technical Exchange and Information Meetings

Efforts in Activity 9.1.1 will continue to coordinate with the ASME Section XI Pipe Flaw Evaluation Task Group.

10.5 References

10.1 Wilkowski, G. M., and others, "Short Cracks in Piping and Piping Welds," Semiannual Report, April 1992 - September 1992, NUREG/CR-4599, Vol. 3, No. 1, September 1993.

10.2 Kiefner, J. F., Maxey, W. A., Eiber, R. J. and Duffey, A. R., "Failure Stress Levels of Flaws in Pressurized Cylinders," *Progress in Flaw Growth and Fracture Toughness Testing*. ASTM STP 536, 1973, pp. 461-481.

10.3 "PVRC Recommendations on Toughness Requirements for Ferritic Materials," WRC Bulletin 175, August 1972.

10.4 Schmidt, R. A., Wilkowski, G. M., and Mayfield, M. E., "The International Piping Integrity Research Group (IPIRG) Program - An Overview," SMiRT-11, Paper G12/1, August 1991.

10.5 Wilkowski, G. M. and Scott, P. M., "A Statistically Based Circumferentially Cracked Pipe Fracture Mechanics Analysis for Design or Code Implementation," *Nuclear Engineering and Design*, Vol. 111, pp. 173-187, 1989.

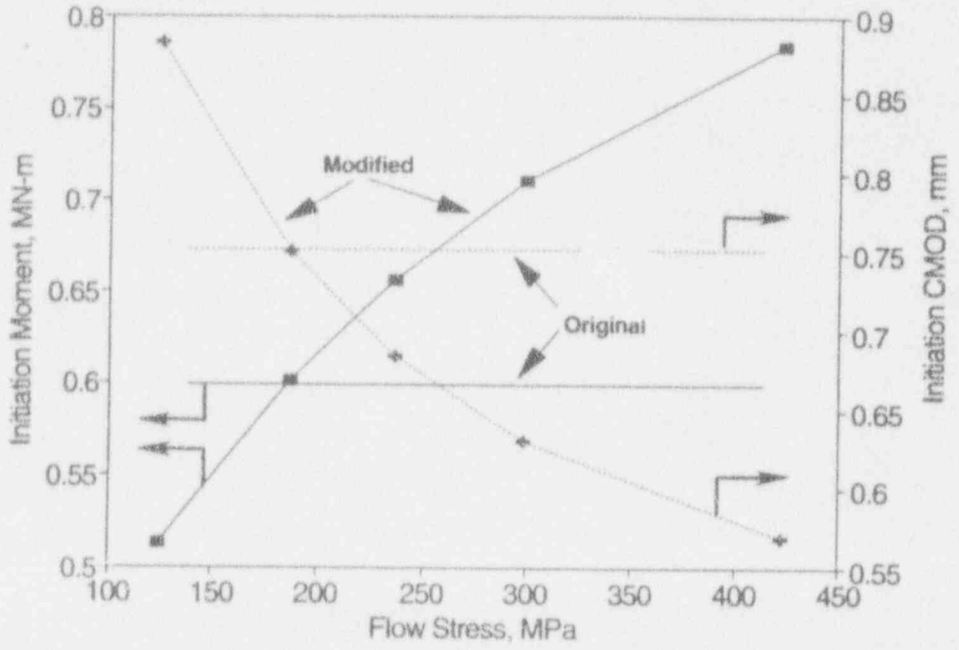

(a) TWC = 10 percent of circumference

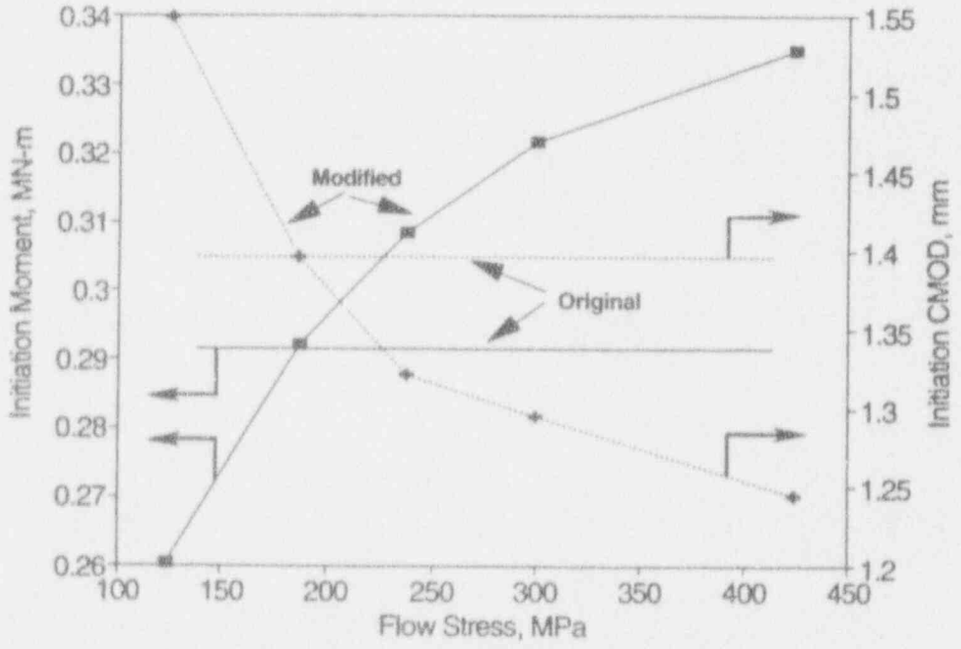

(b) TWC = 30 percent of circumference

Figure 10.11 Comparison of Zahoor modified GE/EPRI with original GE/EPRI predictions using stress-str n curve data from A106 Grade B Pipe F29

10.6 Zahoor, A. and Gamble, R. M., "Evaluation of Flawed-Pipe Experiments", EPRI report NP-4883M, November 1986, see Section 2.0.

10.7 Kumar, V., et al., "An Engineering Approach for Elastic-Plastic Fracture Analysis," EPRI Report NP-1931, July 1981.

10.8 Wilkowski, G. M., and others, "Analysis of Experiments on Stainless Steel Flux Welds", NUREG/CR-4878, April 1987.

NRC FORM 335 (2-89) NRCM 1102, 3201, 3202

U.S. NUCLEAR REGULATORY COMMISSION

BIBLIOGRAPHIC DATA SHEET

(See instructions on the reverse)

1. REPORT NUMBER (Assigned by NRC, Add Vol., Supp., Rev., and Addendum Numbers, if any.)

NUREG/CR-4599
BMI-2173
Vol. 3, No. 2

2. TITLE AND SUBTITLE

Short Cracks in Piping and Piping Welds
Semiannual Report
October 1992 - March 1993

3. DATE REPORT PUBLISHED

MONTH: March
YEAR: 1994

4. FIN OR GRANT NUMBER

B5702

5. AUTHOR(S)

G. M. Wilkowski, F. Brust, R. Francini, N. Ghadiali, T. Kilinski, P. Krishnaswamy, R. Mohan, C. Marschall, S. Rahman, A. Rosenfield, and P. Scott

6. TYPE OF REPORT

Technical

7. PERIOD COVERED (Inclusive Dates)

8. PERFORMING ORGANIZATION - NAME AND ADDRESS (If NRC, provide Division, Office or Region, U.S. Nuclear Regulatory Commission, and mailing address; if contractor, provide name and mailing address.)

Battelle
505 King Avenue
Columbus, Ohio 43201

9. SPONSORING ORGANIZATION - NAME AND ADDRESS (If NRC, type "Same as above"; if contractor, provide NRC Division, Office or Region, U.S. Nuclear Regulatory Commission, and mailing address.)

Division of Engineering
Office of Nuclear Regulatory Research
U.S. Nuclear Regulatory Commission
Washington, D.C. 20555-0001

10. SUPPLEMENTARY NOTES

11. ABSTRACT (200 words or less)

This is the sixth semiannual report of the U.S. Nuclear Regulatory Commission's 4-year research program "Short Cracks in Piping and Piping Welds" which began in March 1990. The objective is to verify and improve fracture analyses for circumferentially cracked nuclear piping with cracks sizes typically found during in-service flaw evaluations.

Progress in the through-wall-cracked pipe efforts invovled (1) verification of deformation plasticity under nonproportional loading, (2) evaluation of the effect of weld metal strength on various J-estimation schemes, and (3) development of new GE/EPRI functions. Surface-cracked pipe evaluations involved (1) material characterization of B&W C-Mn-Mo submerged arc weld metal, and (2) 3D finite-element mesh refinement study. The toughness of the bimetallic weld fusion line was evaluated and showed unusual fracture behavior based on the results of the Charpy tests. The dynamic strain aging J-R tests confirmed the screening criterion developed earlier in the program.

The results from this program to date necessitated several additional efforts. These were initiated and have been reported here. Presentation of the results from this program to the ASME Section XI Pipe Flaw Evaluation Working Group is also summarized here.

12. KEY WORDS/DESCRIPTORS (List words or phrases that will assist researchers in locating the report.)

Pipe, Fracture Mechanics, Cracks, J-Integral/Tearing Modulus, Leak Rate, Elastic-Plastic Fracture Mechanics, Nuclear Piping Steels

13. AVAILABILITY STATEMENT

unlimited

14. SECURITY CLASSIFICATION

(This Page)
unclassified
(This Report)
unclassified

15. NUMBER OF PAGES

16. PRICE

Federal Recycling Program